ADDIS ABABA UNIVERSITY

ADDIS ABABA INSTITUTE OF TECHNOLOGY

AFRICAN RAILWAY CENTRE OF EXCELLENCE

ANALYSIS AND IMPROVEMENT OF SECONDARY SUSPENSION EFFECTS ON RIDE COMFORT OF PASSANGER RAILCAR

(CASE OF ADDIS ABABA LIGHT RAIL TRANSIT SERVICE)

By

Biniam Ejara

Advisor: Celestin Nkundineza (Ph.D.)

A Thesis

Submitted to the School of Graduate Studies of Addis Ababa University in Partial Fulfillment of the Requirements for the Degree of Master of Science in Railway Engineering (Rolling Stock)

October 2021

Addis Ababa, Ethiopia

APPROVAL SHEET

The undersigned have examined the thesis entitled **"**Analyses and Improvement of Secondary Suspension Effects On Ride Comfort (Case Of AALRT) " presented by Biniam Ejara a candidate for the degree of Master of Science and hereby certify that it is worthy of acceptance.

Approved By Board of Examiners

Dr. Celestin Nkundineza(Ph.D.) Signature_____ Date_____

Advisor

Mr. Awel Mohammed

Internal Examiner Signature_____ Date_____

Dr. Samuel Tesfaye (Ph.D.)

External Examiner Signature_____ Date_____

Mr. Birhanu Reesom

Chair person Signature_____ Date_____

DECLARATION

I declare that research work titled “Analysis and improvement of secondary suspension effects on ride comfort” is my own work. The work has not been presented elsewhere for assessment. Where material has been used from other sources it has been properly acknowledged / referred.

_____

Biniam Ejara

ABSTRACT

Speed and track irregularities are the main causes of vibrations in rail vehicles. They bring a discomfort, fatigue and motion sickness to passengers depending on its frequency content. In this thesis the analysis and improvement of the secondary suspension effects on a passenger ride comfort of rail vehicle by considering the current random track irregularities are evaluated via the Sperling ride index. The current track irregularities data were collected from Addis Ababa Light Rail Transit Service (AALRTS) then converted to time domain and curve fitted using sine functions. The half car model of a vehicle with two bogies, two suspension levels, and a flexible carbody for one car is considered for mathematical modeling of the vehicle vibrations. The response due to pitch and bounce were numerically analyzed using MATLAB / Simulink and Universal Mechanism multibody dynamic simulation software (UM-MBS). The results obtained from two numerical simulations matched between each other. The results show that bounce vibrations affect more the ride comfort than pitch vibrations and as the speed increases the ride comfort worsens according to Sperling ride index evaluations. In addition to these analyzes, if the secondary suspension damping ratio falls between 0.1 and 0.3 the ride comfort is improved. Finally, optimizations of suspension parameters were done for worst track irregularities scenario by using MATLAB/Simulink/ Response optimization tool which led to reducing the ride discomfort significantly than the current suspension parameters. The evaluations concluded that the AALRTS vehicle vertical response is at good conditions with current track irregularities. The ride comfort is improved by 9.87%, 14.62%, and 15.17% at the center of the carbody, above bogie front and above rear bogie respectively.

Keywords: AALRTS, passenger rail vehicle, random track irregularities, secondary suspension, ride comfort.

Acknowledgments

Foremost, I would like to express heartfelt sincere gratitude to my advisor Dr.CELESTIN NKUNDINEZA (PhD) next to God, for his follow up, guidance, advice and technical support in strengthening me during the course of my paper work.

Next to him, I would like to thank Addis Ababa Light Rail Transit administration staff and rolling stock department for their appreciable technical support to get data of train and rail irregularities.

Also I would like to acknowledge a company of universal mechanism multi body dynamic simulation software for giving me the license freely for two months.

Finally, I would like to thank Addis Ababa University / African Center of Railway Excellence /and World Bank for covering a fund for this thesis and also all my tuition fee of master's Degree in rail way engineering.

Table of Contents

APPROVAL SHEET i
DECLARATION ii
ABSTRACT iii
Acknowledgments iv
List of Tables vii
List of Figures viii
List of Abbreviations x
CHAPTER ONE 1
INTRODUCTION 1
1.2. Statement of the problem 3
1.3. Research questions 4
1.4. Objective of Study 4
1.4.1. General Objective 4
1.4.2. Specific Objective 4
1.5. Delimitation 5
1.6. Limitation of Study 6
1.7. Significance of the Study 6
CHAPTER TWO 8
LITERATURE REVIEW 8
2.2. Ride comfort evaluation methods 9
2.3. Review of previous ride comfort evaluations and suspension optimization 10
2.5. Summary of the literature 12
CHAPTER THREE 14
METHODOLOGY 14
3.1. The mathematical model of the rail vehicle in the vertical direction. 16
3.1.1. The assumptions made in formulating the model 16
3.1.2. The movement equations for the of a car body. 18
3.1.3. Equations of motion of passenger rail vehicle 25
3.2. Track irregularities 36
3.3. Ride comfort Evaluations 37

3.3 .1 Sperling's Method 37
CHAPTER 4 40
RESULTS AND DISCUSSION 40
4.1. Curve fitting of track irregularities 42
4.2. Numerical simulation results 44
4.2.1. The vehicle vertical vibration response at different vehicle speeds. 44
4.2.2. Response of vertical vibrations of the vehicle at different damping ratio 46
4.2.3. Response of the vertical vibrations of the railcar at different load conditions 47
4.2.4. Time-domain step response analyses of the vehicle vertical vibrations. 48
4.2.5. Frequency response analysis of the vehicle 51
4.2.6. Ride comfort versus variation in speed 54
4.2.7. Ride comfort versus secondary suspension damping ratio variations 56
4.3. Multi-Body System Dynamic Simulation Results 57
4.3.1. Response of the vehicle vibrations versus speed variations 60
4.3.2. Ride comfort versus speed variations at variable damping ratio and under different track irregularities 63
4.4. Optimization of suspension parameter for reducing ride discomfort 65
CHAPTER FIVE 71
CONCLUSION AND RECOMMENDATIONS 71
5.1 Conclusion 71
5.2. Recommendations 72
REFERENCES 73
APPENDIX 78
A. AALRT Vehicle specifications 78
B. Matlab Simulations 79
C. Simulink Block 86
D. Universal Mechanism software programs 90

List of Tables

Table 3. 1 Scale for the ride comfort index Wz. 39

Table 4.1 Vehicle bounces and pitches vibration responses at different loading conditions……..47

Table 4. 2 Peak frequency response of Rail vehicle with respect to passenger loads 48

Table 4. 3 Step response characteristics for bounce movement of the vehicle..... 49

Table 4. 4 Step response characteristics for the pitch movement of the vehicle 50

Table 4.5 Comparison of universal mechanism and Matlab/Simulink results for vehicle bounce vibrations 61

Table 4. 6 optimized parameters of suspensions 66

Table 4. 7 Uncertain variables while optimizations..... 67

Table 4.8 Optimized suspension parameters versus the original suspension parameters. 67

Table A. 1 AALRT vehicle specifications…….78

Table A. 2 Load conditions of AALRT vehicles 79

List of Figures

Figure 3.1 General work flow of the study 15
Figure3.2 The vehicle vertical mechanical model, where ab, ac are the axle bases of bogies and axle base of car body and ξk with k = 1…. 4, the irregularities against the wheelset k..... 17
Figure 3.3 Transverse vibration of thin beams [33]..... 19
Figure 3.4 the measured vertical track irregularities of AALRT at a) north-south and b) East-west lines 37
Figure 3.5 vertical displacements of track irregularities in time domain a)E-W direction track irregularities b) N-S line vertical track irregularities..... 38
Figure 3.6 frequency weighting B [12]..... 39
Figure 4.1 FFT for Vertical acceleration of car body using experimental test and simulations 41
Figure 4.2 Curve fitting of track irregularities of NS line using the sum of sine's at degree 8 and its residual..... 43
Figure 4.3 Symmetrical dynamic response of the vehicle at 20, 40, 60, 80 km/hr. of car body bounce and bogie bounce..... 45
Figure 4.4 The symmetrical dynamic response of the vehicle at 20, 40, 60, and 80 km/hr. of car body pitch and bogie pitch..... 46
Figure 4.5 Change in vehicle response versus damping coefficient for symmetrical bounce movement. 50
Figure 4.6 Step response characteristics of the bounce vibration of the vehicle. 51
Figure 4.7 Step response of pitch vibration of the system..... 51
Figure 4.8 Frequency domain response of the vehicle where ac is carbody accelerations, acb are carbody bending motion and ab is bogie accelerations 52
Figure 4.9 Fast Fourier Transform of bogie bounce vibration accelerations at random track excitation..... 53
Figure 4.10 Frequency response of bounce vibration at random track excitations is in the frequency domain..... 53
Figure 4.11 Frequency responses of pitch accelerations at a) the car body, bending mode, and bogie frequency responses b) the fast Fourier transform of the sampled track

excitations and the bogie pitch output. Ride comfort index for different speeds of vehicle. 54
Figure 4.12 change in ride comfort vs. the speed of the vehicle 56
Figure 4.13 Change in the ride comfort with damping ratio at different vehicle Speeds using Mat lab/Simulink software 57
Figure 4.14 Rail vehicle model of A) wheelset B) bogie, and C) car body using Universal Mechanism Multi-Body System dynamic simulation software 58
Figure 4.15 Track irregularities along vertical rail profile 59
Figure 4.16 Multi-Body System simulation results: variations of bounce accelerations at various speeds for a) bogie and b) rigid carbody. 61
Figure 4.17 Change in pitch vibration at various speed in car body and bogie using UM – MBS software. 63
Figure 4.18 the ride index of AALRT rail vehicles under current track irregularities at various speeds and damping ratio of secondary suspension due to effect of bounce vibrations 64
Figure 4.19 ride comfort versus the vehicle speed and different damping ratios when track excitations UIC bad track. 65
Figure 4.20 Sensitivity Analysis statistical results. 69
Figure 4.21 Optimized versus original ride comfort of AALRT vehicles. 69
Figure 4.22 Optimized versus original ride quality of AALRT vehicles. 70
Figure 4.23 Change in design parameters at corresponding iterations where Czb, Kzb, Kzc, bzc are the primary suspension damping coefficient, primary suspension spring stiffness, secondary suspension spring stiffness and damping coefficients. 70
Figure c. 1 Simulink block of vertical vibrations of the carbody, bending mode carbody, and bogie pitch and bounce vibrations 86
Figure c. 2 vertical track excitation of AALRT 87
Figure c. 3 velocity excitation of the track input 87
Figure c. 4 symmetrical excited bounce vibrations of the vehicle. 88
Figure c. 5 Simulink block for Anti symmetrical excitations of the vehicle pitch vibrations response 89

List of Abbreviations

AALRTS	Addis Ababa Light Rail Transit Service
ISO	International Organization for Standardization
BS	British Standard
UIC	International union of railways
DOE	Design of Experiment
V	Velocity in m/s
L	Longitudinal Length of the car
EI	Bending module
$\boldsymbol{\mu}$	Damping coefficient of car body
$w(x,t)$	Displacement of the carbody section
T	Time in seconds
FEM	Finite Element Method
$Z_{b1,2}, \dot{Z}_{b1,2}, \ddot{Z}_{b1,2}$	Bounce displacement, velocity and accelerations of the bogie at front and rear (at distantl1 and l2) positions respectively.
$\theta_{b1,2}, \dot{\theta}_{b1,2}, \ddot{\theta}_{b1,2}$	Pitch angle, velocity, accelerations at bogie front and rear positions respectively (at distantl1 and l2).
$Z_c, \dot{Z}_c, \ddot{Z}_c$	Bounce displacement, velocity and accelerations at car body
$\theta_c, \dot{\theta}_c, \ddot{\theta}_c$	Pitch angle, velocity, accelerations at car body

m_b, m_c	Mass of bogie and mass carbody respectively
J_b, J_c	Mass moment inertia of bogie and carbody
i_b, i_c	Radius of gyration for bogie and carbody
Kz_b, Cz_b	Vertical Primary suspension stiffness and damping constant.
Kz_c, Cz_c	Vertical secondary suspension stiffness and damping constant
a_b, a_c	Bogie and carbody wheel base respectively
$T(k,t)$	Time dependent coordinates of k^{th} natural bending mode in vertical directions
$W_k(x)$	Eigen or shape function vibration mode k at bending
$\boldsymbol{\rho}$	Density
$\boldsymbol{\omega}$	Natural frequency
m_{mc}, k_{mc}, c_{mc}	Mass ,stiffness and damping constant of the car body bending respectively
F_1, F_2	Vertical bogie forces act on the carbody at front and rear bogie center
F_3, F_4	Vertical wheelset forces due to bounce at front bogie in right and left directions
F_5, F_6	Vertical wheelset forces due to bounce at front bogie in right and left directions
F_7, F_8	Vertical wheelset forces due to pitch at front bogie in right and left directions

F_9, F_{10}	Vertical wheelset forces due to pitch at rear bogie in right and left directions
$\xi_{1,2}, \dot{\xi}_{1,2}$	Vertical track excitations at functions of time and wheel vertical velocity at wheel 1and 2.
$\xi_{3,4}, \dot{\xi}_{3,4}$	Vertical track excitations at functions of time and wheel vertical velocity at wheel 3and 4.
u, v	Symmetrical and axisymmetric excitations Eigen functions respectively
$\zeta_{b,c}$	Damping ratio of bogie and car body
$\zeta_{m2,3}$	Modal damping ratio at mode 2and 3
$\omega_{m2,3}$	Modal angular frequency at mode 2 and 3
s_1, s_2, s_3	Symmetrical excitation bounce displacements at carbody, bending carbody mode and bogie
a_1, a_2, a_3	Axis-symmetrical excitation pitch displacements at carbody, bending carbody mode and bogie

CHAPTER ONE

INTRODUCTION

Because of the need for comfort, security, safety, and rapid transportation demands in the current situation, railway companies are forced to meet more stringent regulations regarding the dynamic behavior of rail vehicles[1]. The ride comfort is regarded as the capability of vehicle suspension to maintain motion within the range of human comfort, and is usually measured by a riding comfort index.

To fulfill the need of current demand related to ride comfort the rail vehicle needs many improvements. From them, the improvement of railway vehicle suspensions is an easy and cheapest way to achieve this goal [2]. Various studies have been conducted regarding improvement of the rail car concerning the factors like comfort, safety, stability, and others related to the dynamic behavior of the rail vehicle during the running of railway vehicles by measuring vibration accelerations [3].

Vibrations are generated because of the interaction between wheel and track in the railway vehicles. The bounce, car body bending and pitch vibrations have impact on the rolling quality, safety, and ride comfort and track quality. The rise in the speed of the vehicle will excite the increase in the vibration behavior at the carbody level, with a negative impact up on the ride comfort, this needs to be improved by the optimization of the suspension parameters[4] or strengthening the car body structural rigidity [5].

If we need to increase the speed of the vehicle further with track irregularities the passive suspension system performance is no more achieve the standard ride comfort level, so using the semi-active or fully active suspension is another solution [6]. Despite the favorable results, the active suspension is not a best operational solution. Because of the cost of implementing, operating, and maintenance, this system is too costly versus its benefits. Therefore, in the case of a low and medium-speed train like of Addis Ababa Light Rail transit (AALRT), it's better to optimize the existing passive suspension element rather than using active suspension system.

There are various international standards for evaluating the ride among them; Sperling Ride Index, ISO 2631, BS 6841, EN-12999, and UIC 513 are widely used [7–11]. They

are used frequency-weighted acceleration to evaluate the vibration level in terms of passenger comfort. From the standards stated above the Sperling ride index measures the ride comfort independently in different directions [12], because its easily interpreted and can measure the vibrations of various element on the car body in different plane independently. In this paper, Sperling Ride Index (Wz) is proposed for evaluating ride comfort.

In the rail way vehicles the passive suspension made of spring and oil dampers. It is characterized by low cost, a high level of simplicity and the absence of an external driving system. Engineers tried to obtain the best performances from such a suspension by careful selection of suspension parameters, design and optimizations for good stability and comfort the rail vehicles [13]. The active suspension system is providing the optimal damping response in each time step. The suspension strategy that takes the advantage of the fully active suspension has the advantage of providing the optimal damping response in each time step. This technology is used in tilting trains for reduction of lateral acceleration which gets in excess when negotiating a curve. It also used in the secondary suspension to improve ride comfort. However, the introduction of new adaptive functional components aims to improve a certain aspect of the performance, while the railway vehicle dynamics is influenced in several different aspects, that is, it is multidisciplinary. Furthermore, the costs of implementing the components are high and there are some open questions regarding robustness and long-term reliability [14].

Passive systems on the other hand can significantly improve performance of the vehicle regarding both comfort and stability especially in the low and medium speed rail vehicles. Because of that it is still a point of interest in such type of rail vehicles. However, it is needs extensive mathematical formulation and optimization problems to get its best performance. Through optimization of passive damper and spring stiffness parameters for both primary and secondary suspension of a railway vehicle good ride comfort and stability are obtained [15].

However, in current AALRTS because of the overload of the passengers during operation as well as the current track irregularities the dynamic behavior of the vehicle is varied. This, change in dynamic behavior of the vehicle especially the effects due to track

irregularities intensify the vibrations of the rail vehicle which have the negative impact on the ride comfort. In order to assess such a problem, this paper studied the effects of the passive secondary suspension parameter during variable speed, overloads condition, and current track irregularities in AALRT line upon ride comfort. Bounce, pitch and car body bending mode motion vibrations are evaluated by the Wz index at frequency weighted accelerations of each type of motions. By using numerical analysis of 2D and 3D multibody body simulation the effects of secondary suspension parameters on the ride comfort is studied at the various speeds of the vehicle and current vertical rail irregularities of AALRT vehicle. Finally, sensitivity analysis using Monte Carlo simulation is done to clearly identify the parameter that have much impacts on the ride comfort from existing suspension parameters and then according to the results the parameter which have greater effect on the ride comfort taken as design parameter for improvement process. The improvement of the ride comfort is done by reducing the vertical vibrations such as bounce, pitch as well as bending car body vibrations to minimum by keeping the suspension deflection according to the standard of the AALRTS for both primary as well as secondary suspension, by using Latin hypercube Algorithm on the Response optimization analysis tool on the MATLAB /SIMULINK environment.

1.1. Statement of the problem

Vibration on the vehicle usually occurs because of different types of rail vehicle forces that act on vehicles carbody under variable factors such as track condition, traction, braking speed, wind effects, wheel polygonization, and rail wheel wear, etc. If this vibration exceeds the allowable limiting values, it leads to ride discomfort of passengers, rail-car instability, wear on rail and wheels. Also, on extreme cases, damages of components of the rolling stock and derailment may happen.

From above stated problems, the vibrations due to track conditions are the major causes of the ride discomfort to passengers and drivers. When the level of the ride comfort worsens, it may cause motion sickness, fatigue, back pain and others related health problems to passengers and drivers. These issues were improved by vibration isolation elements (suspension element) and structural damping concepts. But, the latter one contradicts with speed and energy consumption issues. The secondary suspension

parameters one usually designed according to standard track irregularities. But even over a time track irregularities become worse due to different factors such as aging, improper maintenance, degradation of the soil and other factors.

In order to address the problem of vibrations due track irregularities on the ride comfort, the effects of secondary suspension parameters on the passengers ride comfort of railcar at different speeds, overloads, and track condition will be evaluated for a case of Addis Ababa Light Rail Transit Service. Then we will optimize appropriate suspension parameters according to the condition that will make the AALRT to work with existing standards of ride index in worse track condition of the track AALRT vehicles. But, in this research, the study concentrates on the effects of vibration from bounce, pitch and bending of car body of dynamic forces under different conditions of the track by numerical analysis using MATLAB /Simulink and Universal Mechanism multibody simulation software.

1.2. Research questions

- Do the secondary suspension damper and spring parameters influence on ride comfort?
- Could vibration level caused by vehicle speed, overload of passengers and track conditions affect ride comfort?
- To what level do existing secondary suspensions minimize vibration in the case of AALRT?

1.3. Objective of Study

1.3.1. General Objective

The general objective of this study is to analyze and improve the suspension dynamic influence, with an overload of passengers, variable speed, and random track irregularities, on ride comfort in the case of AALRT rail car.

1.3.2. Specific Objective

This research work specifically aims to:

1. To perform mathematical modeling and analyze the effects of damping of secondary suspension parameters, and vertical dynamic forces passenger rail car at straight track motion of the car under conditions of:-
    - Over loading of passengers
    - Variable speed of the cars
    - Random track irregularities on the ride comfort
2. To analyze numerically the vibration of the car body with frequency weighted acceleration and power spectral density, and to compare with standard values to predict the level of comfort of AALRT.
3. To perform the analyses of a half-car model, simulation, and to find optimum values of secondary suspension parameters that improve the ride comfort for AALRT vehicles in the MATLAB/ Simulink software.
4. To validate the vibration response results from MATLAB by modeling and simulating the complete car in the Universal Mechanism Multi-Body System dynamics simulation software
5. To determine the parameters of the suspension among those obtained in specific objective (5) that lead to improved ride comfort as well as those that do not affect the railcar ride quality of AALRT.

1.4. Delimitation

As mentioned before there are various options to improve the ride comfort of passenger rail vehicles. This thesis only evaluates and improving the effects of passive secondary suspension effects on ride comfort in the case of AALRT. The only vibration due to bounce, pitch, and carboy bending dynamic force with the rigid track is considered. The measure of ride comfort is evaluated according to the standards of the Sperling ride comfort index. However, other parameters such as loading condition, vehicle speed, and vertical track irregularities condition of the trains are taken into account. Lateral irregularities as well as lateral dynamics are not studied in this research because they have a very little influence on vertical and pitching motion of ride comfort indexes.

1.5. Limitation of Study

Some of the limitations of this study are described as follows:

- Experimental analysis and tests will not be performed in this study due to the absence of laboratory and tools used to perform tests.

1.6. Significance of the Study

The method, the results, and the findings obtained from this study shows it has great importance for AALRT, other vehicle operating companies, and researchers who on the evaluation and improvement of ride comfort of the vehicles. The significance of this study in details is described as follows.

- The methodology used in this paper will be adopted for another study regarding vibrations analysis of vehicles.
- A better comfort can also be very important from the customers' point of view who wants to enjoy a smooth ride and possibly want to spend their time reading or working onboard.
- The vehicle may be allowed to run at higher speeds or on lower quality track while maintaining the same comfort as the passive vehicles. Higher speed reduces travel time which is appealing not only to passengers but also to operators who seek more efficient use of infrastructure and rolling stock. Allowance to run on lower track quality can also be very attractive to the infrastructure managers who need to invest substantial time and money to keep very good track quality especially when it comes to high-speed lines.

1.7. Thesis organization

The chapter of this paper is organized to guide the reader from theoretical background to final results.

- Chapter one is about the backgrounds of the dynamics of the rail vehicle, track irregularities, suspension system, and ride comfort, the problem to be solved, the scope, objectives, and significance of the study were described.

- In chapter two, review of several papers related to the suspension system, ride comfort, vehicle dynamics, track irregularities and optimizations of vehicle responses.
- Chapter three covers the analytical modeling of the car body bending, vehicle dynamics in the bounce and pitch vibrations, different parameters needed for modeling the vehicle, Sperling evaluations method for the ride comfort for passenger vehicles.
- Chapter four includes analysis and discussion of the results of this study subject using numerical simulations of MATLAB/SIMULINK and UM-MBS simulation for the evaluations of curve fitting of track irregularities, vehicles speed variations on vibrations response of the vehicle during pitch and bounce motions, effects of suspension parameters variations on the vehicle response, speed and secondary suspension variations on ride index of vehicle and improvement of suspension parameter for ride comfort is carried out. The results of those simulations were presented accordingly.
- Finally, recommendation, future work and conclusion of the whole study of the simulation are described briefly.

CHAPTER TWO

LITERATURE REVIEW

There are many studies conducted regarding evaluations of rail vehicle ride comfort but this paper only considered the literature that is related to this study especially with the secondary suspension of the rail vehicle. Summary or reviews of those papers have been presented in the next sub-sections.

2.1. Suspension system of rail vehicles

In terms of vehicle dynamics aspects, the suspension system should maintain good ride quality and curving performance against track irregularities especially in the case of high speed trains. These suspensions can be categorized into three groups: passive, semi-active, and fully active systems[16].

A passive suspension system has conventional springs and pneumatic or oil dampers. These systems contain no sensors, electronics, or controls [13]. A well-designed passive suspension which has advantage of design simplicity and cost-effectiveness is commonly used in rail vehicles. However as the parameters of the passive damper are fixed, its performance on the wide frequency range and different rail conditions are limited[17].

Semi-active suspension systems provide controlled real-time dissipation of energy. The main semi-active devices that have been considered for transit engineering applications are variable orifice which is composed of oil cylinders and mechanical valves, so the system reliability may be reduced and the maintenance may be costly [18]. Another type of semi-active dampers uses controllable fluids, which include electro rheological (ER) and magneto rheological (MR) fluids. In comparison with the semi-active dampers described above, an advantage of controllable fluid devices is that they contain no moving parts other than the pistons in the dampers, which makes them simple and reliable. Liao and Wang[18] presented the feasibility for applying MR fluid dampers to control the vertical vibrations of a railway vehicle and improves ride comfort significantly.

Fully active suspensions use hydraulic actuators which create the desired force in the suspension system. Both the semi-active and fully active suspensions require sensors to

be located on the vehicle which measures the motions of the body, suspension system, and/or the bogie mass. Fully active suspension scans consume large amounts of power to provide the control forces. However, for lower speed vehicles a passive suspension is a good option because it's simple in constructions and cost effective.

2.2. Ride comfort evaluation methods

It is important to evaluate the ride comfort to assess the quality and experience of a passenger on a train journey. The comfort level of passengers depends on a combination of both physiological and physical factors. The ride comfort mainly affected by parameters such as humidity, smell, visual stimuli, vibration, temperature, acoustic noise, and design layout. Vibration is the main parameter that affects the users' comfort because of interaction with different parts of the vehicle body [11] and [20–23].

Because of the vibration factor, the ride comfort evaluation methods are based on the passenger's exposure durations and their level. The condition of the railway vehicles and the track conditions as railway profile, rail irregularities or curvature, and wheel defects, influence the passenger's perception of comfort. However, these parameters are not regular in all the countries; it is difficult to establish a unified standard for ride comfort of railway vehicles. Three methods that are commonly used throughout the world are the root -mean –square(R.M.S), statistical, and Sperling's methods [12].

The R.M.S method is an evaluation procedure proposed and revised on the ISO 2631 standard by the International Organization for Standardization (ISO). It depends on the rate of human exposure to whole-body vibration. But, the statistical method, developed in EN 12299, was created based on the R.M.S method. Considering the fluctuations in both acceleration and frequency levels that occur during train travel, the ISO 2631 standard is appropriated for the evaluation of trips with small variations, while the EN 12299 method is more accurate for travels with variations associated with passengers and also minimizes the sensitivity to artifacts.

When proceeding to a comparison between two or more train comfort rides, the more appropriate method is Sperling's method. ‘’This method was introduced in the mid of the last century in Germany by Sperling, is currently used in countries like Sweden, China or India. The special characteristic of this method is the fact that it is determined for each

direction using frequency-weighted accelerations. Which are different in three directions .Even when the intensities for all frequencies of vibration are equal, the human feeling during its exposure to vibration varies depending on the direction of motion in different parts of the body''[5, 24, 25]. Thus, to convert the vibration into the human feeling a frequency weighting curve is used. Higher levels of weighting factor corresponding to the frequencies where humans are more sensitive. For ISO 2631 the sensitive ranges for vertical and lateral vibration are 4-12 Hz and 0.6-2 Hz, respectively. On the EN 12299, the sensitive ranges found are 4-16.5 Hz for vertical vibration and 0.6-2 Hz for lateral vibration. For Sperling's method, both vertical and lateral vibration ranges are 3-7 Hz.

2.3. Review of previous ride comfort evaluations and suspension optimization

Johansson et al. [15] studied the optimization of damping characteristics in bogie suspensions using a multi-objective optimization methodology. The damping is investigated and optimized in terms of the resulting performances of a railway vehicle concerning safety, comfort, and wear considerations. A complete multi-body system model describing the railway vehicle dynamics is implemented in commercial software GENESYS and used in the optimization. Pareto fronts concerning safety, comfort, and wear objectives are obtained, showing the trade-off behavior between the objectives suffers from relevant degradation which in critical cases may lead to component failure, derailment, and loss of life. Finally, he concludes that the railway companies should have to consider ride comfort and safety issues during the operation to compete with other modes of transportation industries.

Jason et al [26] investigated the possibility of improving the ride quality of a two-axle railway vehicle with a single-stage suspension employing passive suspensions employing an inerter device. The goal of this study is to improve the ride quality in both the vertical and lateral motions in response to track irregularities. The elastic effects of the damper and inerter device are then taken into consideration for practical purposes. But, widespread use of this vehicle has been limited because a single-stage suspension leads to unsatisfactory ride quality**.** Non-ideal behavior of the damper and inerter devices (e.g. compliance effects) has not been considered.

Lozia et al [27] proposed the methodology of optimizing the parameters of the passive suspension system of a railway vehicle. A linear half-vehicle model and an example of the procedure carried out to optimize a selected parameter of the model have been demonstrated. In this study, considerations that need to be carried out with employing a half-vehicle model, such issues as nonlinearities of spring characteristics of the suspension system, asymmetry and nonlinearities of shock absorber characteristics, dry friction in the suspension system, and wheel lift-off are not included.

Sharma et al [28] studied on" improving the ride quality and comfort of railway vehicles using semi-active secondary suspension based on magneto- rheological fluid dampers". Non-linear stiffness and damping functions of the passive suspension system are extracted from experimental data and magneto rheological damper is integrated into the secondary vertical suspension system for improving ride quality and comfort of the rail vehicle. The finding of the research establishes magneto rheological damper strategies in the secondary suspension system of railway vehicles improve the ride quality and passenger comfort to a great extent compared to the existing passive system by only reducing the vertical vibrations. However, the highly nonlinear behavior of a Magneto rheological damper related to its semi-active nature increases the level of complexity in numerical modeling; especially when parametric models are used and they are considered only the vertical dynamics of the vehicle.

Javad et al**.** [29] investigated to improve ride comfort based on springs and damper settings by using the design of experiment method (DOE). Pitch and bounce equation motions for 7 degrees of freedom are modeled .by using the RMS accelerations of bounce accelerations and a pitch angle of the car body as objective functions optimize the existed suspension settings. The optimized suspension settings improve the ride comfort significantly.

Dumitriu et al. [30] analyze the suspension damping influence on the ride comfort evaluated by the Sperling ride index. While modeling the vehicle they considering the flexible car body, wheelset vertical dynamics as the derivative of track irregularities, and static random track excitations to determine the vibrations response at three critical points that are at a car body center and above two bogies. Their results from numerical

simulations show the secondary suspension damping greatly reduces the ride discomfort at above two bogies while at the center of the car body it may intensify the vibration and the primary suspension doesn't have much effect on the ride comfort. He also did another investigation by adding longitudinal suspension element to the secondary suspension on its mathematical modeling to see the influence of the car body flexibility on the ride comfort. The vertical bending mode of symmetrical vibrations significantly affects ride comfort and so for such cases, the longitudinal suspension element has great importance in reducing such vibrations when the vehicle is at high speed[31].In his recent research that was published in 2021 by using the mean comfort method (EN12299) and Sperling ride index, he evaluates the ride comfort of the second model in [31] to compare the results of the two standards. From the results he concludes under the same conditions of vehicle operation, the ride comfort indices of Sperling ride index results indicate a weaker ride comfort than in the case of the ride comfort indices of Mean Comfort Method. While frequency weighting does not change the dominant vibration modes, such as bounce and pitch, it does reduce their impact on the dynamic response of the car body; the weighting function related with Sperling's method significantly decreases the influence of the dominant vibration modes on the dynamic behavior of the car body less than the weighting function related with the mean comfort method [32].

2.5. Summary of the literature

In this part, a summary of works of literature that related to the stated problem and the gaps filled with this literature is presented.

There are many types of research and investigation that were done regarding improvement of the ride comfort due to vibrations of the rail vehicles by employing different suspension systems and improving structural stiffness of the system. While improvement of ride comfort their assumptions and considerations for all the researches are very different. In case of track irregularities, almost all of the researches were done based on static random excitations and periodic excitations based ORE sample but a few works of literature is used the measured track irregularities of the operating railway system.

However, in the case of AALRT, almost all works were done before working with rigid car bodies to evaluate the ride comfort. There is no sufficient study regarding evaluations of the dynamic effects of secondary suspension parameters for light rail trains that consider a factor such as an overload and current track irregularities. Generally, we need to study more on this area by considering the effects of secondary suspension dynamics which are related to sensitivity issues that depend on overload of the passengers, variable speed, and random track irregularities to evaluate the current conditions of the AALRT trains ride comfort.

CHAPTER THREE

METHODOLOGY

In this section, the method to achieve the objectives that are put in chapter one is briefly described as follows.

- First, the system is modeled mathematically by considering the vehicle as one car, two bogies, and four wheel sets and the flexible car body by using the AALRT vehicle parameters.
- Then current data from the AALRT track is designed and sampled and curve fitted using Matlab as stationary random track irregularities.
- The procedures followed to analyze the response of the system due to speed variations and secondary suspension parameters variation on MATLAB /SIMULINK software will be presented.
- The method of modeling and analyzing the vehicle in Universal Mechanism MBS was also demonstrated.
- Finally, the way of evaluating the ride comfort according to the Sperling index is presented.

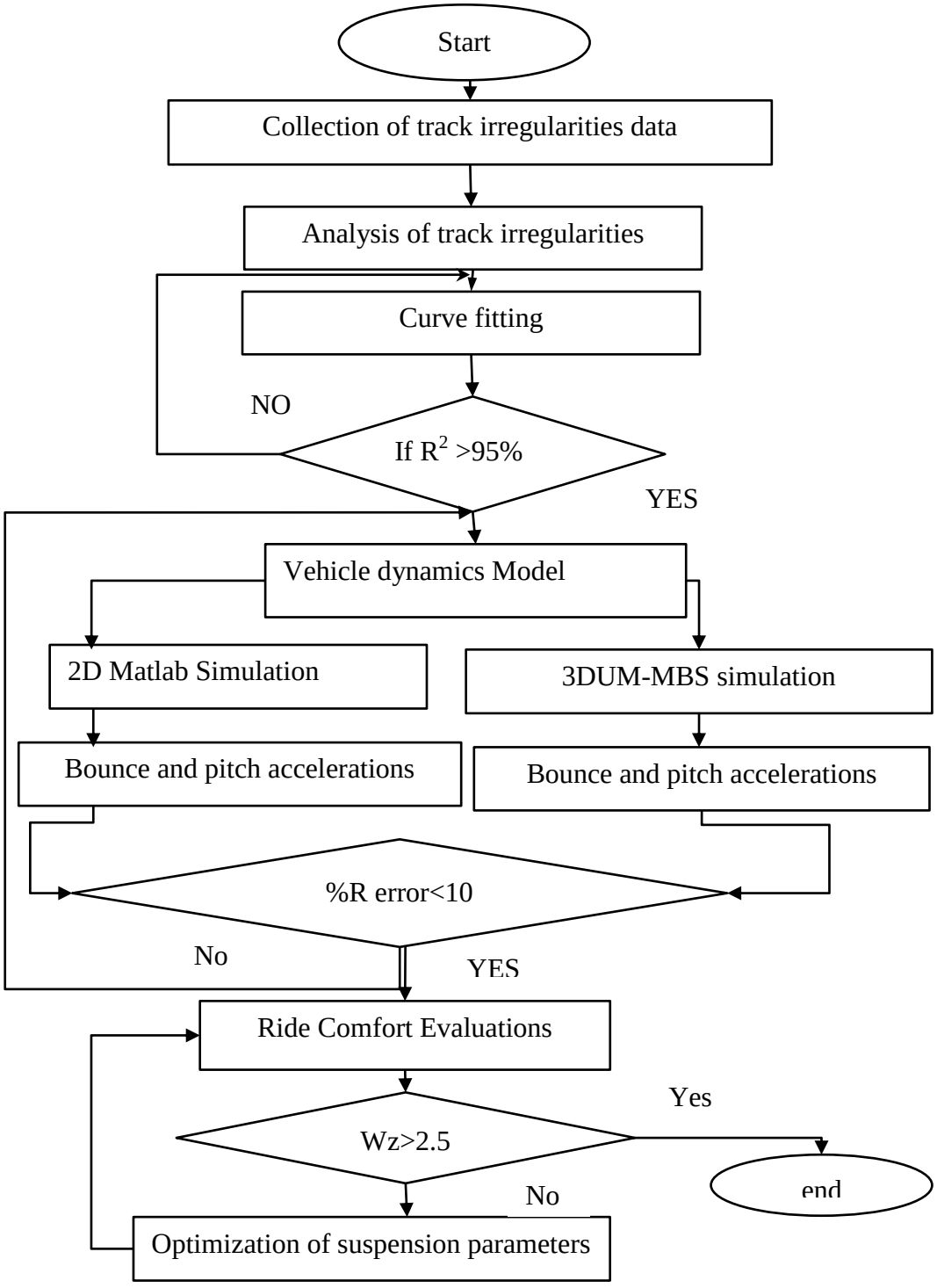

Figure 3.1 General work flow of the study

3.1. The mathematical model of the rail vehicle in the vertical direction.

The vehicle should be represented as a multi-body system for analysis of dynamic behavior of the rail vehicle system. The model of the system is represented in a Figure 3.2.

3.1.1. The assumptions made in formulating the model

- ✓ Vertical half rail car model is considered (bounce, pitching for car body and carbody bending motion). The rail vehicle bounce and pitching motion was decoupled from lateral motions (yaw and lateral displacement). Researches have shown that these two motion types have a very weak coupling.
- ✓ The springs and dampers of the suspension system elements have linear characteristics and the vehicle is moving on a standard gauge and on the rigid track.
- ✓ Only one car motion with two bogies that have four axles is considered.
- ✓ Excitations of the vertical left and right rail is considered as the same shape in this model. The data collected from the AALRTS field measurement and converted to general form of equations accordingly.
- ✓ The vehicle car body of length $'l'$ is modeled by taking assumptions as an Euler-Bernoulli beam of uniformly distributed mass and constant section.
- ✓ Because of the frequencies of wheel sets on the track are much higher than the vehicle vibration and the track rigidity is much higher than the one of the vehicle suspension the track is considered as a rigid track.

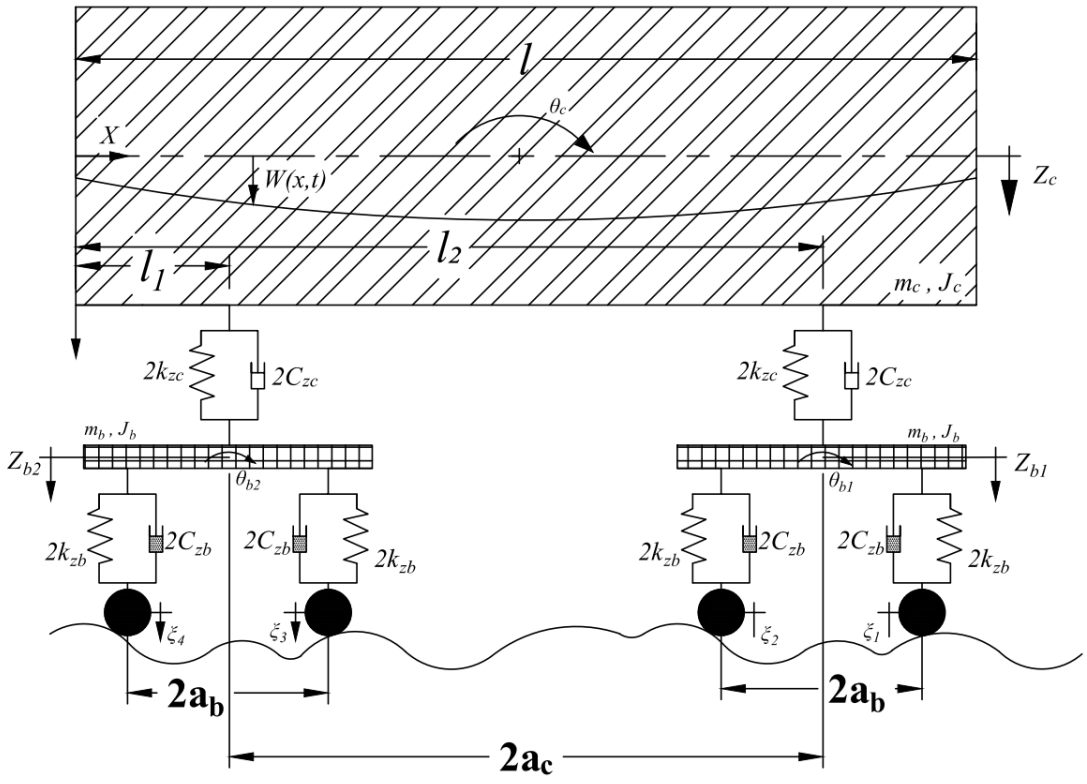

Figure 3.2 The vehicle vertical mechanical model, where $a_{b,}a_c$ are the axle bases of bogies and axle base of car body and ξ_k with k = 1…. 4, the irregularities against the wheelset k.

Two-floor suspension of railway vehicle with two bogies and four axles that travels on a with random track irregularities is considered for the model of the vehicle (Figure 3.2). A Kelvin-Voigt system is used for modeling both the secondary and the primary suspensions level. The spring stiffness and damping constants for the car body and bogies are k_{zc} , k_{zb} , c_{zb} and c_{zc} respectively.

The bogies masses are considered as 2-DOF rigid bodies, namely the bounce movement z_{bk} and pitch θ_{bk}, with k = 1, 2.Becuase of the rigid track is considered in the model, the vertical wheelset displacement equals the velocity of corresponding irregularities.

Before modeling the system we need to get the mode shape functions of the vertical displacements of the carbody as follows.

3.1.2. The movement equations for the of a car body.

Due to the modal superposition of rigid and bending modes considered the vertical displacement of the car body are given by [33]

$$w(x,t) = Z_c(t) + \left(\frac{L}{2} - x\right)\theta_c(t) + \sum_{k=1}^{\infty} W(x)T_k(t) \qquad (3.1)$$

Where, $w(x,t) -$ is displacement of the car body at a time t.

$Z_c(t) -$ It's the bounce vibration of the car-bodies at a time t.

$\theta_c(t) -$ Pitch vibration of car body rigid modes.

$W(x) -$ Shape function of vibration mode k at bending.

$T_k(t) -$ Time-dependent coordinate

By considering the car body as Euler Bernoulli constant section(Figure 3.3) and uniformly distributed mass from equations above the shape function($W(x)$) of vibration at mode k are derived as follows.

Where, $M(x,l)$ are bending moment, $V(x,t)$ shear force, and $f(x,t)$ external transverse across the length of the beam? Since inertia force acting on element beam is $f = ma$

where $m = \rho v$ and $v = dx \times A(x)$

From equations 3.1 and 3.2 inertia force becomes,

$$f = \rho dx A(x)\,(\partial^2 w(x,t)/\partial t^2) \qquad (3.2)$$

From Figure 3.3 the force equation in the vertical (Z) direction and Moment Equation about Y-axis could be

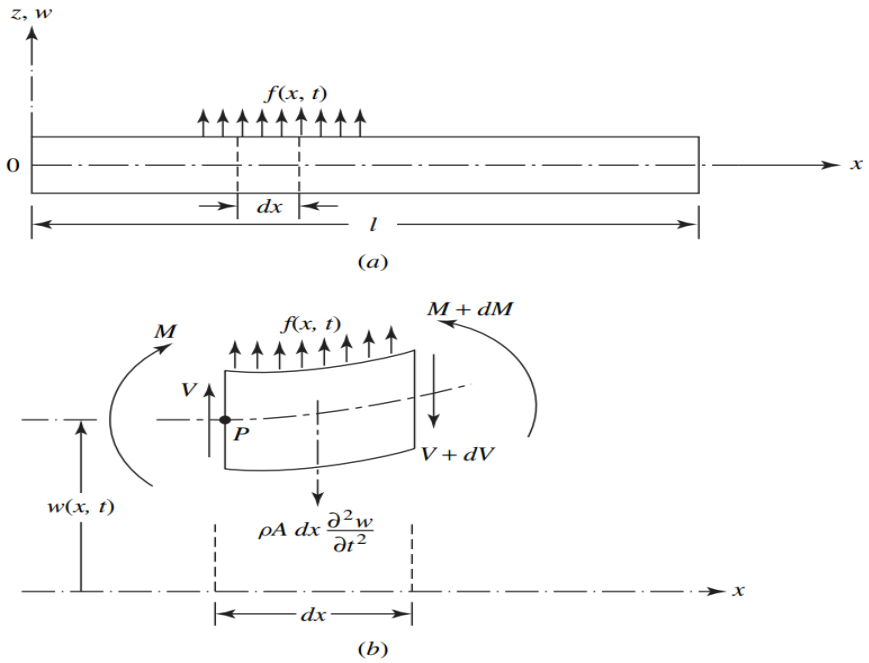

Figure 3.3 Transverse vibration of thin beams [33].

$$-(V + dV) + f(x,t)dx + V = \rho dx A(x)\,(\partial^2 w(x,t)/\partial t^2) \tag{3.3}$$

$$(M + dM) - (V + dV) + f(x,t)dx \times \frac{dx}{2} - M + Vdx = 0 \tag{3.4}$$

where $dV = \frac{\partial v}{\partial x}dx \quad dM = \frac{\partial M dx}{\partial x}$

$$dx\left(-\frac{\partial V(x,t)}{\partial x} + f(x,t)\right) = \rho dx A(x)\,(\partial^2 w(x,t)/\partial t^2) \tag{3.5}$$

Then dx can be canceled out the equation (3.6) becomes

$$-\frac{\partial V(x,t)}{\partial x} + f(x,t) = \rho A(x)\,(\partial^2 w(x,t)/\partial t^2) \tag{3.6}$$

From (3.6) disregarding terms involving second powers of dx since it's too small

$$\frac{\partial M dx}{\partial x} - Vdx + \frac{\partial V dx}{\partial x} + \frac{f(x,t)dxdx}{2} = 0 \tag{3.7}$$

This means

$$\frac{\partial M(x,t)}{\partial x} - V dx = 0 \tag{3.8}$$

Then by substitute equations (3.7) and (3.8)

$$\frac{\partial^2 M(x,t)}{\partial x^2} + f(x,t) = \rho A(x)\ (\partial^2 w(x,t)/\ \partial t^2) \tag{3.9}$$

From the elementary theory of bending beams (Euler- Bernoulli thin beam theory) the relationship between bending moment and deflection can be

where E is young's modulus and I(x) is the moment of inertia of beam cross-section about the X-axis

$$w(x,t) = EI(x)\frac{\partial^2 w(x,t)}{\partial x^2} \tag{3.10}$$

Form (3.9) and (3.10) the equation of transverse vibration of a uniform beam will be the following

$$\frac{\partial^2}{\partial x^2}\left[EI(x)\frac{\partial^2 w(x,t)}{\partial x^2}\right] + \rho A(x)\ (\partial^2 w(x,t)/\partial t^2) = f(x,t) \tag{3.11}$$

$$\left[EI(x)\frac{\partial^4 w(x,t)}{\partial x^4}\right] + \rho A(x)\ (\partial^2 w(x,t)/\partial t^2) = f(x,t) \tag{3.12}$$

For free-free vibration, external vibration assumed to be zero ($f(x,t) = 0$). So equation (3.12) becomes

$$\left[EI(x)\frac{\partial^4 w(x,t)}{\partial x^4}\right] + \rho A(x)\ (\partial^2 w(x,t)/\partial t^2) = 0$$

For uniform beam

$$\left[c^2\frac{\partial^4 w(x,t)}{\partial x^4}\right] +\ (\partial^2 w(x,t)/\ \partial t^2) = 0, \qquad \text{But} \ldots . c^2 = \frac{EI(x)}{\rho A(x)} \tag{3.13}$$

Using the separation of variables method the solution of free vibration become [33]

$$w(x,t) = W(x)T(t) \tag{3.14}$$

$$\left[c^2 \frac{\partial^4 W(x)T(t)}{\partial x^4}\right] + \frac{\partial^2 W(x)T(t)}{\partial t^2} = 0, \tag{3.15}$$

From (3.13) and (3.14)

$$\left[c^2 \frac{T(t)\,\partial^4 W(x)}{\partial x^4}\right] + \frac{W(x)\,\partial^2 T(t)}{\partial t^2} = 0,$$

$$\left[\frac{c^2}{w(x)} \frac{\partial^4 W(x)}{\partial x^4}\right] - \frac{\partial^2 T(t)}{T(t)\,\partial t^2} = 0$$

$$\left[\frac{c^2}{W(x)} \frac{\partial^4 W(x)}{\partial x^4}\right] = -\frac{\partial^2 T(t)}{T(t)\,\partial t^2} = a \tag{3.16}$$

Where, $a = \omega^2$ a is a positive constant

Equation (3.16) can be written in the two forms of equations (3.17) and (3.18)

$$\left[\frac{c^2}{W(x)} \frac{\partial^4 W(x)}{\partial x^4}\right] = a \tag{3.17}$$

$$-\frac{\partial^2 T(t)}{T(t)\,\partial t^2} = a \tag{3.18}$$

From (3.18)

$$\frac{d^4 W(x)}{dx^4} - \frac{a}{c^2}\big(W(x)\big) = 0 \tag{3.19}$$

From (3.19)

$$\frac{d^2 T(t)}{dt^2} - aT(t) = 0 \tag{3.20}$$

Let $\frac{a}{c^2} = \beta^4$, Equation (3.13)becomes

$$\frac{\omega^2}{c^2} = \beta^4 = \frac{\omega^2}{\left[\frac{EI}{\rho A}\right]} = \frac{\rho A \omega^2}{EI} \tag{3.21}$$

$$\frac{d^4 W(x)}{dx^4} - \beta^4 \big(W(x)\big) = 0 \tag{3.22}$$

The solution (3.19) can be written as from

$$T(t) = A\cos\omega(t) + B\sin\omega(t) \tag{3.23}$$

where, A and B are constants that can be found from the initials conditions in (3.23).

The solution of equation (3.16) is assumed to be from exponentials

$$W(x) = ce^{sx} \tag{3.24}$$

where, c and s are constants. We get by substituting (3.24) into (3.22).

$$\frac{d^4 ce^{sx}}{dx^4} - \beta^4 (ce^{sx}) = 0 \tag{3.25}$$

$$s^4 ce^{sx} - \beta^4 (ce^{sx}) = 0 \qquad \rightarrow s^4 - \beta^4 = 0 \tag{3.26}$$

So the roots of the equations (3.26) become

$$s_{1,2} = \pm\beta, s_{3,4} = \pm i\beta \tag{3.27}$$

So the solution of equation (3.17) is expressed as

$$W(x) = c_1 e^{\beta x} + c_2 e^{-\beta x} + c_3 e^{i\beta x} + c_4 e^{-i\beta x} \tag{3.28}$$

where c_1, c_2, c_3, c_4 are constants

Form equation (3.28) W(x) can be expressed by sine and cosine functions

$$W(x) = c_1(\cos\beta x + \cosh\beta x) + c_2(\cos\beta x - \cosh\beta x) + c_3(\sin\beta x + \sinh\beta x) + c_4(\sin\beta x - \sinh\beta x) \tag{3.29}$$

From $\beta^4 = \frac{\rho A \omega^2}{EI}$

$$\omega^2 = \frac{EI\beta^4}{\rho A} = \omega = \beta^2\sqrt{EI/\rho A} = (\beta l)^2\sqrt{EI/\rho A l^4} \tag{3.30}$$

$\omega, W(x)$, is the natural frequency vibration of the beam and normal mode (characteristics of the beams) respectively.

For any beam, there will be an infinite number of normal modes with one natural frequency associated with it. The value of c_1 to $c_4$is determined from the boundary conditions equation (3.31). Since the railway car is assumed as a free-free end at both ends take both free ends as boundary conditions.

The boundary condition is stated in equation (3.31).

$$\begin{aligned} \frac{EId^2W(0)}{dx^2} &= 0 & \frac{d^2W(0)}{dx^2} &= 0 \\ \frac{EId^3W(0)}{dx^3} &= 0 & \frac{d^3W(0)}{dx^3} &= 0 \\ \frac{EId^2W(l)}{dx^2} &= 0 & \frac{d^2W(l)}{dx^2} &= 0 \\ \frac{EI3W(l)}{dx^3} &= 0, & \frac{d^3W(l)}{dx^3} &= 0 \end{aligned} \tag{3.31}$$

Since at free end bending moment and shear force are zero by differentiating (3.22) for boundary equations (3.31) it yields (3.32)

$$\begin{aligned} \frac{d^2W(x)}{dx^2} = \beta^2 \; [&c_1(-\cos\beta x + \cosh\beta x) + c_2(-\cos\beta x - \cosh\beta x) \\ &+ c_3(\sin\beta x + \sinh\beta x) + c_4(-\sin\beta x - \sinh\beta x)] \end{aligned} \tag{3.32}$$

$$\frac{d^3W(x)}{dx^3} = \beta^3 [c_1(\sin\beta x + \sinh\beta x) + c_2(\sin\beta x - \sinh\beta x) + c_3(-\cos\beta x + \cosh\beta x) + c_4(-\cos\beta x - \cosh\beta x)] \quad (3.33)$$

$$\text{For } \frac{d^2W(x)}{dx^2} = 0, \text{gives } c_2 = 0$$

$$\frac{d^3W(0)}{dx^3} = 0, c_4 = 0 \quad (3.34)$$

$$\text{So at } x = 0, c_2 \text{ and} c_4 = 0$$

For a non-trivial solution of the constants, C_1 and C_3 since the Eigen mode functions is orthogonal, the determinant formed by coefficients are equal to zero.

$$\frac{d^2w(l,t)}{dx^2} = 0 = c_1(-\cos\beta l + \cosh\beta l) + c_3(\sin\beta l + \sinh\beta l) \quad (3.35)$$

$$\frac{d^3w(l,t)}{dx^3} = 0 = c_3(-\cos\beta l + \cosh\beta l) + c_1(\sin\beta l + \sinh\beta l)$$

The above equation (3.35) when expressed in matrices form

$$\begin{bmatrix} c_1 \\ c_3 \end{bmatrix} \begin{bmatrix} -\cos\beta l + \cosh\beta l & \sin\beta l + \sinh\beta l \\ \sin\beta l + \sinh\beta l & -\cos\beta l + \cosh\beta l \end{bmatrix} = 0 \quad (3.36)$$

Since the Eigen function is assumed to be orthogonal this determinant of equation (3.36) is equal to zero

$$\det \begin{bmatrix} -\cos\beta l + \cosh\beta l & \sin\beta l + \sinh\beta l \\ \sin\beta l + \sinh\beta l & -\cos\beta l + \cosh\beta l \end{bmatrix} = 0 \quad (3.37)$$

$$\cos\beta l \cosh\beta l - 1 = 0 \quad (3.38)$$

Value of $\beta_o l = 0$ for rigid body mode in case of free - free beam

So for i^{th} mode shape of the beam can be expressed as

$$c_1(-\cos\beta l + \cosh\beta l) + c_3(\sin\beta l + \sinh\beta l) = 0 \quad (3.39)$$

$$c_3(-\cos\beta l + \cosh\beta l) + c_1(\sin\beta l + \sinh\beta l) = 0 \quad (3.40)$$

From equations (3.39) and (3.40)

$$c_1 = c_3 \frac{(\sin\beta l + \sinh\beta l)}{(-\cos\beta l + \cosh\beta l)} \quad (3.41)$$

$$= -c_3 \frac{(-\sin\beta l + \sinh\beta l)}{-\cos\beta l + \cosh\beta l} + c_3(-\sin\beta l + \sinh\beta l)$$

From equation (3.41) and (3.29)

$$W_k(x) = (\sin\beta ix + \sinh\beta ix) - (\sin\beta l - \sinh\beta l)/(\cos\beta l - \cosh\beta l)(\cos\beta l - \cosh\beta l \quad (3.42)$$

where, equations (3.42) indicate the modal shape functions at k mode of bending carbody, which it simplified form is described below

$$W_k(x) = \sin\beta_k x + \sin h\beta_k x - \frac{(\sin\beta_k l - \sin h\beta_k l)}{\cos\beta_i l - \cos h\beta_k l}(\cos\beta_k x - \cos h\beta_k x) \quad (3.43)$$

3.1.3. Equations of motion of passenger rail vehicle

The vertical motion of the vehicle is described by both the equations of bogie bounce and pitch, vibration rigid modes in the car body and the equation of the first and second mode of vertical bending of the car body.

The equation of motion of flexible the rail car body in the vertical direction [2, 34–37] presented in Figure 3.1 is given by:

$$EI(\partial^4 \frac{w(x,t)}{\partial x^4}) + \mu I \frac{\partial^5 w(x,t)}{\partial x^4 \partial t} + m \frac{\partial^2 w(x,t)}{\partial t^2} = \sum_{k=1}^{2} F_k \delta(x - l_k) \quad (3.44)$$

Since the higher order modes of frequency have less impact on the vibration response only the first two bending modes that are symmetrical and anti-symmetrical carbody bending vibration movements are considered.

By substituting equation 3.1 into 3.44 , applying the separation of variables method, and considering the orthogonal property of the Eigen function in the car body vertical bending [30], the equation of motion turns into three two-order differential equations with ordinary derivatives

$$m_c \ddot{z}_c = \sum_{i=1}^{2} F_{zck} \tag{3.45}$$

$$J_c \ddot{\theta}_c = \sum_{k=1}^{2} F_{zck}(l_k - \frac{L}{2}) \tag{3.46}$$

$$m_{mk}\ddot{T}_c + c_{mk}\dot{T}_c + k_{mk}T_c = \sum_{i=1}^{2} F_{zck} W_c(l_k) \tag{3.47}$$

where stiffness, damping, and the car body modal mass are given as follows.

$$k_{m2,3} = EI \iint_0^L \frac{d^2 W_c}{dx^2} dx, c_{m2,3} = \mu I \iint_0^L (\frac{d^2 W_k}{dx^2})^2 dx, m_{m2,3} = m \int_0^L {W_k}^2 dx \tag{3.48}$$

$m_{m2,3}, c_{m2,3}$, and $k_{m2,3}$, are the mass, damping, and stiffness of the second and third mode of carbody bending respectively.

Where, EIis bending module, m mass on length unit and $'\mu'$ damping coefficient, $w(x,t)$ is displacement of a beam section $('t')$ is time, δ (.) is Dirac's delta function, and F_k represents the force due to the secondary bogie suspension.

$$F_k = -2K_{zc}(w(l_1,t) - Z_{b1}) - 2C_{zc}\left(w(l_1,t) - \dot{Z}_{b1}\right) - 2K_{zc}(w(l_2,t) - Z_{b2}) - 2C_{zc}\left(w(l_2,t) - \dot{Z}_{b2}\right) \tag{3.49}$$

This force acts at the distancel_k from the car body end

Derivations of the equations of pitch and bounce for rigid carbody as well as for rigid bogie can be expressed as follows

1. Equation of motion of carbody for translation in the vertical direction

$$m_c\ddot{Z}_c = F_1 + F_2 \tag{3.50}$$

where,

$$F_2 = -2K_{zc}(w(l_1,t) - Z_{b2}) - 2C_{zc}\left(w(l_2,t) - \dot{Z}_{b2}\right)$$

$$F_1 = -2K_{zc}(w(l_1,t) - Z_{b1}) - 2C_{zc}\left(w(l_1,t) - \dot{Z}_{b1}\right)$$

F_1 and F_2 are the secondary suspension force due to bounce motion of front bogie and rear bogie respectively.

$$m_c\ddot{Z}_c = -2K_{zc}(w(l_1,t) - Z_{b1}) - 2C_{zc}\left(w(l_1,t) - \dot{Z}_{b1}\right) - 2K_{zc}(w(l_2,t) - Z_{b2}) - 2C_{zc}\left(w(l_2,t) - \dot{Z}_{b1}\right)) \tag{3.51}$$

2. Equation of motion for rotation of the carbody

$$J_c\ddot{\theta}_c = F_1 a_c + F_2 a_c \tag{3.52}$$

$$J_c\ddot{\theta}_c = \left(-2K_{zc}(w(l_1,t) - Z_{b1}) - 2C_{zc}\left(w(l_1,t) - \dot{Z}_{b1}\right)\right) a_c + \left(-2K_{zc}(w(l_2,t) - Z_{b2}) - 2C_{zc}\left(w(l_2,t) - \dot{Z}_{b2}\right)\right) a_c \tag{3.53}$$

3. Equation of motion of front and rear bogies in the vertical direction
   F_3 and F_4 are Right and left wheel bounce forces for front bogies and F_5 and F_6 are right and left bounce forces for rear bogies

$$F_3 = -2K_{zb}(Z_{b1} - \xi_1) - 2C_{zb}\left(\dot{Z}_{b1} - \dot{\xi}_1\right) \tag{3.54}$$

$$F_4 = -2K_{zb}(Z_{b1} - \xi_2) - 2C_{zb}\left(\dot{Z}_{b1} - \dot{\xi}_2\right) \tag{3.55}$$

$$F_5 = -2K_{zb}(Z_{b2} - \xi_3) - 2C_{zb}\left(\dot{Z}_{b2} - \dot{\xi_3}\right) \tag{3.56}$$

$$F_6 = -2K_{zb}(Z_{b2} - \xi_4) - 2C_{zb}\left(\dot{Z}_{b2} - \dot{\xi_4}\right) \tag{3.57}$$

$$m_b \ddot{z_{b1}} = F_1 - F_3 - F_4 \tag{3.58}$$

$$m_b \ddot{z}_{b1} = 2K_{zc}(w(l_1,t) - Z_{b1}) + 2C_{zc}\left(w(l_1,t) - \dot{Z}_{b1}\right) - 2K_{zb}(Z_{b1} - \xi_1) - 2C_{zb}\left(\dot{Z}_{b1} - \dot{\xi_1}\right) - 2K_{zb}(Z_{b1} - \xi_2) - 2C_{zb}\left(\dot{Z}_{b1} - \dot{\xi_2}\right) \tag{3.59}$$

$$m_b \ddot{z}_{b2} = F_2 - F_5 - F_6 \tag{3.60}$$

$$m_b \ddot{z}_{b2} = 2K_{zc}(w(l_2,t) - Z_{b2}) + 2C_{zc}\left(w(l2,t) - \dot{Z_{b2}}\right) - 2K_{zb}(Z_{b2} - \xi_3) - 2C_{zb}\left(\dot{Z_{b1}} - \dot{\xi_3}\right) - 2K_{zb}(Z_{b2} - \xi_4) - 2C_{zb}\left(\dot{Z_{b1}} - \dot{\xi_4}\right) \tag{3.61}$$

$$\text{let } Z_{b1} + Z_{b2} = Z_{b1,2}, \dot{Z}_{b1} + \dot{Z}_{b2} = \dot{Z}_{b1,2}, \ddot{z}_{b1} + \ddot{z}_{b2} = \ddot{z}_{b1,2}, w(l_1,t) + w(l_2,t) = w\left(l_{1,2},t\right), \xi_1 + \xi_3 = \xi_{1,3}, \dot{\xi_1} + \dot{\xi_3} = \dot{\xi_{1,3}}, \xi_2 + \xi_4 = \xi_{2,4} \tag{3.62}$$

$$m_b \ddot{z}_{b1,2} = -2C_{zb}\left(2\dot{Z}_{b1,2} - (\dot{\xi_{1,3}} + \dot{\xi_{2,4}}\right) - 2K_{zb}\left(2Z_{b1,2} - (\xi_{1,3} + \xi_{2,4})\right) + 2C_{zc}\left(w\left(l_{1,2},t\right) - \dot{Z}_{b1,2}\right) + 2K_{zc}\left(w\left(l_{1,2},t\right) - Z_{b1,2}\right) \tag{3.63}$$

4. Equation of motion for the pitch of the bogies

F_7 and F_8 are Right and left wheel pitch forces for front bogies and F_9 and F_{10} are right and left pitch forces for rear bogies.

$$J_b \ddot{\theta}_{b1} = F_7 a_b - F_8 a_b \tag{3.64}$$

$$F_7 = -2K_{zb}(a_b\theta_{b1} - \xi_2) - 2C_{zb}\left(a_b\dot{\theta}_{b1} - \dot{\xi_2}\right) \tag{3.65}$$

$$F_8 = -2K_{zb}(a_b\theta_{b1} - \xi_1) - 2C_{zb}\left(a_b\dot{\theta}_{b1} - \dot{\xi_1}\right) \tag{3.66}$$

$$F_9 = -2K_{zb}(a_b\theta_{b2} - \xi_4) - 2C_{zb}\left(a_b\dot{\theta}_{b2} - \dot{\xi_4}\right) \tag{3.67}$$

$$F_{10} = -2K_{zb}(a_b\theta_{b2} - \xi_3) - 2C_{zb}\left(a_b\dot{\theta}_{b2} - \dot{\xi_3}\right) \tag{3.68}$$

$$J_b\ddot{\theta}_{b1} = F_7a_b - F_8a_b \tag{3.69}$$

$$\begin{aligned} J_b\ddot{\theta}_{b1} = a_b\left(-2K_{zb}(a_b\theta_{b1} - \xi_2) - 2C_{zb}\left(a_b\dot{\theta}_{b1} - \dot{\xi_2}\right)\right) \\ - a_b(-2K_{zb}(a_b\theta_{b1} - \xi_1) - 2C_{zb}\left(a_b\dot{\theta}_{b1} - \dot{\xi_1}\right)) \end{aligned} \tag{3.70}$$

$$J_b\ddot{\theta}_{b2} = F_9a_b - F_{10}a_b \tag{3.71}$$

$$\begin{aligned} J_b\ddot{\theta}_{b2} = a_b\left(-2K_{zb}(a_b\theta_{b2} - \xi_4) - 2C_{zb}\left(a_b\dot{\theta}_{b2} - \dot{\xi_4}\right)\right) \\ - a_b(-2K_{zb}(a_b\theta_{b2} - \xi_3) - 2C_{zb}\left(a_b\dot{\theta}_{b2} - \dot{\xi_3}\right) \end{aligned} \tag{3.72}$$

$$\text{let}, \theta_{b1} + \theta_{b2} = \theta_{b1,2}, \qquad \dot{\theta}_{b1} + \dot{\theta}_{b2} = \dot{\theta}_{b1,2} \qquad \ddot{\theta}_{b1} + \ddot{\theta}_{b2} = \ddot{\theta}_{b1,2}$$

$$J_b\ddot{\theta}_{b1,2} = -2a_bK_{zb}\left(2a_b\theta_{b1,2} + \xi_{1,3} - \xi_{2,4}\right) - 2a_bC_{zb}\left(2a_b\dot{\theta}_{b2} + \dot{\xi_{1,3}} - \dot{\xi_{2,4}}\right) \tag{3.73}$$

Finally, the equations of motions for the bounce of bogies and pitch of bogies become the following,

$$\begin{aligned} m_b\ddot{z}_{b1,2} + 2C_{zb}(2\dot{z}_{b1,2} - \dot{\xi}_{1,3} - \dot{\xi}_{2,4}) + 2K_{zb}(2Z_{b1,2} - \xi_{1,3} - \xi_{2,4}) \\ + 2Czc\left[\dot{z}_{b1,2} - \frac{\partial w(l_{1,2}, t)}{\partial t}\right] + 2Kzc\left[Z_{b1,2} - \partial w(l_{1,2}, t)\right] = 0 \end{aligned} \tag{3.74}$$

$$J_b\ddot{\theta}_{b1,2} + 2Czb\ a_b\left(2a_b\ \dot{\theta}_{b1,2} - \dot{\xi}_{1,3} - \dot{\xi}_{2,4}\right) + 2k_{zb}a_b\left(2a_b\ \dot{\theta}_{b1,2} - \xi_{1,3} - \xi_{2,4}\right) \tag{3.75}$$

The mass of a bogie is m_b and its inertia moment$J_b = m_bi_b{}^2$, where 'i_b' is the bogie gyration radius.

By substituting the (3.76) below into (3.51),(3.50),(3.74),(3.75). Those four coupled equations above decoupled into six independent equations as follows

$$s_1 = Z_c; a_1 = \theta_c; s_2 = T_2\ ; a_2 = T_3; s_3 = \frac{1}{2}(Z_{b1} + Z_{b2});$$

$$a_3 = \frac{1}{2}(\theta_{b1} - \theta_{b2});$$

$$W_2(l_1) = W_2(l_2) = u; W_3(l_1) = -W_3(l_2) = v \tag{3.76}$$

The movement equation at center carbody ($\theta_c(t) = 0$) from (3.1) becomes

$$W(x,t) = Z_c(t) + \sum_{k=1}^{\infty} W_k(x)T_k(t) \tag{3.77}$$

For the case we only consider the second and third modes. Then we can write the bending equation for center of carbody.

$$W(x,t) = Z_c(t) + W_2(x)T_2(t) \tag{3.78}$$

$$W(x,t) = Z_c(t) + W_3(x)T_3(t) \tag{3.79}$$

From the equation of car body equation (3.54), (3.79), and (3.81)

$$\begin{aligned} m_c\ddot{Z_c} &= -2K_{zc}(w(l_1,t)+w(l_2,t) - (Z_{b1} + Z_{b2})) \\ &\quad - 2C_{zc}\big(w(l_1,t) + w(l_2,t) - (\dot{Z}_{b1} + \dot{Z}_{b2})\big) \\ &= -2K_{zc}\big(2\big(z_c(t) + W_2(l)T_2(t)\big) - (Z_{b1} + Z_{b2})\big) \\ &\quad - 2C_{zc}\big(2\big(\dot{z}_c(t) + W_2(l)\dot{T}_2(t)\big) - (\dot{Z}_{b1} + \dot{Z}_{b2})\big) \end{aligned}$$

$$m_c\ddot{s_1} = -4C_{zc}(\dot{s_1} + u\dot{s_2} - \dot{s_3}) - 4K_{zc}(s_1 + us_2 - s_3) \tag{3.80}$$

From equation (3.47) and (3.76)

It becomes

$$\begin{aligned} m_{m2}\ddot{s_2} = &-C_{m2}\dot{s_2} - C_{m2}s_2 - 4C_{zc}(\dot{s_1} + u\dot{s_2} - \dot{s_3}) \\ &-4K_{zc}(s_1 + us_2 - s_3) \end{aligned} \tag{3.81}$$

For bogie bounce motion from equations (3.66), (3.76), and (3.78).

$$m_b\ddot{z}_{b1,2} = -2C_{zb}\big(2\dot{z_{b1,2}} - (\dot{\xi}_{1,3} + \dot{\xi}_{2,4}\big) - 2K_{zb}\big(2Z_{b1,2} - (\xi_{1,3} + \xi_{2,4})\big)$$

$$+2C_{zc}\left(w\left(l_{1,2},t\right)-\dot{Z_{b1,2}}\right)+2K_{zc}\left(w\left(l_{1,2},t\right)-Z_{b1,2}\right)$$

$$m_{m2}\ddot{s_3}=-2C_{zb}\left(\dot{s_3}-\dot{\xi}\right)-2K_{zb}(s_3-\xi)-2C_{zc}(\dot{s_1}+u\dot{s_2}-\dot{s_3})-2K_{zc}(s_1+us_2-s_3) \quad (3.82)$$

For pitch movement from equations (3.1), (3.56), and (3.79)

$$J_c\ddot{\theta}_c=\left(-2K_{zc}(w(l1,t)-Z_{b1})-2C_{zc}\left(w(l1,t)-\dot{Z}_{b1}\right)\right)a_c+\left(-2K_{zc}(w(l2,t)-Z_{b2})-2C_{zc}\left(w(l2,t)-\dot{Z}_{b2}\right)\right)a_c.$$

$$J_c\ddot{a_1}=-2C_{zc}a_c(a_c\dot{a_1}-v\dot{a_2}+\dot{a_3})-2K_{zc}a_c(a_c\dot{a_1}-v\dot{a_2}+\dot{a_3}) \quad (3.83)$$

From equation (3.47), (3.79), and (3.82)

$$EI(\partial^4\frac{w\,(x,t)}{\partial x^4})+\mu I\frac{\partial^5 w\,(x,t)}{\partial x^4\,\partial t}+m\frac{\partial^2 w\,(x,t)}{\partial t^2}=$$
$$-2K_{zc}(w(l1,t)-Z_{b1})-2C_{zc}\left(w(l1,t)-\dot{Z_{b1}}\right)-2K_{zc}(w(l2,t)-Z_{b2})-2C_{zc}\left(w(l2,t)-\dot{Z_{b2}}\right)$$
$$m_{m3}\ddot{a_2}=-C_{m3}\dot{a_2}-k_{m3}a_2+2C_{zc}a_c(a_c\dot{a_1}-v\dot{a_2}+\dot{a_3})+2a_cK_{zc}(a_ca_1-va_2+a_3) \quad (3.84)$$

From equation (3.76) and (3.79)

$$J_b\ddot{\theta}_{b1,2}=-2a_bK_{zb}\left(2a_b\theta_{b1,2}+\xi_{1,3}-\xi_{2,4}\right)-2a_bC_{zb}\left(2a_b\dot{\theta}_{b2}+\dot{\xi}_{1,3}-\dot{\xi}_{2,4}\right)$$

$$J_b\ddot{a_3}=-4C_{zb}a_b\left(a_b\dot{a_3}-\dot{\xi^-}\right)-4K_{zb}a_b(a_ba_3-\xi^-)+4C_{zc}a_c(a_c\dot{a_1}-v\dot{a_2}-\dot{a_3})+4K_{zc}a_c(a_ca_1-va_2-a_3) \quad (3.85)$$

The independent carbody bounce, carbody bending mode, bogie bounce equations due to symmetrical excitations of the track that derived in (3.80),(3.81), and(3.82)

$$m_c\ddot{s_1}+4c_{zc}(\dot{s_1}+u\dot{s_2}-\dot{s_3})+4K_{zc}(s_1+us_2-s_3)=0$$

$$m_{m2}\ddot{s_2}+C_{m2}\dot{s_2}+C_{m2}s_2+4C_{zc}(\dot{s_1}+u\dot{s_2}-\dot{s_3})+4K_{zc}(s_1+us_2-s_3)=0$$

$$m_b\ddot{s}_3 + 4C_{zb}\left(\dot{s}_3 - \dot{\xi}^{+}\right) + 4K_{zb}(s_3 - \xi^{+}) - 4C_{zc}(\dot{s}_1 + u\dot{s}_2 - \dot{s}_3) - 4K_{zc}(s_1 + us_2 - s_3) = 0$$

The independent carbody pitch, carbody bending mode and bogie pitch due to anti-symmetrical excitations of the track from (3.83),(3.84) and (3.85).

$$J_c\ddot{a}_1 + 4C_{zc}a_c(a_c\dot{a}_1 - v\dot{a}_2 + \dot{a}_3) + 4K_{zc}a_c(a_c a_1 - va_2 + a_3)$$

$$m_{m3}\ddot{a}_2 + C_{m3}\dot{a}_2 + k_{m3}a_2 + 4C_{zc}v(-\dot{a}_1 + v\dot{a}_2 - \dot{a}_3) + 4K_{zc}v(-a_1 + va_2 - a_3) = 0$$

$$J_b\ddot{a}_3 + 4C_{zb}\left(\dot{a}_3 - \dot{\xi}_1^{-}\right) + 4K_{zb}(a_3 - \xi_1^{-}) + 4C_{zc}a_c(\dot{a}_3 - v\dot{a}_2 - a_c\dot{a}_1) + 4K_{zc}a_c(a_3 - va_2 - a_c a_1) = 0$$

, where $m_c$and $J_c = m_c ic^2$ are the car body mass and inertia moment with i_c its gyration radius and.

State-space formulations

The motion equations for the car body and bogies make up a seven-equation system with ordinary derivatives. The system can be matrix-like, written where **M, C, K,** are inertia damping and stiffness matrices **P** and **R,** are displacement and velocity input matrices, with **Zw** the vector of heterogeneous terms

$$M\ddot{q} + C\dot{q} + Kq = P\left[\dot{\xi}\right] + R[\xi] \tag{3.86}$$

Generalized state space form linear equations

$$A\dot{Z} + BZ = F(t)$$

Note that the second order differential equations is changed to first order differential equation in order to solve analytically

Then final equation is reduced to

$$A = \begin{bmatrix} C & M \\ M & 0 \end{bmatrix}, \qquad B = \begin{bmatrix} K & 0 \\ 0 & -M \end{bmatrix}, \text{and } F = \begin{bmatrix} P(t) \\ \dot{P}(t) \end{bmatrix}$$

where,

$$M1 = \begin{bmatrix} m_c & 0 & 0 \\ 0 & m_{m2} & 0 \\ 0 & 0 & m_b \end{bmatrix}; C1 = \begin{bmatrix} 4C_{zc} & 0 & 0 \\ 0 & 4C_{zc}v + C_{m2} & 0 \\ 0 & 0 & 4C_{zb} + 4C_{zc} \end{bmatrix};$$

$$K1 = \begin{bmatrix} 4K_{zc} & 0 & 0 \\ 0 & 4K_{zc}v + K_{m2} & 0 \\ 0 & 0 & 4K_{zb} + 4K_{zc} \end{bmatrix}; P1 = \begin{bmatrix} 0 \\ 0 \\ -4C_{zb} \end{bmatrix}; R1 = \begin{bmatrix} 0 \\ 0 \\ -K_{zb} \end{bmatrix}$$

$$M2 = \begin{bmatrix} J_c & 0 & 0 \\ 0 & m_{m3} & 0 \\ 0 & 0 & J_b \end{bmatrix};$$

C2

$$= \begin{bmatrix} 4C_{zc}{a_c}^2 - 4C_{zc} - 4C_{zc}a_c & 0 & 0 \\ 0 & -4C_{zc}a_c v - 4C_{zc}(v)^2 - 4C_{zc}v + C_{m3} & 0 \\ 0 & 0 & 4C_{zc}a_c + 4C_{zc}v + 4C_{zb} + 4C_{zc} \end{bmatrix}$$

$$\mathbf{K2} = \begin{bmatrix} 4K_{zc}{a_c}^2 - 4K_{zc}V - 4K_{zc}a_c & 0 & 0 \\ 0 & -4K_{zc}a_c V - 4K_{zc}(V)^2 - 4K_{zc}V + C_{m3} & 0 \\ 0 & 0 & 4K_{zc}a_c + 4K_{zc}V + 4K_{zb} + 4k_{zc} \end{bmatrix}$$

$$\dot{P2} = \begin{bmatrix} 0 \\ 0 \\ -4C_{zb} \end{bmatrix}; P2 = \begin{bmatrix} 0 \\ 0 \\ -4K_{zb} \end{bmatrix};$$

$$M = M1 + M2 = \begin{bmatrix} m_c & 0 & 0 & 0 & 0 & 0 \\ 0 & m_{m2} & 0 & 0 & 0 & 0 \\ 0 & 0 & m_b & 0 & 0 & 0 \\ 0 & 0 & 0 & J_c & 0 & 0 \\ 0 & 0 & 0 & 0 & m_{m3} & 0 \\ 0 & 0 & 0 & 0 & 0 & J_b \end{bmatrix}$$

$$\mathbf{C} = \begin{bmatrix} 4C_{zc} & 0 & 0 & 0 & 0 & 0 \\ 0 & 4c_{zc}u + C_{m2} & 0 & 0 & 0 & 0 \\ 0 & 0 & 4C_{zb} + 4C_{zc} & 0 & 0 & 0 \\ 0 & 0 & 0 & 4C_{zc}a_c{}^2 - 4C_{zc}\mathbf{V} - 4C_{zc}a_c & 0 & 0 \\ 0 & 0 & 0 & 0 & -4c_{zc}a_c v - 4c_{zc}(\mathbf{V})^2 - 4C_{zc}\mathbf{V} + C_{m3} & 0 \\ 0 & 0 & 0 & 0 & 0 & 4C_{zc}a_c + 4C_{zc}\mathbf{V} + 4C_{zb} + 4C_{zc} \end{bmatrix}$$

$$\dot{P} = \begin{bmatrix} 0 \\ 0 \\ 0 \\ 0 \\ 0 \\ -4K_{zb} \end{bmatrix} [\dot{\xi}_1 \quad \dot{\xi}_2]; R = \begin{bmatrix} 0 \\ 0 \\ 0 \\ 0 \\ 0 \\ -4K_{zb} \end{bmatrix} [\xi_1 \quad \xi_2];$$

$$\mathbf{K} = \begin{bmatrix} 4K_{zc} & 0 & 0 & 0 & 0 & 0 \\ 0 & 4K_{zc}u + K_{m2} & 0 & 0 & 0 & 0 \\ 0 & 0 & 4K_{zb} + 4K_{zc} & 0 & 0 & 0 \\ 0 & 0 & 0 & 4K_{zc}a_c{}^2 - 4K_{zc}\mathbf{V} - 4K_{zc}a_c & 0 & 0 \\ 0 & 0 & 0 & 0 & -4K_{zc}a_c\mathbf{V} \quad -4K_{zc}(\mathbf{V})^2 - 4K_{zc}\mathbf{V} + k_{m3} & 0 \\ 0 & 0 & 0 & 0 & 0 & 4K_{zc}a_c + 4K_{zc}\mathbf{V} + 4K_{zb} + 4k_{zc} \end{bmatrix}$$

The below equations include the excitation mode of symmetrical and the anti-symmetrical movements

$$\xi^{+} = \frac{(\xi_1{}^{+} + \xi_2{}^{+} + \xi_3{}^{+} + \xi_4{}^{+})}{4}, \xi^{-} = \frac{(\xi_1{}^{-} + \xi_2{}^{-} - \xi_3{}^{-} - \xi_4{}^{-})}{4}, \tag{3.87}$$

The parameters of the car body bending vibration are the modal angular frequency and the damping ratio.

$$\omega_{m2,3} = \sqrt{\frac{k_{m2,3}}{m_{m2,3}}}, \zeta_{m2,3} = \frac{c_{m2,3}}{2\sqrt{k_{m2,3}m_{m2,3}}} \tag{3.88}$$

To facilitate the analysis of vibrations, the damping ratio of the suspension levels is considered uncoupled, as below

$$\zeta_{b,c} = \frac{c_{b,c}}{\sqrt{k_{b,c}m_{b,c}}} \tag{3.89}$$

3.2. Track irregularities

The irregularities of AALRT‟s track are always measured along the line Easter-West (Ayat-Torhailoch) and North-South (Kalit-Menelick II) lines. If they find during the measurement the worse deviation from the company standards, in the night the maintenance of the track should be done on that track portion. In this work, only the vertical ride comfort of AALRTS vehicle is considered. The sample of rail irregularities used is shown in Figure 3.4and Figure 3.5 for the AALRT track.

The plot had 122 points measured during inspection and maintenance by AALRT at a distance interval of 5m for each measurement. During inspection track level on up line segment, the acceptance standard limit from reference rail is 0.004m.

The graph plotted using sampled irregularities was at a distance of 500 m. To use them as irregularities inputs for the vibration equation of rail vehicle using MATLAB, the graph was divided into 1000 segments and imported in MATLAB main code to simulate the vibration responses of the vehicle (Appendix C Figure c. 2and Figure c. 3). These segments allow the wheels to follow the path of the irregularities. Therefore, this helps the wheels to follow all the points along with the irregularities. The track excitations inputs are designed according to delay and wheel base and bogie base.

For the vehicle model in the Figure 3.1, the track excitations inputs vector is

$$\xi_k(t) = \begin{pmatrix} \xi_1(t) \\ \xi_2(t) \\ \xi_3(t) \\ \xi_4(t) \end{pmatrix} = \begin{pmatrix} \xi_1(t) \\ \xi_2(t-\phi_1) \\ \xi_3(t-\phi_2) \\ \xi_4(t-\phi_3) \end{pmatrix} \tag{3.90}$$

Where $\phi_1 = \frac{2a_b}{v}; \phi_2 = \frac{2a_c}{v}; \phi_3 = (2a_b + 2a_c)/v$ and v is the longitudinal running velocity of the vehicle.

(a) (b)

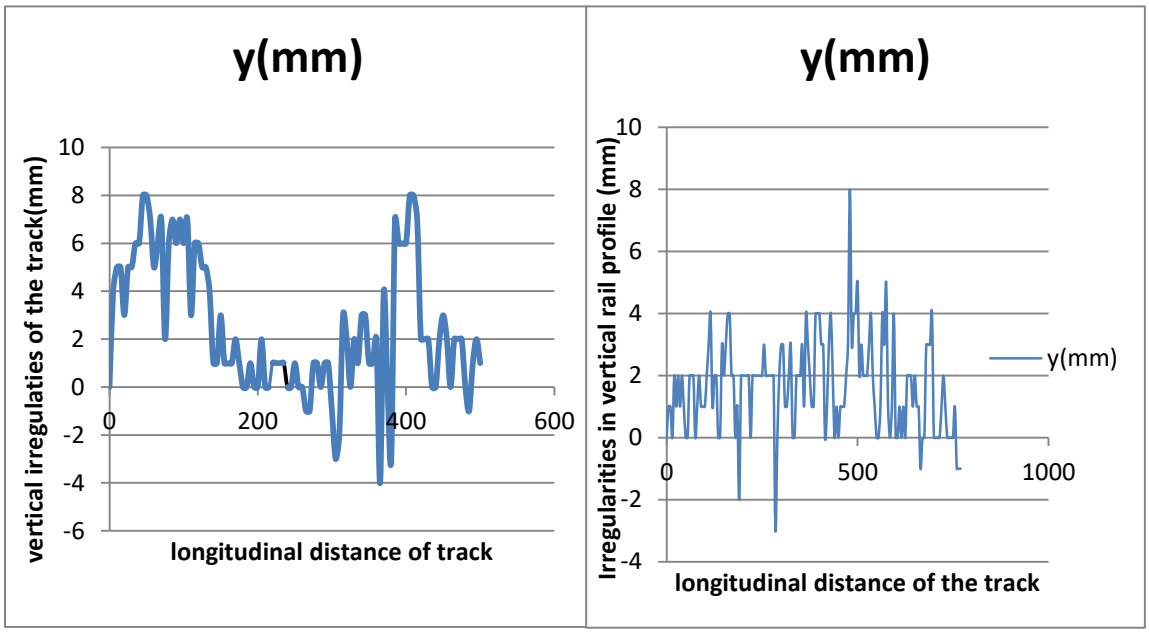

Figure 3.4 the measured vertical track irregularities of AALRT at a) north-south and b) East-west lines

3.3. Ride comfort Evaluations

There are many different evaluations standards in the world from them Sperling ride index is briefly discussed here.

3.3 .1 Sperling's Method

As Sperling's method is concerned; the passengers' perception of the vibrations occurring during the running of the railway vehicle is based on the comfort index Wz. The scale of values of the comfort index Wz and the significance of each value is featured in Table3.1. Assuming that the spectrum of accelerations is a continuous frequency function and the energy of vibrations is concentrated between 0.5 and 30 Hz, the following. Figure 3.6 shows the frequency weighting function and highlights the fact that the higher sensitivity of the human body to vertical vibrations is manifested in the frequency interval of 3 to 7 Hz [11]. Equation 3.90 can be used to calculate the comfort index Wz,

a)

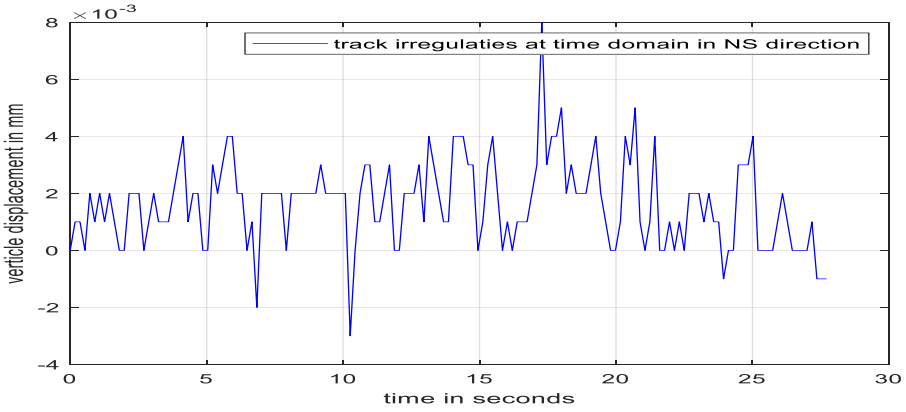

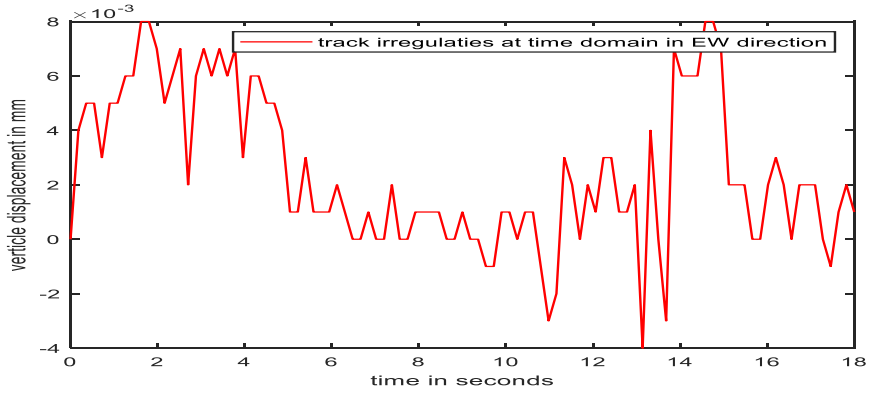

b)

Figure 3.5 vertical displacements of track irregularities in time domain a)E-W direction track irregularities b) N-S line vertical track irregularities

$$W_z = \sqrt[10]{\int_{0.5}^{30} a^3(f)B^3(f)df} \tag{3.91}$$

where a is the acceleration amplitude in cm/s ^{2}, B represents the frequency weighting function that expresses human vibration sensitivity, and f= ω/2π

To assess the ride comfort at the vertical vibrations, the weighting function B comes from

$$B(f) = 0.588\sqrt{\frac{1.911f^2 + (0.25f^2)^2}{(1 - 0.277f^2)^2 + (1.563f - 0.0368f^3)^2}} \tag{3.92}$$

Table3. 1 Scale for the ride comfort index Wz[31].

Ride comfort index Wz	Vibration sensitivity
1.0	Just noticeable
2.0	Clearly noticeable
2.5	More pronounced, but not unpleasant
3.0	Strong irregular, but still tolerable
3.25	Very irregular
3.5	Extremely irregular, unpleasant, and annoying prolonged exposure intolerable
4.0	Extremely unpleasant; prolonged exposure harmful

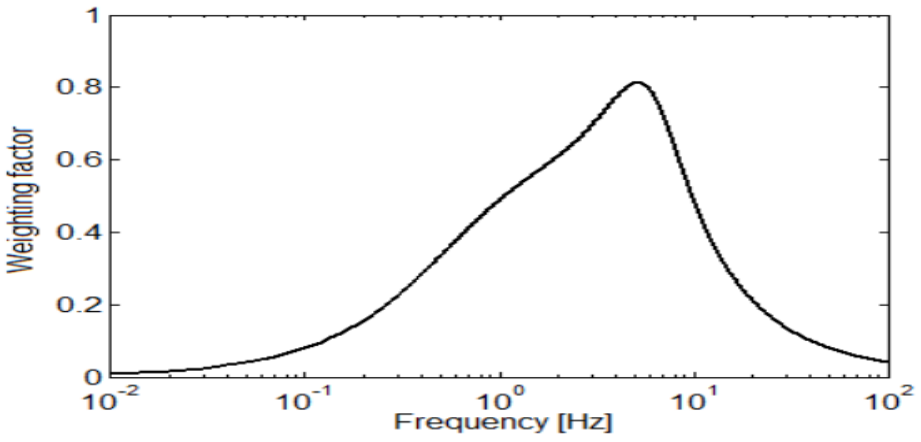

Figure 3.6 frequency weighting B [12]

CHAPTER 4

RESULTS AND DISCUSSION

In this chapter results, findings, analyses, and discussion of the study will be presented and discussed. In the first section, the conversion, analysis, and curve fitting of track excitations data will be discussed. In the second section, the factors such as the response of vehicle vibrations at various speeds of vehicle, the secondary suspension damping variations with speed, time-domain analysis, frequency response analysis, and evaluation of ride comfort using Sperling ride index will be analyzed using MATLAB/Simulink software' and their results presented graphically and discussed one by one. In the third section, all parameters analyzed in section two will be analyzed using Universal Mechanism software for validations of MATLAB results and some additional futures of dynamics of the vehicle of the results between the two software and validations. In the final section, the results of optimization of suspension parameters for the improvement of ride comfort will be discussed.

Validation

The simulated findings were compared to results acquired from acceleration measurements gathered through actual testing to validate the software simulation results. The findings of actual testing were obtained from the Research Designs Organization For standardization, and now it's only a matter of chance [38].Over a straight track, the rail vehicle traveled at a constant speed of 80 km/h is considered for validation. The data collection process was composed of two parts. The record was established in first stage. The record was set for a 2Km straight specimen run down track, and the record was verified over a lengthy distance. In the second stage, you'll run around 25 kilometers. A strain gauge accelerometer (Range: +1g &+2g; Frequency response: 25Hz; Excitation: 5V AC/DC; Sensitivity: 360 mV/V/g; Damping: silicon fluid). The acceleration data was recorded in the time domain using National Instruments cards (Sampling rate: 100 Samples/s, Resolution: 12 Bit) and then transformed to the spectral domain using Fast Fourier Transformations (FFT).

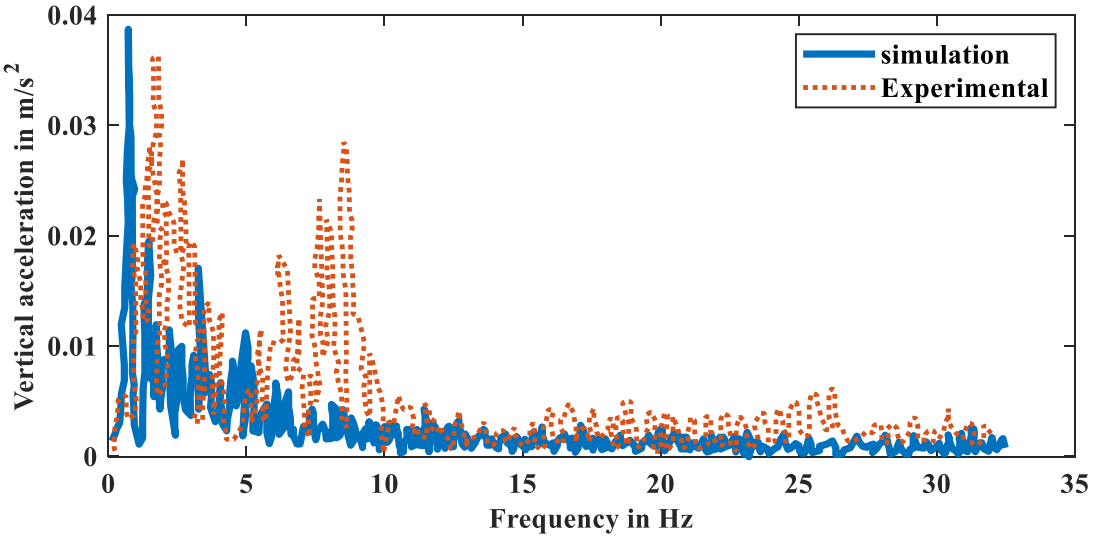

Figure4.1 FFT for Vertical acceleration of car body using experimental test and simulations

The results of the Fast Fourier transform of the vertical accelerations versus frequency is shown in Figure 4.1 the results shows that the experimental result peak is 0.0362m/s^2 and simulation peak was 0.0387m/s^2 the difference between the two is 6.5% relative error between each other the result is only validated against the experiment for only first 30 Hz frequency since the Sperling ride index measured with this range only the vertical vibration result is validated due to the this study focuses on the vertical vibrations only. Other than the peak frequency response there is some difference in the waveform due to different factors.

- In practice, problems such as wheel flats, faults in the bearings of the wheel axle sets, and other moving parts might occur with the aging process, resulting in additional force inputs.
- It's also likely that there would be a time gap between random inputs measurements of the track and vehicle acceleration readings, leading the track profile to change.
- In both the real world and the simulation, the track irregularities aren't the same.

4.1. Curve fitting of track irregularities

Sometimes, measured track irregularities data are difficult to work with. Because of it has random and non-deterministic behavior. To deal with such a case there are various international standards that estimate track irregularity based on different track quality. This standard value is only used in frequency domain analysis which is designed in power spectral density notation. It doesn't describe perfectly the current AALRT track conditions.

In the case of AALRT, the track defects are measured with a specified maintenance schedule. To evaluate the behavior of such a track under different dynamic random irregularities we need to design a generalized form of equation that estimates the current track irregularities. From the measured data, by converting it into a time function and convert it into generalized form of equation by curve fitting methodology then can use it for numerical analysis as stationary random track excitation. To analyze, this issue, the MATLAB curve fitting tool is used for converting existing random data into generalized form of the equation. While transforming the data to fit the measurement data of the system the curve fitting model have above 95 % of correlation with measured data (as expressed by correlation coefficient). So to determine the behavior of the system within the specified model from over 500m measured data 120 m track data is sampled in an area where track conditions are worst (in AALRT when it is above 4mm amplitude). By testing with a different curve-fitting algorithm, the sine functions at degree eight that specified at (4.1) suits best the vertical irregular rail profile. This function has a correlation coefficient (R^2) of 0.99. Generally, the acceptance range for curve fitting is when the value of correlation coefficient is greater than 0.95 is best to use.

General model Sin8:

$$\begin{aligned} f(x) = {} & a_1\sin(b_1x + c_1) + a_2\sin(b_2x + c_2) + a_3\sin(3x + c_3) + \\ & a_4\sin(b_4x + c_4) + a_5\sin(b_5x + c_5) + a_6\sin(b_6x + c_7) + \\ & a_7\sin(b_7x + c_7) + a_8\sin(b_8x + c_8) \end{aligned} \tag{4.1}$$

where, ‘x’ is vertical profile track irregularity data.

Coefficients:

$$a_1 = 3.593 \quad b_1 = 0.0167 \quad c_1 = -0.5327$$
$$a_2 = 1.815 \quad b_2 = 0.0556 \quad c_2 = 0.186$$
$$a_3 = 0.6803 \quad b_3 = 0.3018 \quad c_3 = 1.114$$
$$a_4 = 0.8014 \quad b_4 = 0.1746 \quad c_4 = -0.06319$$
$$a_5 = 0.5126 \quad b_6 = 0.6124 \quad c_5 = 1.455$$
$$a_6 = 0.3223 \quad b_6 = 0.4833 \quad c_6 = -1.023$$
$$a_7 = 0.9545 \quad b_7 = 0.1178 \quad c_7 = -0.3799$$
$$a_8 = 1.089 \quad b_8 = 0.2023 \quad c_8 = 1.278$$

The goodness of fit:

SSE: 0.05425 R-square: 0.9977 where, SSE is steady state error

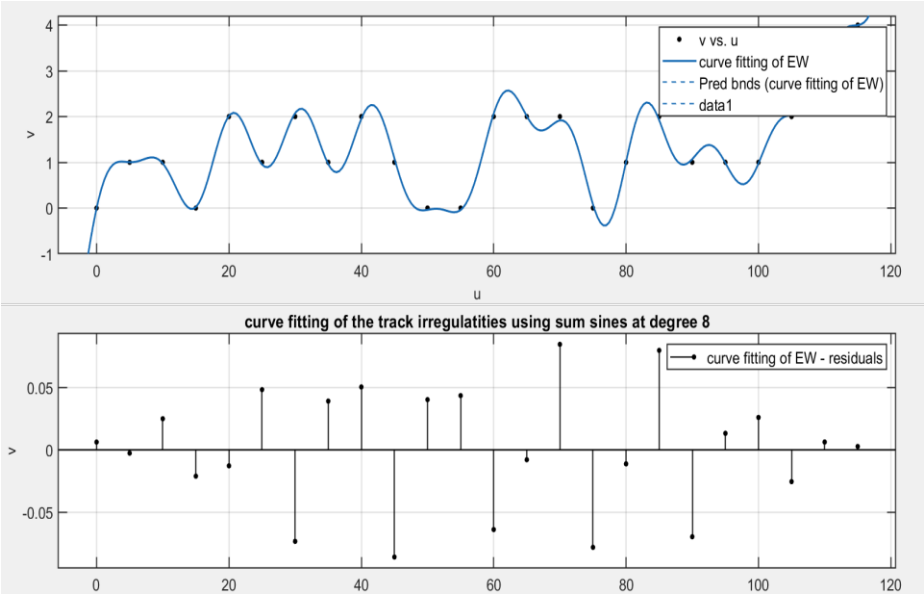

Figure 4.2 Curve fitting of track irregularities of NS line using the sum of sine’s at degree 8 and its residual.

4.2. Numerical simulation results

In this section, the numerical simulation results of responses of vibrations and evaluations of the ride comfort for the 2D vertical car model under different conditions will be presented and discussed. The modeling and simulation signal flow charts in Simulink are show in Appendix C. For evaluation of the ride comfort, Matlab code are presented in appendix A. AALRT vehicle parameters are described in Table A. 1and Table A. 2 in the appendix A.

4.2.1. The vehicle vertical vibration response at different vehicle speeds.

Speed is the main contributing factor of vibration in all types of vehicles. In rail vehicles, the designer aims to increase the speed with reasonable safety and stability.

As shown in Figure 4.3 when the speed of vehicle increases from 20 km/hr to 80 km/hr, the amplitude of car body bounce acceleration increases significantly with its root mean square value. Therefore, the speed boosts the bounce vibration of the rigid car body, bogie as well as elastic car body vibrations.

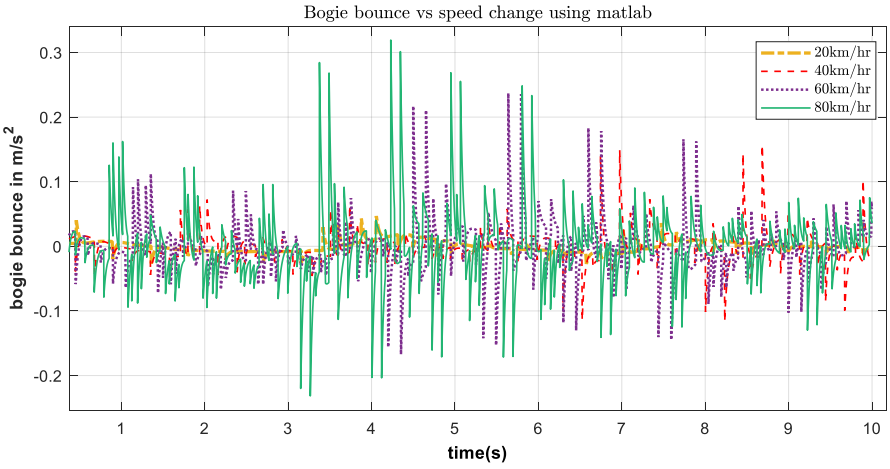

(a)

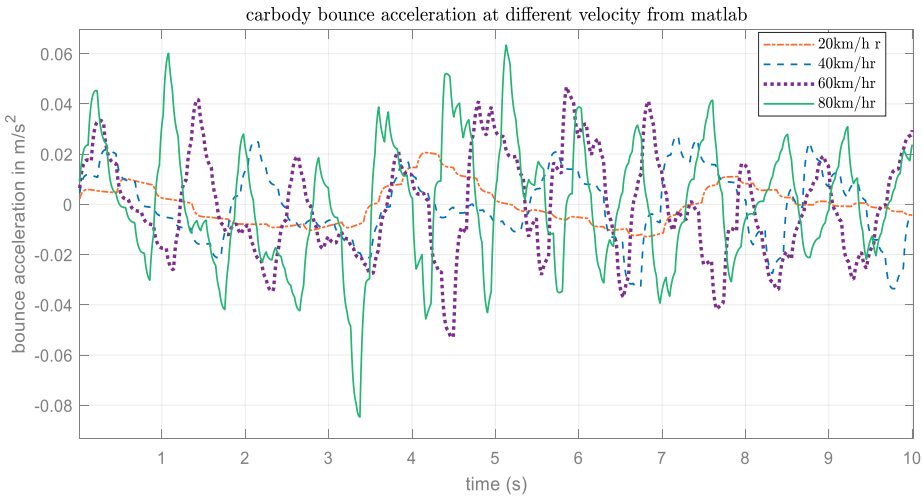

(b)

Figure 4.3 Symmetrical dynamic response of the vehicle at 20, 40, 60, 80 km/hr. of car body bounce and bogie bounce

The pitching acceleration results, which are shown in Figure 4.4 indicate that the maximum difference in amplitude between 20 km/hr to 80 km/hr of vehicle speeds are 0.0283 m/s^2 ,0.17635 m/s^2 and 0.29298 m/s^2 for carboy, flexible car body and bogies respectively. These results show that the car body acceleration in the pitch plane is less than the bounce response. As shown in the Table 4.4 the acceleration due to pitch motion is lesser than the bounce for the car body and bogie while in the car body bending mode it's a little bit higher.

The rate of deviation of magnitude of vibration acceleration is greater in the bounce movement than pitch because the change in vertical displacement of the car body is greater than the rate of change of angular displacement.

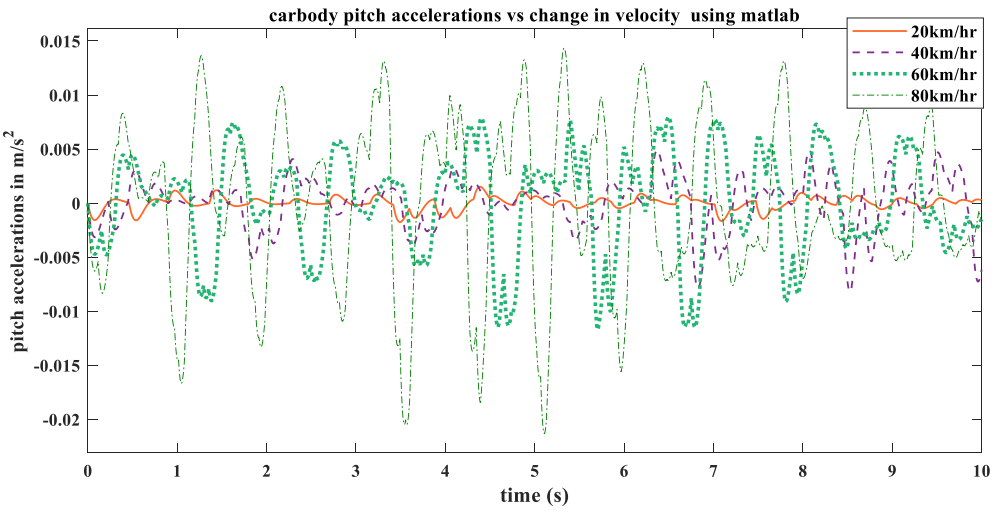

(a)

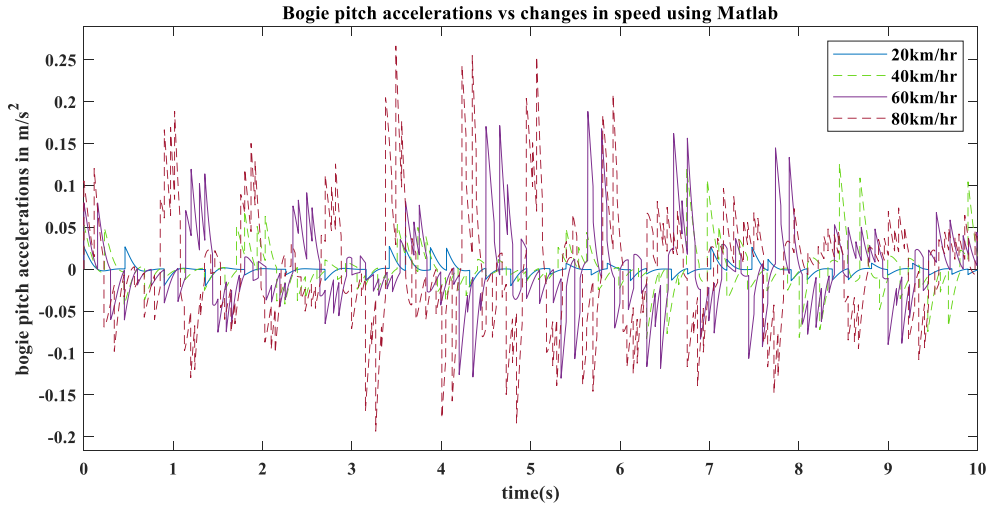

(b)

Figure 4.4 The symmetrical dynamic response of the vehicle at 20, 40, 60, and 80 km/hr. of car body pitch and bogie pitch

4.2.2. Response of vertical vibrations of the vehicle at different damping ratio

The response of the vertical vibrations of the vehicle is evaluated under different secondary suspension damping ratios at vehicle speed 20km/hr and load of 47325 kg which are the normal working condition at AALRT and other primary and secondary suspension parameters were constant.

As seen from Figure 4.5 while the damping ratio rises from 0.1 to 0.7 the response of car body bounce falls in amplitude from 0.02436 m/s^2 to 0.01214 m/s^2. But the bogie

vibration response rises in amplitude significantly from 0.0062 to 0.0117 m/s^2. It means an increase of around 88.7 % for bogies and a decrease of 50.16% car body vibration responses respectively. These facts show that an increase of the damping coefficient of secondary suspension leads to an increase in the vibration amplitudes of the bogie, which affects the stability of the car. Therefore, care must be taken while increasing the damping coefficients of secondary suspension.

4.2.3. Response of the vertical vibrations of the railcar at different load conditions

AALRT operations are such that the number of passengers during peak hour is higher than the one of standard operating conditions. Therefore, in order to evaluate this condition the vehicle suspension parameter and its speed should be at normal operating conditions as indicated in company operation manual.

Table4.1 Vehicle bounces and pitches vibration responses at different loading conditions

	Carbody	**Bending mode**	**Bogie**	**Carbody**	**Bending mode**	**Bogie**
44320	0.0332	6.59e-4	0.058	6.3e-04	2.21e-4	8.74e-3
47900	0.0299	6.62e-4	0.0577	6.2e-04	2.24e-4	8.72e-4
59700	0.02493	6.73e-4	0.0566	6.0e-04	2.37e-4	8.71e-4
63000	0.02407	6.75e-4	0.0567	5.9e-04	2.41e-4	-

The results under the change in load as shown in Table 4.1 shows that the peak vibration response of vehicle in both pitch and bounce motion for the car body and bogie as well as its RMS acceleration decrease in small amount while the car body bending mode vibration increases slightly.

Since the time domain doesn't show the effects of loading briefly, the frequency response of the system under different loads is estimated. From the several loading conditions, where the maximum load is 63000kg the vibration response results are presented in

Table4. 2 It shows that the peak frequency response amplitudes didn't change with the load for car body bending mode and carbody in a pitch vibration motion.

Table4. 2 Peak frequency response of Rail vehicle with respect to passenger loads

Load(Kg.)	**Bounce accelerations(RMS)(Hz)**			**Pitch accelerations(RMS)(Hz)**		
	Rigid carbody	Carbody bending mode	bogie	Rigid carbody	Carbody bending mode	Bogie
44735	4	4	4	0.5	2.5	0.5
47900	3.4	3.4	4	0.5	2.5	0.5
57900	3.4	3.4	4	0.5	2.5	0.5
6300	4	4	4	0.5	2.5	0.5

But for the rigid carbody its peak pitch accelerations frequency response occurs at 0.5Hz while for flexible carbody it occurs at 2.5 Hz. This fact indicates that modeling the carbody without flexibility changes human sensitivity to vibrations from medium (discomfort) to high (motion sickness). But for bounce accelerations the peak frequency response didn't change because of vertical vibrations didn't affect by the load.

4.2.4. Time-domain step response analyses of the vehicle vertical vibrations.

The vehicle model is linearized using linear system analyzer application available in MATLAB/Simulink. The response of the system for a step input is checked and the results are summarized in .

Table4. 3.

As seen from Figure 4.6 the smaller peak response shows less vibration effects on the car body. Bogie peak response is seven times the car body peak response, which shows that

the bogie components are subjected to the vibration, which affects the stability of the rail vehicle which in turn may cause the wear and failure of the bogie parts.

The settling time of the carbody is greater than the bogie which indicates the damping ratio in the primary suspension is greater than the secondary suspension. Because as the damping ratio increases the ride comfort increases but the system goes unstable. The rise time of bogie and car body vibration response zero means the damper has good damping ability to transient vibration excited from the track irregularities. But, the vibration due to bending car body mode is -0.00917 which indicates the carbody bending mode of vibrations affects the vehicle vibrations responses.

Table4. 3 Step response characteristics for bounce movement of the vehicle

	Carbody	Bending mode	Bogie
Peak response(m/s^2)	1.3	-0.00917	8.1
Settling time(sec)	26	5.4	12.1
Over-shoot (%)	Infinity	Infinity	Infinity
Rise time(sec)	1.44e-16	2.91e-16	0.0604

The step response of pitch vibration as shown in Figure 4.7 and Table 4.4 has the rise time of car body bounce same as the rise time of bogie bounce motion. But, the rise time of car body bending motion is greater than the rise time of bounce motion of rigid rail car. Because of its elastic properties it takes a long time to initialize. It results in a slower response than the two rigid body modes. All of them have lesser settling time, which means the damping ratio is too small because we didn't use the damper in pitch plane. But, since pitch motion has some vertical motion that effects is get out in this result.

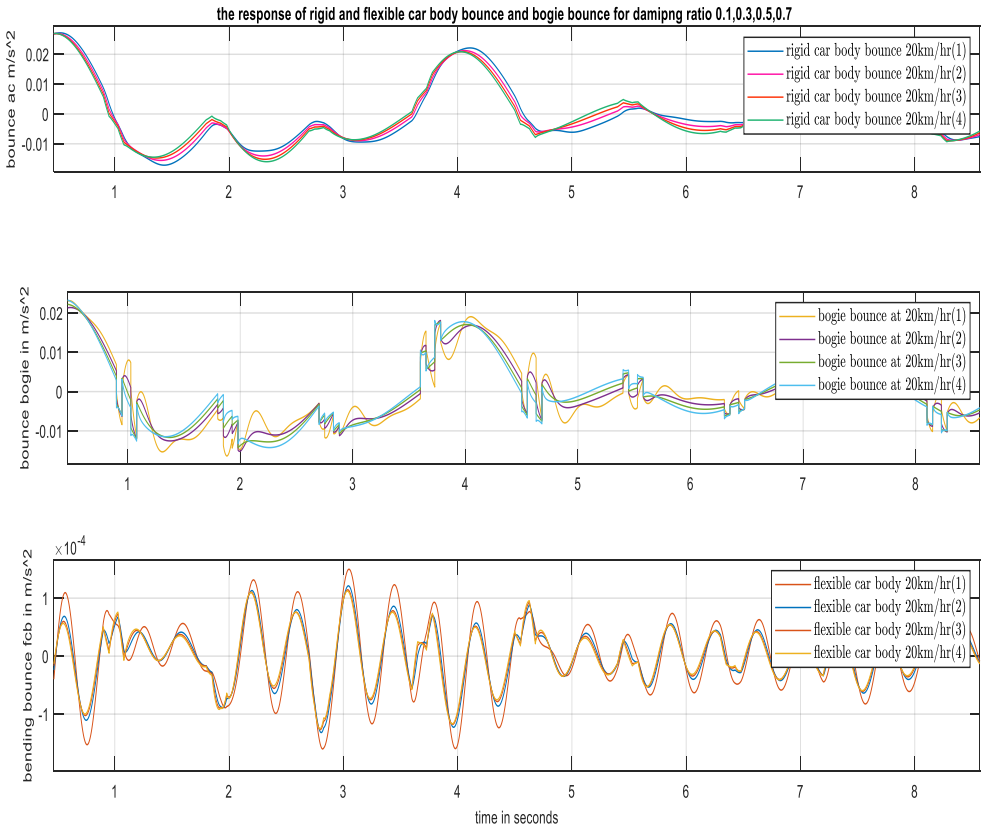

Figure 4.5 Change in vehicle response versus damping coefficient for symmetrical bounce movement.

Table4. 4 Step response characteristics for the pitch movement of the vehicle

	Carbody	**Bending mode**	**Bogie**
Peak response(m/s^2)	-0.293	0.107	5.94
Settling time(sec)	0.809	0.759	0.698
Overshoot (%)	Infinity	1.54e+18	Infinity
Rise time(sec)	0	0.059	0

Generally, the time domain step response indicates that the bounce vibrations affect more the ride comfort while the pitch vibration response has effect on the stability of the rail vehicle.

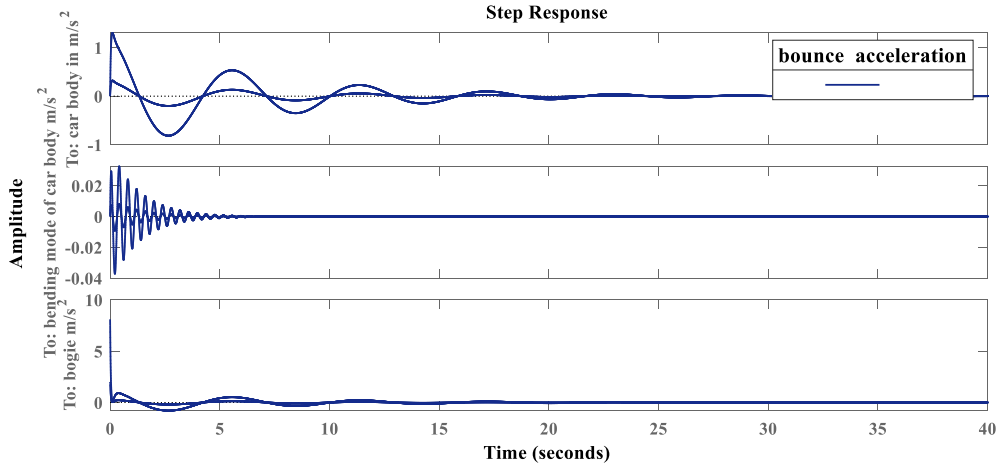

Figure 4.6 Step response characteristics of the bounce vibration of the vehicle.

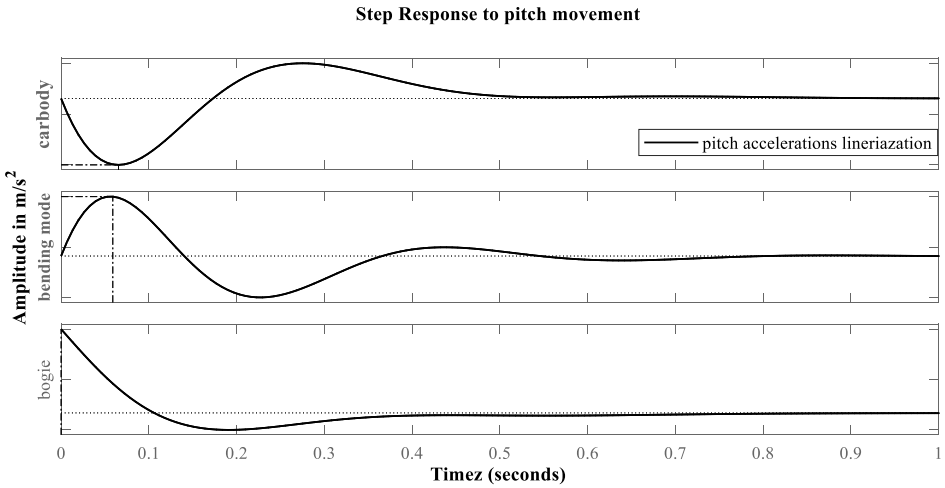

Figure 4.7 Step response of pitch vibration of the system

4.2.5. Frequency response analysis of the vehicle

The collected data is all in the time domain. However, because the vibration is transferred through the suspensions to the passengers, and the influence of vibration on passengers is contained all the time, what is more interesting is in the frequency domain. Therefore, Fourier transformation is applied to the time signal to transfer it into the frequency domain. By performing the Fourier Transform, the time signal is chopped into small sections and each section is applied to get a periodic signal. Then Fast Fourier Transform (FFT) is performed, and the signal is transferred into the frequency domain. From the frequency band of the signal, the distribution of frequencies in the acceleration signal can

be seen. Therefore, it provides information about frequencies where large amplitude of acceleration appear.

The frequency response of the system is estimated from the linearized Simulink block by using perturbed Gaussian random input on the Simulink/linear analysis toolbox. Gaussian random input has amplitude of 0.001m and the sample time 0.001s and number of samples of 10000 then the sampled track data in the time domain will be transformed to the frequency domain using Fast Fourier Transform algorithm (Figure 4.9).The result obtained using frequency estimation is shown in Figure 4.10 and Figure 4.11.

The measurement was taken when the critical vibrations are at the car body center. The pitch acceleration responses of the car body, car body bending, and bogie have peak response at 4Hz. It means that according to ISO 2631, EN12 999, and the Sperling index the human body is sensitive to low vibration frequency range between 3 to 7 Hz. Because it's between these ranges, it causes discomfort based on the magnitude and duration of the vibration time for this vehicle. Hence, this frequency is within the range of the resonance frequency of abdominal pain and respiration difficulties.

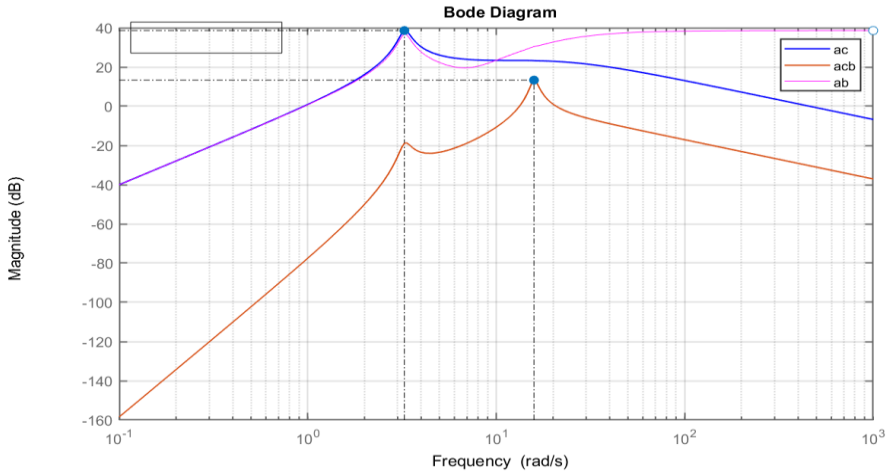

Figure 4.8 Frequency domain response of the vehicle where ac is carbody accelerations, acb are carbody bending motion and ab is bogie accelerations

As shown in Figure 4.8, at the higher frequency the peak frequency response decreases for carbody bounce and it stabilizes to a certain value for the bogie bounce motion.

While during bounce vibration, accelerations peak response occurs at 0.5 Hz for car body and bogie. But the car body bending mode, it occurs at 2.5 Hz. It indicates that the

vibration due to bounce on the rigid car body and bogie causes motion sickness because it occurs between 0.2-1 Hz range. Therefore, considering flexibility while modeling the car body have significant change on the peak acceleration responses.

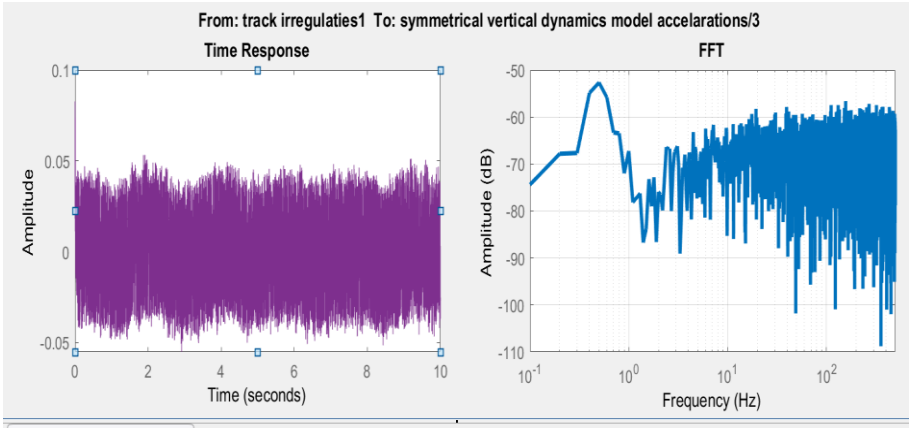

Figure 4.9 Fast Fourier Transform of bogie bounce vibration accelerations at random track excitation.

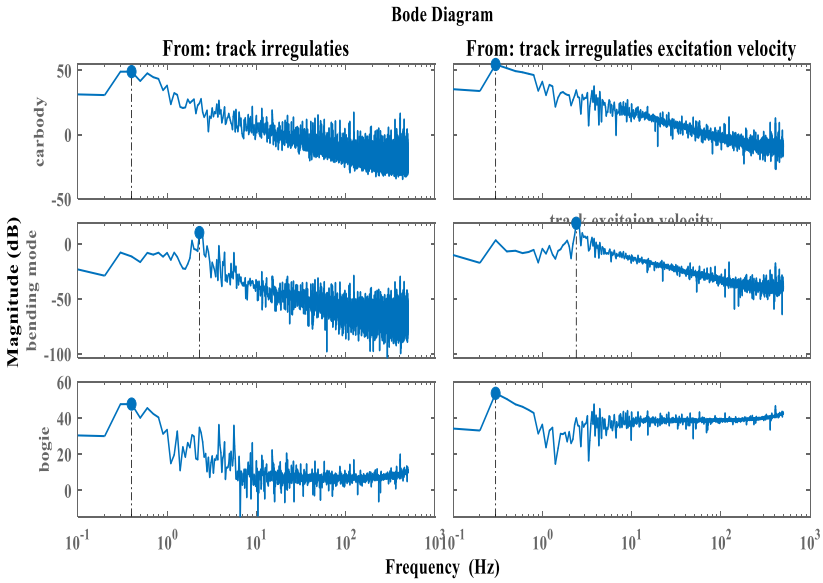

Figure 4.10 Frequency response of bounce vibration at random track excitations is in the frequency domain.

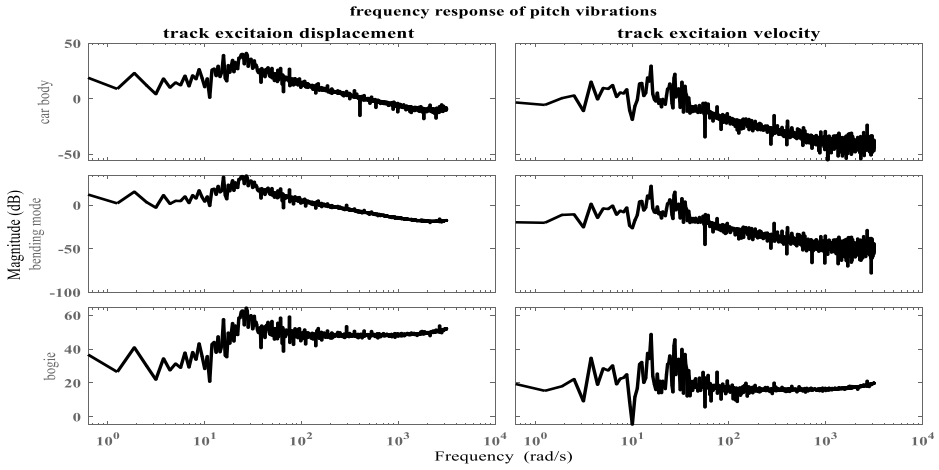

a)

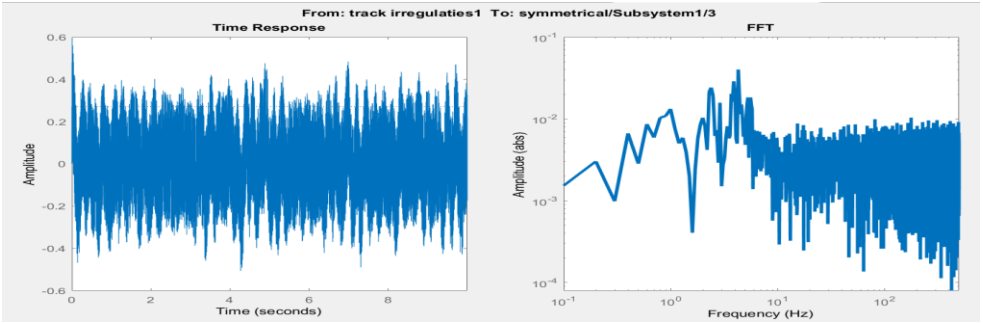

b)

Figure 4.11 Frequency responses of pitch accelerations at a) the car body, bending mode, and bogie frequency responses b) the fast Fourier transform of the sampled track excitations and the bogie pitch output. Ride comfort index for different speeds of vehicle.

4.2.6. Ride comfort versus variation in speed

The ride comfort of the vehicle at car body floor is measured using Sperling Index at current measured irregularities of AALRT and designed track irregularities of European standard under the different speed of the vehicle. The result of the r ide comfort index to vehicle speed for standard track irregularities are shown in Figure 4.12

The ride comforts of the car body worsen with increasing speed when the vehicle speed is around 20 km/hr for bounce vibrations Wz is 1.65. It means the current rail operation in" clearly noticeable range ".In the case of pitch accelerations when the vehicle speed is at

20 km/hr its WZ is 0.8, which indicates the pitch vibrations have a lower effect on ride comfort than the bounce vibrations at the car body floor.

At 40 km/hr the bounce and pitch vibrations ride index are 2.2 and 1 respectively. It means when the speed of the vehicle doubles the bounce and pitch accelerations effect on the ride discomfort increases by 33% and 25% respectively. For the former type of vibration, the level is on a "more pronounced but pleasant "and the latter is in the level of "just noticeable". In this range, the bounce vibration is felt by the passengers but doesn't affect the comfort, which tells us the maintenance team needs to be vigilant before a further problem happens.

When speed triples from the first speed conditions at just 60 km/hr the Wz is 2.65 and 1.25 for bounce and pitch vibrations respectively. It indicates that as the bounce vibration rises from 60 to 80km/hr ride comfort is deteriorated at a rate of 60.6%. This speed made the ride comfort level "strong and irregular but still tolerable ".However, according to the standards of the manufacturers, the ride index should be below 2.5 for AALRT service. Therefore, when the speed rises above 50 km/hr the ride index will be above 2.5 that it surpasses the allowable ride comfort index by the manufacturer. It means, to keep speeds higher than 50 km/hr the track should be repaired to eliminate the current track irregularities. Otherwise, the speed should stay below 50 km/hr.

When the speed is 80 km/hr and above, the bounce vibrations yield a ride comfort index of 3.1 which is in a very irregular comfort index range, while for the pitch Wz is below 2 which means a level of pronounced but not unpleasant ride index.

. For vehicle speed above 80 km/hr the vibration due to bounce affects the system very significantly. It is not recommended to use the vehicle speed above 50 km/hr within this type of track irregularities.

Generally, the bounce vibrations are the major driver of ride discomfort for such vehicle while the pitch vibrations don't affect the ride comfort of the AALRT according to this analysis results.

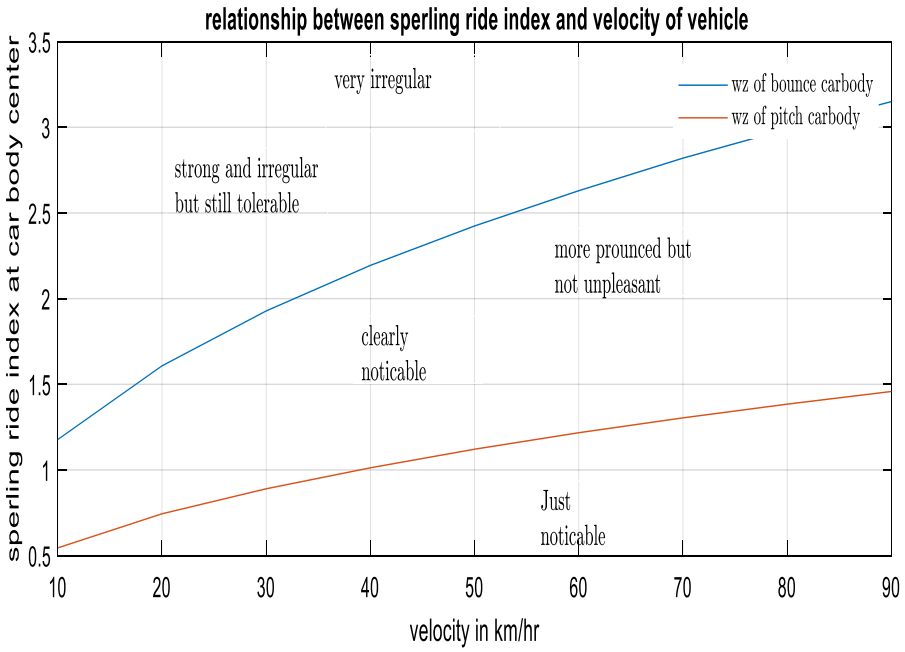

Figure 4.12 change in ride comfort vs. the speed of the vehicle

4.2.7. Ride comfort versus secondary suspension damping ratio variations

In this section we evaluate the change in secondary suspension damping ratio from 0.1 to0.45 For 20 km/hr by keeping other parameters constant at three critical positions such as at center of the carbody, above bogie front, and above rear bogie. The effect of secondary suspension damping ratio on the ride comfort effects results for different critical positions are shown below in Figure 4.13.

Between the damping ratios of 0.05 to 0.3, the variation on the ride comfort is greater. But, between the damping ratios of 0.05 to 0.3, the variation on the ride comfort is greater. When the damping ratio is below 0.1 both ride quality and ride comfort deteriorates significantly. Therefore care must be taken while choosing the damping ratio.

.Between 0.07 to 0.1 the ride comfort and ride quality changes by 65.7% and 42.8 % but above 0.3 the change is below 10%.

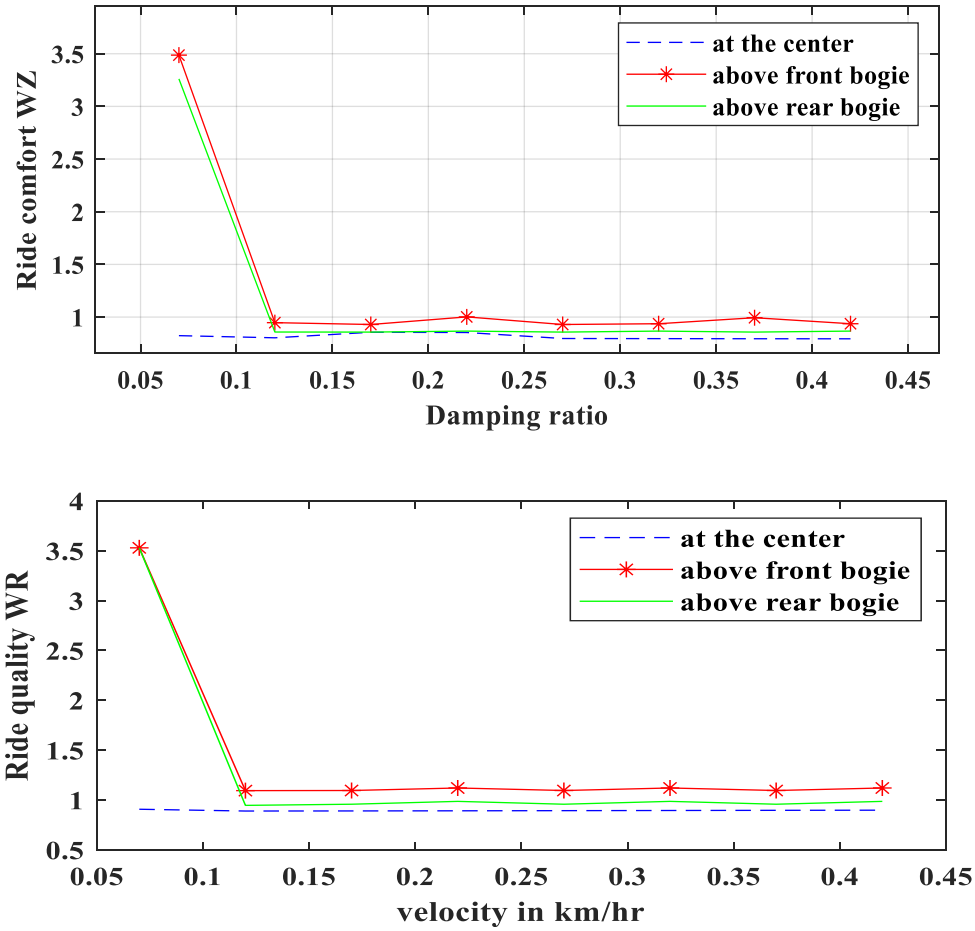

Figure 4.13 Change in the ride comfort with damping ratio at different vehicle Speeds using Mat lab/Simulink software

4.3. Multi-Body System Dynamic Simulation Results

Here we validated the results provided by a numerical simulation using a MATLAB, by comparing them with the results provided by Multi-Body System (MBS) dynamic simulation using Universal Mechanism (UM) software. Universal Mechanism software is MBS software that studies the dynamics of rail vehicles and other machinery using numerical computation [39]. In this paper, the software is used for studying the secondary suspension parameter effect on the vertical dynamics of the light rail car under technical specifications of AALRT rail vehicles. Each parameter that used for this simulation is described under appendix A in the Table A. 1 and Table A. 2. The passenger car was run on the track model created from gauge parameters corresponding to AALRT service. The UIC rail profile and the S1002 wheel profile were used. The

track model contains also measured track irregularities during the maintenance operation at AALRT. The track is considered a rigid track. The vehicle was tested for speeds in range between 20 km/hr and 80 km/hr. The software uses the park solver method for numerical computations at 0.005 s step size and 500 m longitudinal track distance.

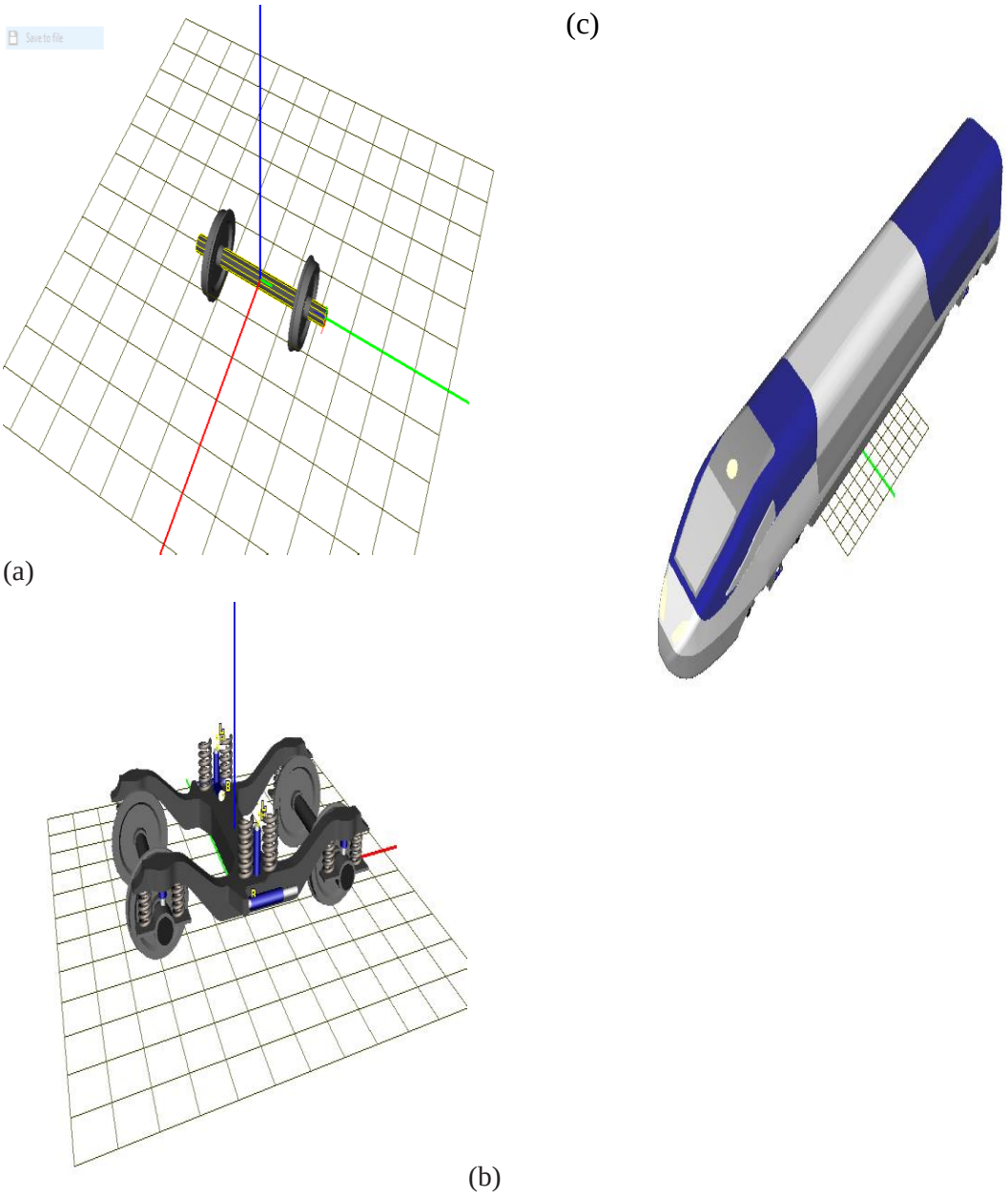

(a)

(b)

(c)

Figure 4.14 Rail vehicle model of a) wheelset b) bogie, and c) car body using Universal Mechanism Multi-Body System dynamic simulation software

The wheelset of the AALRT vehicle developed according to the dimension given in Appendix A. All four wheelset are the standard type wheelset because the right and left vertical displacements are taken as equal the final wheelset model expressed in Figure 4.14.

Bogie part is developed by using already developed bogie frame in the software then convert its dimension according to the measurement of AALRT that explained in Appendix A then connected to the primary and secondary suspension by considering the spring element as well as damper are a linear element and also added the axle box to the wheelset and connecting the wheelset with the bogie frame with primary suspension then the carbody and the bogie are connected with secondary suspension element on the UM input window.

Before car body modeled on Universal Mechanism, modeled on the SOLID WORK software according to specifications then integrates it with the universal mechanism models then connected with two bogies as external subsystems. The car body model dimension parameter then modifies it according to the AALRT car body sizes.

After the vehicle is modeled finally the track is designed and the designed vertical rail profile explained below. Track inputs the already measured vertical rail profile value in excel form is send to the track irregularities modeling part the universal simulation part then convert to the track irregularities data .then track is considered as rigid track.

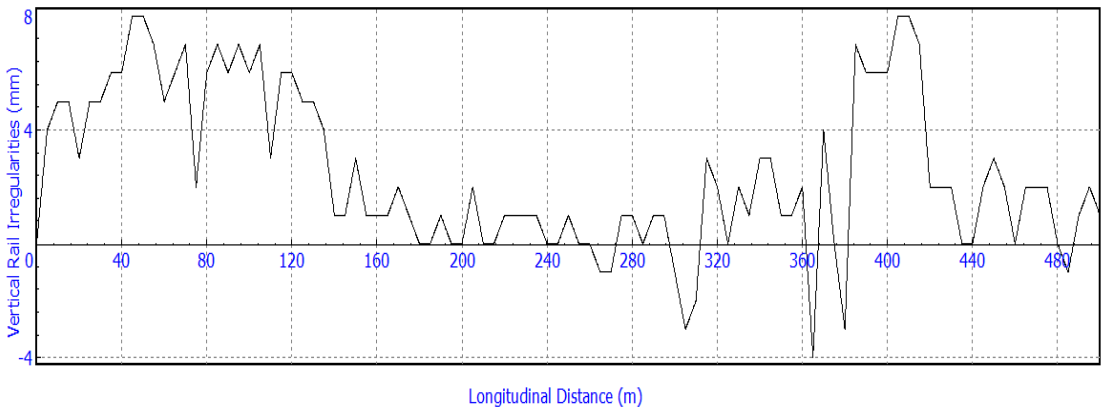

Figure 4.15 Track irregularities along vertical rail profile

The rail profile is taken as UIC rail profile that is not defected and the left and right rail profile have the same irregularities in the vertical direction and there are no rail

irregularities in the lateral directions. The wheel rail contact as taken as Fast-Sim model since, this contact model is simple and takes small computation time.

4.3.1. Response of the vehicle vibrations versus speed variations

In bounce motion, as the speed of the vehicle increases the bounce accelerations also increase in magnitude and energy content. However, for pitch motion, at car body level it does not vary significantly as bounce accelerations as speed varies.

Figure 4.16 shows that the multi-body system simulation results of carbody and bogie bounce accelerations under AALRT current track excitation with various speed considerations. The result from MATLAB/ Simulink and MBS has an average relative difference of 9.5 % for car body and 7.25% for the bogie root mean square accelerations.

a)

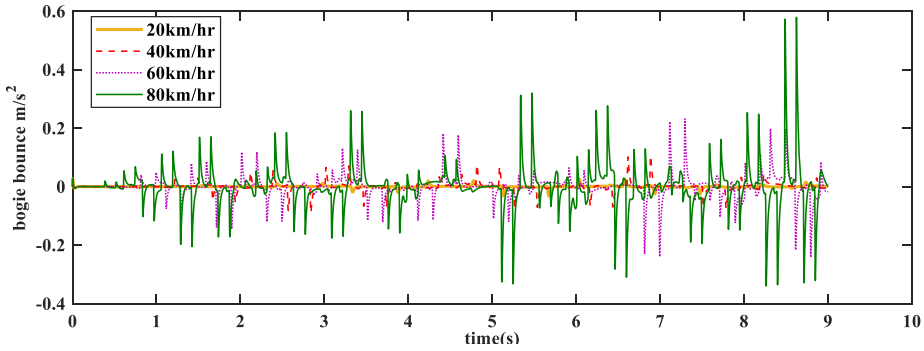

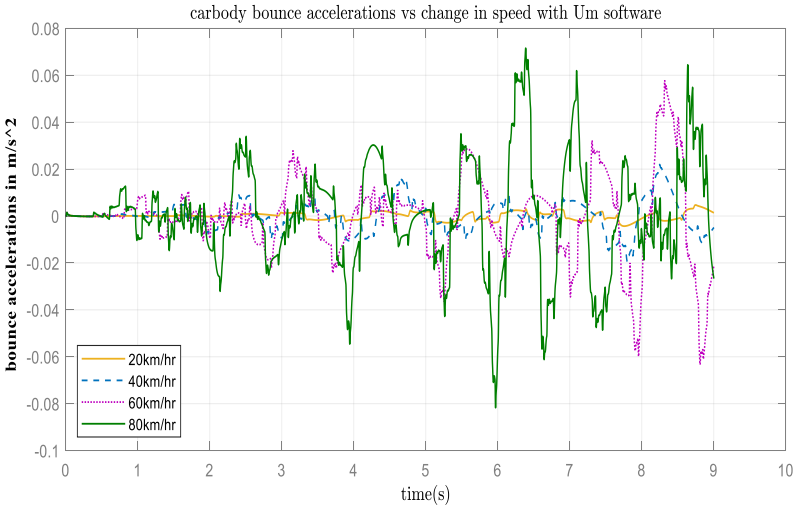

b)

Figure 4.16 Multi-Body System simulation results: variations of bounce accelerations at various speeds for a) bogie and b) rigid carbody.

The root mean square accelerations are used for comparing two software results. Because it's the main parameter that measures the energy content of vibrations, which used as the main parameter for measuring the Sperling ride index of the vehicle.

At lower vehicle velocity, the car body vibration amplitudes from the numerical simulation deviate from vibrations results provided by MBS simulation because the wheelset dynamic effect was not considered in mathematical modeling. When the acceleration is below $1\ \mathrm{cm/s^2}$ there is a higher percentage of difference between the two methods.

To achieve high accuracy all dynamic behaviors of the wheel-set need to be modeled. However, for the ride comfort evaluations since the wheel and track flexibility doesn't have much effect on the vertical dynamics of the vehicle ignoring the two factors in this study is acceptable.

Table4.5 Comparison of universal mechanism and Matlab/Simulink results for vehicle bounce vibrations

Velocity (km/hr)	Universal Mechanism out-put for bounce R.M.S accelerations(m/s^2)		MATLAB output for bounce R.M.S accelerations (m/s^2)		Average Error (%)	
	Bogie	Carbody	Bogie	Carbody	Bogie rms	Carbody
20	0.082	0.00575	0.0862	0.0078	4.8%	20%
40	0.22	0.01034	0.218	0.0138	8%	5.5%
60	0.40	0.0194	0.364	0.0205	8.1%	5.36%
80	0.58	0.023	0.53	0.0248	9.4%	7.25%

Whenever the value of bounce vibration is above 1cm/s^2 range of relative difference between two methods falls below 10% which shows the modeling through study assumption has good estimation accuracy for the ride comfort calculations.

As shown in Figure 4.17 and Figure 4.4 pitch vibrations accelerations of the bogies and carbody have effects on vibrations root mean accelerations of less than 1rad /s when using UM MBS as well as when using MATLAB/Simulink. Therefore, pitch vibration effects have less impact on the ride comfort variation for such a type of vehicle.

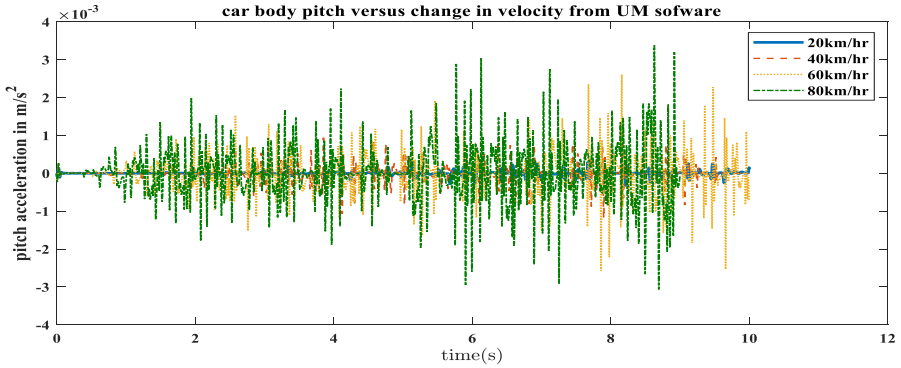

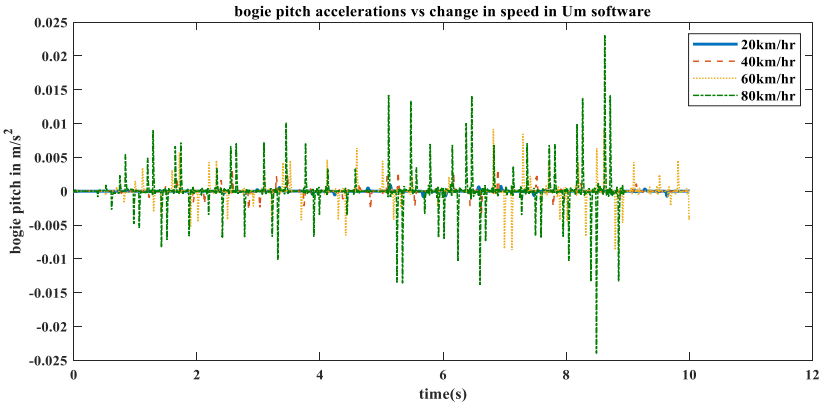

Figure 4.17 Change in pitch vibration at various speed in car body and bogie using UM – MBS software.

Generally, the results show that for high degree measurement accuracy, such as wheel-rail contact, vehicle stability, and other parameters that affect the vehicle dynamics should be included in the mathematical model. But if the system not needed a high degree of accuracy such as an evaluations of bounce vibration effect on the ride comfort ignoring wheelset dynamics parameters can be accepted.

4.3.2. Ride comfort versus speed variations at variable damping ratio and under different track irregularities.

Using UM MBS software several track irregularities data are generated. From them the responses of vehicles under two different types of track irregularities are tested. They are the AALRT track under current irregularities and UIC bad track and their results are presented in Figure 4.18 and Figure 4.19.

First test was carried out using current track irregularities data of AALRT on the UM-MBS simulation environments. The results show that as the velocity increases from 20km/hr to 80km/hr, the ride comfort worsens by 58% when damping ratio of secondary suspension is 0.2 under current AALRT rail vehicle track working conditions. Fundamentally, whenever increasing the speed, always ride discomfort increases.

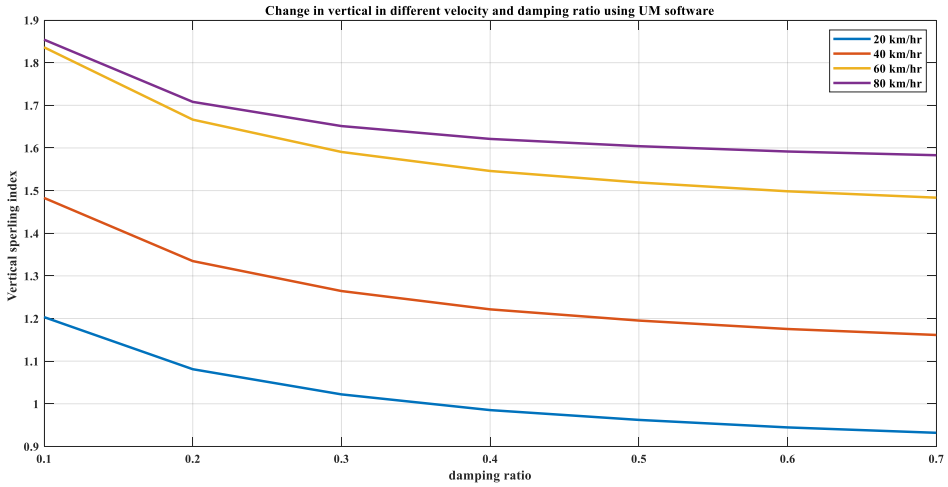

Figure 4.18 the ride index of AALRT rail vehicles under current track irregularities at various speeds and damping ratio of secondary suspension due to effect of bounce vibrations.

When vehicle travels at 20km/hr ,60km/hr and 80km/hr and the secondary suspension damping ratio increases from 0.1 to 0.2, 0.2 to 0.3, and 0.3 to 0.7 or each of speed variables the Wz increases by (10% ,5% ,3%), (9.2%,4.1%,2%) and (7%, 3%and 1%) respectively. It indicates that increasing the secondary suspension damping ratio up to 0.3 will increase the ride comfort significantly. But, when it's above 0. 3 it does not have significant effect on the ride comfort of the vehicle. Therefore, whenever designing suspension damping ratio is always between 0.1 and 0.3 there can be a significant improvement of the ride comfort. But, if it's above that it doesn't have a significant effect on the reduction of ride discomfort.

The second test was carried out using the track irregularities data of bad UIC track conditions and applying them to AALRT rail vehicle model. The ride comfort index variation with respect to speed is shown in Figure 4.19. As the speed increases the comfort will worsen. To reduce this, when damping ratio falls in the range of 0.1 to 0.3 almost there is significant improvement in the ride comfort. According to AALRT vehicle ride comfort index should be below 2.5 when vehicle speed increases beyond 40 km/hr the vehicle bounce response is very irregular. While for the pitch vibrations the vehicle is in comfortable range in the whole speed. For this vehicle under the current assumption, the pitch vibrations have not affected the vehicle comfort.

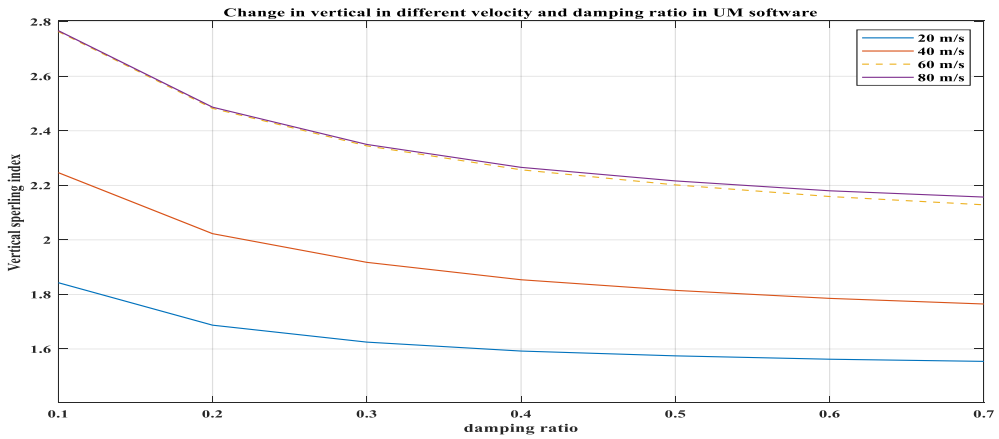

Figure 4.19 ride comfort versus the vehicle speed and different damping ratios when track excitations UIC bad track.

4.4. Improvement of ride comfort

The improvement is need for decreasing ride discomfort by selecting optimum operating conditions for the suspension parameters. It is done by utilizing MATLAB/SIMULINK response optimizations analysis tool. Pattern search Algorithm with Latin hypercube optimization method is used under 50 loop iterations. Four suspension parameters for reducing the vibration accelerations are selected. Those are primary and secondary suspensions damping and spring stiffness. Two uncertain conditions of vehicles are also considered while performing improvement. They are the load of car body and the speed of the AALRT vehicle because it is changed while operating the rail vehicle.

Objective functions

In order to reduce ride discomfort the RMS accelerations of the carbody floor should be minimized. Since, the assumptions measurement of the ride comfort for this vehicle at carbody floor. We made the signal output from the Simulink block RMS acceleration become minimized below 0.01m/s^2 as an equation(4.1). The root mean Suspension deflections response should be less than 0.028mm and 0.016mm for primary and secondary suspension respectively according to AALRT vehicles standard. The suspension deflections considered as constraints for the minimizations of the Rms accelerations of vibrations at the carbody level.

$$a_{rms}(t) = \sqrt{\int_0^{\infty}(\ddot{Z}_c(t) + \left(\frac{L}{2} - x\right)\ddot{\theta}_c(t) + \sum_{i=2}^{\infty} X_i\,(x)\ddot{T}_i(t))} < 0.05 m/s^2 \qquad 4.1)$$

Constraints

$$\delta_{primary}(t) = \sqrt{\int_0^{\infty}(Z_b(t) - \xi(t))} < 0.028 \qquad (4.2)$$

$$\delta_{secondary} = \sqrt{\int_0^{\infty}(Z_c(t) - Z_b(t))} < 0.016 mm \qquad (4.3)$$

$$0.1 \leq \zeta_c \leq 0.3 \qquad (4.4)$$

Where $a_{rms}, \zeta_c, \delta primary$ and $\delta_{secondary}$ are root mean accelerations above rear bogie, secondary suspension damping ratio, and root mean spring deflections for primary and secondary suspensions.

Upper and lower limit for optimized and uncertain parameters are described in Table 4.6 and Table 4.7. For a mass of a carbody the tare and the overload conditions are considered as lower and upper limit respectively but for velocity minimum velocity taken as 20km/hr and maximum velocity as 72 km/hr.

Table4. 6 optimized parameters of suspensions

Parameter	**Description**	**Lower limit**	**Upper limit**
Czb	Primary damping coefficient	10000Ns/m	20000Ns/m
Kzb	Primary spring stiffness	40000N/m	90000N/m
Bzc	Secondary spring stiffness	90000Ns/m	200000Ns/m
Kzc	Secondary damping coefficient	1500000N/m	3000000N/m

Table4. 7 Uncertain variables while optimizations

Uncertain variables	Minimum values	Maximum
Velocity	20km/hr	80km/hr
Mass of carbody	15750kg	25750kg

Sensitivity analysis was done using MATLAB/Simulink to know the relationship between the objective function or the RMS accelerations and the suspension parameters. To do this, 50 uniformly random Gaussian values for each suspension parameters selected and evaluated. Their results and statistical correlation are expressed in the Figure 4.20.

The results show that secondary suspension spring deflections are positively influenced by mass and velocity of the vehicle and decreases with increasing the primary and secondary spring stiffness. While the primary suspension spring deflection increases with the velocity and mass of carbody but greatly reduced with primary suspension spring stiffness. However, other parameters such as primary and secondary damping coefficient and secondary suspension stiffness have less impact on the primary suspension deflections.

The RMS accelerations of the carbody at above bogie front position are greatly influenced by the primary suspension spring stiffness and damping coefficient while they affect the primary and secondary suspension spring deflections. But, primary and secondary suspension spring stiffness and damping coefficient have less impact on the primary suspension deflections and RMS accelerations. Therefore, while doing optimization this conflicting issue should be considered.

Table4.8 Optimized suspension parameters versus the original suspension parameters

Parameters	Original suspension parameters in the vertical directions	Optimized suspension parameters in the vertical directions

Primary damping coefficient	16800 Ns/m	19976.2Ns/m
Primary spring stiffness	680000N/m	899569 N/m
Secondary spring stiffness	2200000N/m	1689936 N/m
Secondary damping coefficient	120000Ns/m	160168Ns/m

The optimized results as shown on the Figure 4.21 and Figure 4.22 it significantly increases the car body ride comfort and the ride quality at different vibrations critical positions. The ride comfort is improved by 9.87%, 14.62% and 15.17% at center of car body, above front bogie ,and above rear bogie respectively. The damping ratio of secondary suspension is 0.234 it meets the criteria.

The ride quality also improved by 9.9%,17.97%,and 18.12% at the center of carbody ,above front bogie and aboe the rear of the bogie.

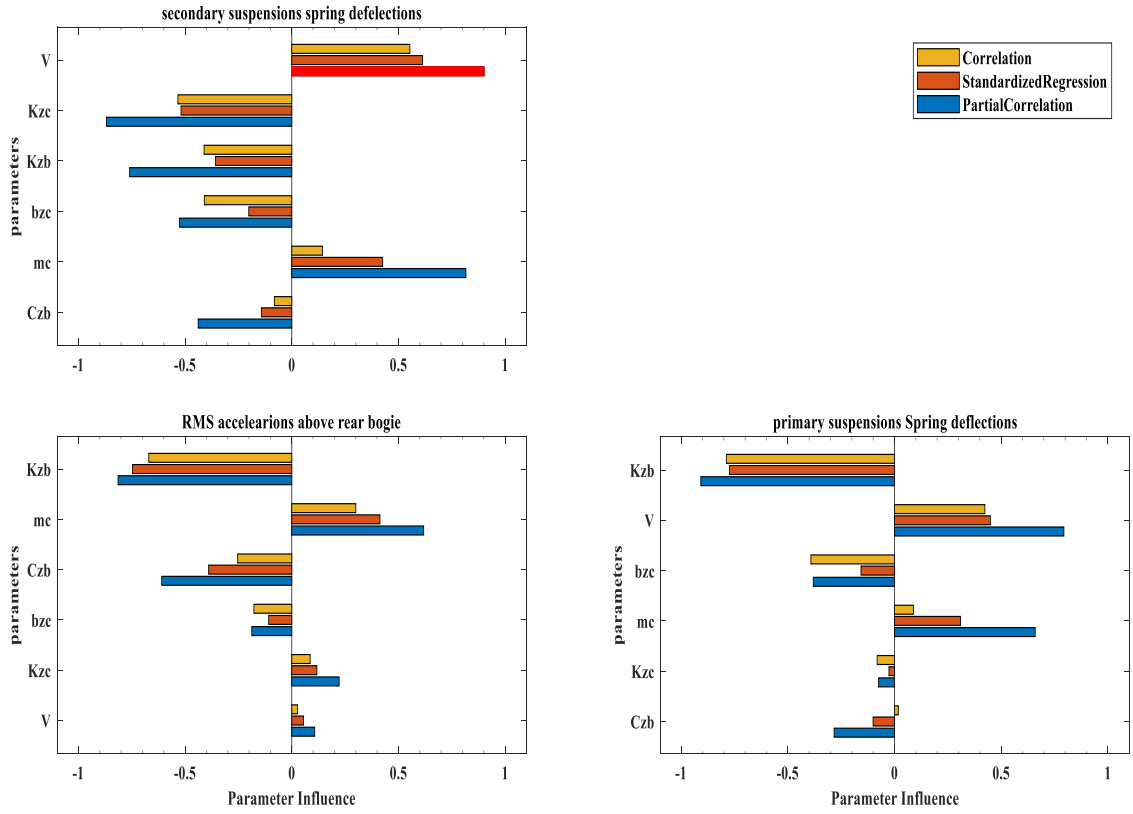

Figure 4.20 Sensitivity Analysis statistical results.

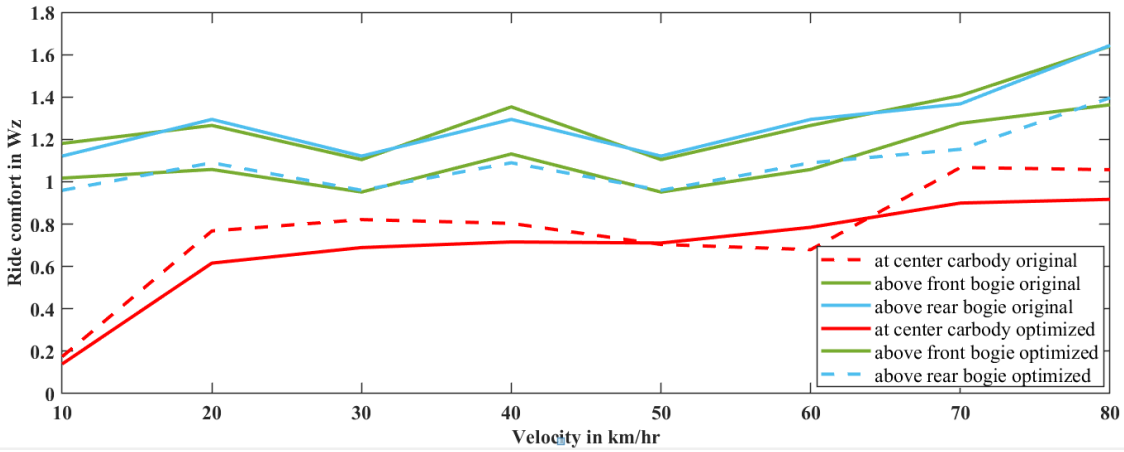

Figure 4.21 Optimized versus original ride comfort of AALRT vehicles.

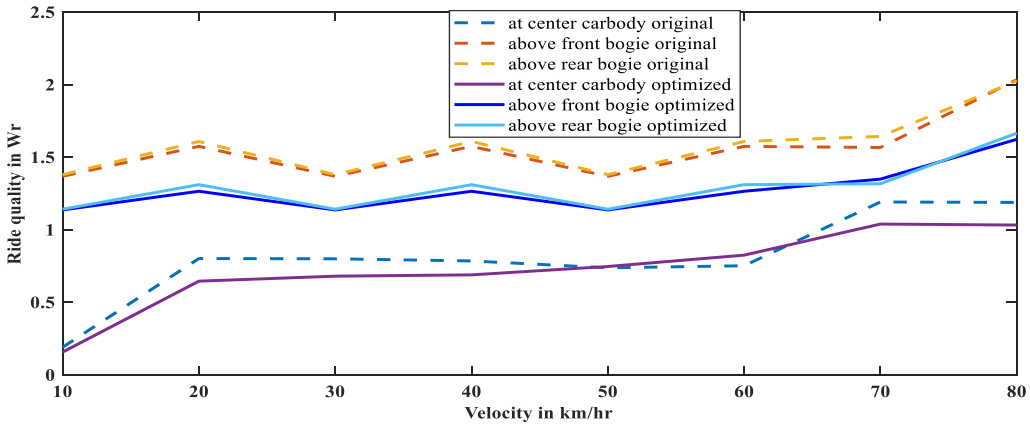

Figure 4.22 Optimized versus original ride quality of AALRT vehicles.

The change in each design parameters with corresponding iterations are shown in Figure 4.23.It shows the parameters are converged after fifth iterations.

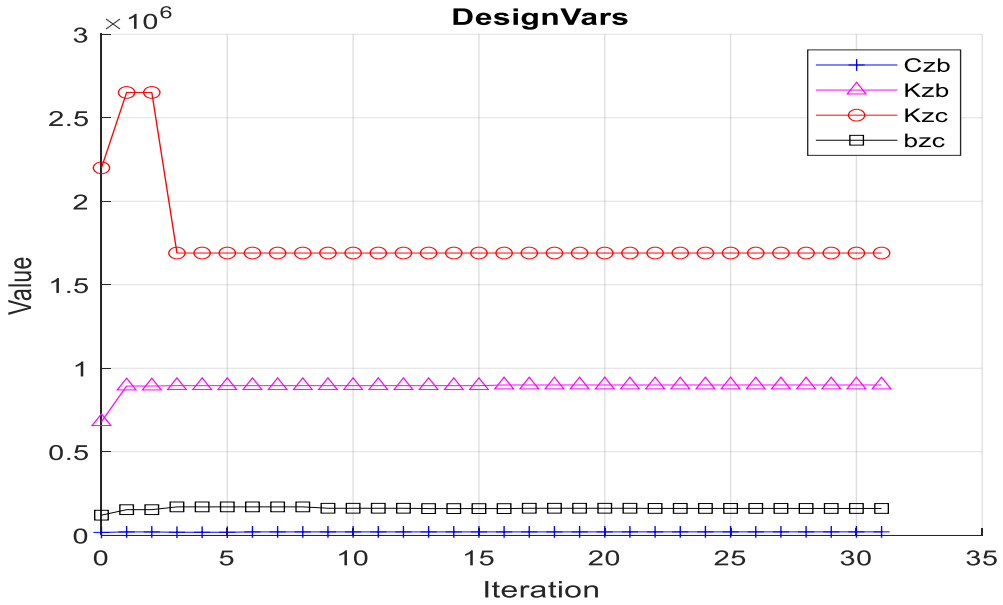

Figure 4.23 Change in design parameters at corresponding iterations where Czb, Kzb, Kzc, bzc are the primary suspension damping coefficient, primary suspension spring stiffness, secondary suspension spring stiffness and damping coefficients.

CHAPTER FIVE

CONCLUSION AND RECOMMENDATIONS

5.1 Conclusion

In this research analysis of the secondary suspension parameter effects on the ride comfort is done for the AALRT vehicles. Several works of literature related to the topic were reviewed. A mathematical model of the rail vehicle for one car, two bogies with seven degrees of freedom that includes bounce, pitch, and bending car body is developed.

Before numerically solving the equations of motion of the vehicle, first, the rail track irregularities data that were collected from the AALRT are converted to the mathematical equations by using MATLAB regression tool. The regression model chooses a sum of trigonometric sine functions of 8^{th} order for a sample of 120m track random irregularities. The regression coefficients yielded a correlation coefficient 0f 0.997, which means a high accurate regression model.

Then the responses of the vehicle to pitch and bounce vibrations at 20km/hr, 40km/hr, 60km/hr and 80km/hr have been analyzed. The results show as the speed increases the vibration increases both in the pitch and bounce in each body mode. Frequency response estimation is done to further study the vibration using MATLAB/Simulink system tool. The results show that the vibrations that are caused by bounce motion are the main source of motion sickness and ride discomfort at car body floor. But, pitch vibrations of the car body and bogie, and car body bending mode motion are the source of ride discomfort. However, they do not any peak frequency response that causes motion sickness.

The ride comfort of the car body is evaluated using the Sperling index and the result shows that within assumptions made and current track conditions AALRT vehicles, there is a good ride comfort condition. Then, we compared MATLAB results with the results from UM MBS software for validating our mathematical model. At different speeds and vibration modes, the two methods yielded a good agreement between their results. Finally, optimizations are done using the Matlab design optimization tool for parameters of vehicle suspensions under worst track conditions and the results show that the optimized parameters reduce the ride discomfort significantly.

5.2. Recommendations

This study methodology used to evaluate ride comfort using a Matlab by considering half-car 2D vertical model, as well as multi-body simulations, shows it is possible to analyze and evaluate the comfort range of other vehicles similar to AALRT under its current track irregularity vertical conditions.

The ride comfort according to evaluations under current track irregularities is in a good comfort range. No discomfort affects passengers that come from the vertical vibrations of the under current assumptions of track irregularities of 120 m. It is recommended future work be done on a whole track irregularities.

The current operations can increase the comfort the of the rail vehicles under current track conditions using optimized suspension parameters. However, the effects of optimized parameters must be tested against other dynamic performance such as derailment indexes before being deployed into design. Also, this study recommends company to use these optimized parameters by further test in its real track conditions to work with in the worst-case scenario.

REFERENCES

[1] M. J. Griffin and J. Erdreich, Handbook of Human Vibration vol. 90, no. 4. 1991.

[2] M. Dumitriu, “Evaluation of the Comfort Index in Railway Vehicles Depending on the Vertical Suspension,” no. August, 2015.

[3] Y. J. Shin, W. H. You, H. M. Hur, J. H. Park, and G. S. Lee, “Improvement of Ride Quality of Railway Vehicle by Semiactive Secondary Suspension System on Roller Rig Using Magnetorheological Damper,” *Adv. Mech. Eng.*, vol. 2014, 2014, doi: 10.1155/2014/298382.

[4] M. J. Thoresson, P. E. Uys, P. S. Els, and J. A. Snyman, “Efficient optimisation of a vehicle suspension system, using a gradient-based approximation method, Part 1: Mathematical modelling,” *Math. Comput. Model.*, vol. 50, no. 9–10, pp. 1421–1436, 2009, doi: 10.1016/j.mcm.2009.07.011.

[5] S. Pradhan, A. K. Samantaray, and R. Bhattacharyya, “Evaluation of ride comfort in a railway passenger vehicle with integrated vehicle and human body bond graph model,” *ASME Int. Mech. Eng. Congr. Expo. Proc.*, vol. 12, no. January 2018, 2017, doi: 10.1115/IMECE2017-71288.

[6] D. Younesian and A. Nankali, “Spectral Optimization of High-Speed Train Suspension Systems,” *Int. J. Veh. Struct. Syst.*, vol. 1, no. 4, 2009, doi: 10.4273/ijvss.1.4.21.

[7] “Evaluation of human exposure to whole-body vibration — Part 4: Guidelines for the evaluation of the effects of vibration and rotational motion on passenger and crew comfort in fixed-guideway transport systems,” *ISO 2631-4:2001(en) Mechanical vibration and shock —*, 2016. .

[8] C. B. E. Sperling, “, Beitrag zur beurteilung des fahrkomforts in schienenfahrzeugen, Glasers Annalen,” 1956. .

[9] BS 6841, *Guide to measurement and evaluation of human exposure tobody mechanical vibration and repeated shock,*. 1987.

[10] UIC 513R, *Guidelines for evaluating passenger comfort in relation to vibration in*

railway vehicle, International Union of Railways. 1994.

[11] Y. Jiang, B. K. Chen, and C. Thompson, "A comparison study of ride comfort indices between Sperling's method and EN 12299," *Int. J. Rail Transp.*, vol. 7, no. 4, pp. 279–296, 2019, doi: 10.1080/23248378.2019.1616329.

[12] C. Deng, J. Zhou, D. Thompson, D. Gong, W. Sun, and Y. Sun, "Analysis of the consistency of the Sperling index for rail vehicles based on different algorithms," *Veh. Syst. Dyn.*, vol. 59, no. 2, pp. 313–330, 2021, doi: 10.1080/00423114.2019.1677923.

[13] H. C. NGUYEN, A. SONE, D. IBA, and A. MASUDA, "Design of Passive Suspension System of Railway Vehicles via Control Theory," *J. Syst. Des. Dyn.*, vol. 2, no. 2, pp. 518–527, 2008, doi: 10.1299/jsdd.2.518.

[14] B. Fu, R. L. Giossi, R. Persson, S. Stichel, S. Bruni, and R. Goodall, "Active suspension in railway vehicles: a literature survey," *Railw. Eng. Sci.*, vol. 28, no. 1, pp. 3–35, 2020, doi: 10.1007/s40534-020-00207-w.

[15] A. Johnsson, V. Berbyuk, and M. Enelund, "Pareto optimisation of railway bogie suspension damping to enhance safety and comfort," *Veh. Syst. Dyn.*, vol. 50, no. 9, pp. 1379–1407, 2012, doi: 10.1080/00423114.2012.659846.

[16] M. M. Moheyeldein, A. M. Abd-El-Tawwab, K. A. Abd El-gwwad, and M. M. M. Salem, "An analytical study of the performance indices of air spring suspensions over the passive suspension," *Beni-Suef Univ. J. Basic Appl. Sci.*, vol. 7, no. 4, pp. 525–534, 2018, doi: 10.1016/j.bjbas.2018.06.004.

[17] S. Sun, H. Deng, and W. Li, "Variable stiffness and damping suspension system for train," *Act. Passiv. Smart Struct. Integr. Syst. 2014*, vol. 9057, no. March 2014, p. 90570P, 2014, doi: 10.1117/12.2045023.

[18] D.-H. Wang and W.-H. Liao, "Ride quality improvement ability of semi-active, active, and passive suspension systems for railway vehicles," *Smart Struct. Mater. 2003 Smart Struct. Integr. Syst.*, vol. 5056, no. August 2003, p. 201, 2003, doi: 10.1117/12.483462.

[19] D. H. Wang and W. H. Liao, "Semi-active suspension systems for railway vehicles

using magnetorheological dampers. Part I: System integration and modelling," *Veh. Syst. Dyn.*, vol. 47, no. 11, pp. 1305–1325, 2009, doi: 10.1080/00423110802538328.

[20] S. J. Park and M. Subramaniyam, "Evaluating Methods of Vibration Exposure and Ride Comfort in Car," *J. Ergon. Soc. Korea*, vol. 32, no. 4, pp. 381–387, 2013, doi: 10.5143/jesk.2013.32.4.381.

[21] M. Nastac, S., Picu, "Whole-Body-Vibration Exposure in Trains," *Ann. "Dunarea Jos" Univ. Galati, Fascicle XIV Mech. Eng.*, vol. 6841, no. 2010, pp. 55–60, 2010.

[22] M. Khan and J. Sundström, "Vibration comfort in Swedish Inter-City trains—a survey on passenger posture and activities," *... 17th Int. Conf. ...*, pp. 3733–3736, 2004, [Online]. Available: http://lib.ioa.ac.cn/ScienceDB/18TH-ICA/pdf/Fr3.X1.2.pdf.

[23] M. S. Khan and J. Sundström, "Vibration measurements in Swedish Inter-city trains: Evaluation of discomfort values," in *12th International Congress on Sound and Vibration 2005, ICSV 2005*, 2005, vol. 4, pp. 3115–3122.

[24] M. Dumitriu and M. Leu, "Correlation between Ride Comfort Index and Sperling's Index for Evaluation Ride Comfort in Railway Vehicles," *Appl. Mech. Mater.*, vol. 880, no. February, pp. 201–206, 2018, doi: 10.4028/www.scientific.net/amm.880.201.

[25] S. Pradhan and A. K. Samantaray, "Integrated modeling and simulation of vehicle and human multi-body dynamics for comfort assessment in railway vehicles," *J. Mech. Sci. Technol.*, vol. 32, no. 1, pp. 109–119, 2018, doi: 10.1007/s12206-017-1212-z.

[26] J. Z. Jiang, A. Z. Matamoros-Sanchez, A. Zolotas, R. M. Goodall, and M. C. Smith, "Passive suspensions for ride quality improvement of two-axle railway vehicles," *Proc. Inst. Mech. Eng. Part F J. Rail Rapid Transit*, vol. 229, no. 3, pp. 315–329, 2015, doi: 10.1177/0954409713511592.

[27] Z. Lozia and E. Kardas-Cinal, "The use of a linear half-vehicle model for the optimization of damping in the passive suspension system of a railway car," *Arch.*

Transp., vol. 39, no. 3, pp. 31–49, 2016, doi: 10.5604/08669546.1225448.

[28] S. K. Sharma and A. Kumar, "Ride comfort of a higher speed rail vehicle using a magnetorheological suspension system," *Proc. Inst. Mech. Eng. Part K J. Multi-body Dyn.*, vol. 232, no. 1, pp. 32–48, 2018, doi: 10.1177/1464419317706873.

[29] J. Marzbanrad, "Optimization of a passive vehicle suspension system for ride comfort enhancement with different speeds based on design of experiment method (DOE) method," *J. Mech. Eng. Res.*, vol. 5, no. 3, pp. 50–59, 2013, doi: 10.5897/jmer10.061.

[30] D. Mădălina and D. I. Stănică, "Influence of the primary suspension damping on the ride comfort in the railway vehicles," *Mater. Sci. Forum*, vol. 957 MSF, no. August, pp. 53–62, 2019, doi: 10.4028/www.scientific.net/MSF.957.53.

[31] M. Dumitriu, "A new passive approach to reducing the carbody vertical bending vibration of railway vehicles," *Veh. Syst. Dyn.*, vol. 55, no. 11, pp. 1787–1806, 2017, doi: 10.1080/00423114.2017.1330962.

[32] M. Dumitriu and D. I. Stănică, "Study on the evaluation methods of the vertical ride comfort of railway vehicle—mean comfort method and sperling's method," *Appl. Sci.*, vol. 11, no. 9, 2021, doi: 10.3390/app11093953.

[33] S. S. Rao, *Vibration of continuous systems*. 2019.

[34] J. Guo, H. Shi, R. Luo, and P. Wu, "Parametric Analysis of the Car Body Suspended Equipment for Railway Vehicles Vibration Reduction," *IEEE Access*, vol. 7, pp. 88116–88125, 2019, doi: 10.1109/ACCESS.2019.2918777.

[35] H. Ye, J. Zeng, Q. Wang, and X. Han, "Study on Carbody Flexible Vibration Considering Layout of underneath Equipment and Doors," no. Icsmim 2015, pp. 1177–1183, 2016, doi: 10.2991/icsmim-15.2016.217.

[36] Y. Wang, Z. Dimitrovová, and J. D. Yau, "Dynamic response of a vehicle with flexible car body moving on a ballasted track," *MATEC Web Conf.*, vol. 211, pp. 1–6, 2018, doi: 10.1051/matecconf/201821111003.

[37] D. Gong, J. S. Zhou, and W. J. Sun, "On the resonant vibration of a flexible

railway car body and its suppression with a dynamic vibration absorber," *JVC/Journal Vib. Control*, vol. 19, no. 5, pp. 649–657, 2013, doi: 10.1177/1077546312437435.

[38] H. Sayyaadi and S. H. Zareh, "Intelligent control of an MR prosthesis knee using of a hybrid self-organizing fuzzy controller and multidimensional wavelet NN," *J. Mech. Sci. Technol.*, vol. 31, no. 7, pp. 3509–3518, 2017, doi: 10.1007/s12206-016-1236-9.

[39] V. Petrenko, "Simulation of Railway Vehicle Dynamics in Universal Mechanism Software," *Procedia Eng.*, vol. 134, pp. 23–29, 2016, doi: 10.1016/j.proeng.2016.01.033.

APPENDIX

A. AALRT Vehicle specifications

Table A. 1 AALRT vehicle specifications

No	Vehicle parameter	Value
1	Track gauge	1.435m
2	Bogie base	10.8m
3	Wheel set base for motor bogie	1.9m
4	Wheel set base for trailer bogie	1.8m
5	Bogie mass for motor bogie	5120kg
6	Bogie mass for trailer bogie	3120kg
7	Car body A or B mass (front and rear car body)	17500kg
8	Car body movement of inertia along x direction	4375
9	Car body movement of inertia along y direction	8750
10	Car body movement of inertia along z direction	8750
11	Car body B mass	12325
12	Car B movement of inertia along x direction	3081.25
13	Car B movement of inertia along y direction	6162.5
14	Car B movement of inertia along z direction	6162.5
15	Bogie movement of inertia along x direction	1250
16	Bogie movement of inertia along y direction	1870
17	Bogie movement of inertia along z direction	2182
	Front and rear car body length	11.800m
19	Middle car body length	3.600m

20	Height car body including pantograph	3.750m
21	Width of car body	2.650m
22	Vertical mass center of Car body	-0.9m
23	Vertical mass center of bogie	-0.528m
24	Primary spring stiffness along z	170000N/m
25	Primary damping ration along z	4200Ns/m
26	Secondary spring stiffness value along z	550000N/m
27	Secondary damper z	60000Ns/m

Table A. 2 Load conditions of AALRT vehicles

Working condition	**Seating capacity (person)**	**Standing capacity in (person)**	**Total capacity (person)**	**Total weight (ton)**
AW_0	0	0	0	44
AW_1	65	0	65	47.9
AW_2	65	189	254	59.2
AW_3	65	252	317	63

B. Matlab Simulations

B1. Matlab code

```
%% 1.track irregularities data
close all
clear
load Book2.csv                  % load the vertical track irregularities data in North south direction
load Book1.csv                  % load the vertical track irregularities data in East west direction
distance_ewx=Book1(:,1);        % east west longitudinal track distance
distance_nsx=Book2(:,1);        % north south longitudinal track distance
```

```
y1=Book2(:,2)./100;                 % vertical distance at north south rail in mm
y2=Book1(:,2)./100;                 % vertical distance at east west rail in mm
v=80;
D=v.*(ones(1,length(v)));
V=D/3.6;                            %velocity of the vehicle in km/hr
time1=distance_ewx./                % Equivalent time in second of longitudinal   distance(ns) by t=s/v
taking as a constant velocity
time2=distance_nsx./V;              % Equivalent time in second of longitudinal….      %distance(ew) by
t=s/v taking as a constant velocity
trir_d1=[time1,y2];
trir_d2=[time2,y1];
plot(time1,y2,'b-')
grid on
legend('track irregulaties at time domain in NS direction')
xlabel('time in seconds')
ylabel ('verticle displacement in mm')
figure()
plot(time2,y1,'r-')
legend('track irregulaties at time domain in EW direction')
xlabel('time in seconds')
ylabel ('verticle displacement in mm')
figure()
```

%% 2.Equation of curve fitting

%% 2.Equation of curve fitting result for Measured Random irregularities of AALRT

% the result of sine at degree 8 curve fitting equation

```
a1 = 0.005159;          % constants of sin 8 function
b1 = 1.131;
c1 =0.299 ;
a2 = 0.002746;
b2 = 2.319;
c2 = 0.5805 ;
a3 = 0.0006797;
b3 = 11.34 ;
c3 = 0.9565 ;
```

```
a4 = 0.0006438  ;
b4 = 4.521;
c4 = -2.632;
a5 = 0.0002434;
b5 = 45.44;
c5 =-1.676;
a6 = 0.0004685;
b6 = 22.49;
c6 = -1.058;
a7 = 0.0004681;
b7 = 13.34;
c7 = -0.3326;
a8 = 0.0003131;
b8 = 8.597;
c8 = -2.155;
x=0.01*(0:1000)';
f=0.5:1:30;
B1=0.588*sqrt((1.911*f.^2+(0.025*f.^2).^2)./((1-0.277*f.^2).^2+(1.563*f-
0.0368*f.^3).^2));
df=f(2)-f(1);
C=(x*(ones(1,length(x))));
B=C.*v;
A = a1*sin(b1*x+c1) + a2*sin(b2*x+c2) + a3*sin(b3*x+c3) +...
a4*sin(b4*x+c4) + a5*sin(b5*x+c5) + a6*sin(b6*x+c6) + ...
a7*sin(b7*x+c7) + a8*sin(b8*x*+c8);
simin = [B A];
plot(B,A)
```

%% 3.parameters of AALRT for analytical equations

```
mc=17500;                    %mass of car body
mb =8000;          %the total mass of bogie 1 and 2
Czb= 16800;    %damping coefficient of vertical primary suspension
Kzb=680000;    %stiffness coefficient of vertical primary suspension
bzc=120000;                  %damping coefficient of vertical secondary suspension
```

```
Kzc=2200000;                %stiffness coefficient of vertical secondary suspension
mmc = 352000;               %mass of car body bending  moment at mode 2.
kmc=89*10^6;                %stiffness coefficient at mode 2
bmc=53.1*10^4;              %damping coefficient at mode 2
bmb=53.1*10^5;
kmb=89*10^6;
mmb=mmc;                    % mass, stiffness and damping coefficient at mode3
wi=8.36;                    % natural at frequency at i bending mode in rad/s
L=11.8;                     % longitudinal length of the car body in m
x_i=5.9;                    % Eigen function of car bending moment
mg=3250;
ac=10.8/2;                  % longitudinal distance between two bogies in m
ab=1.9/2;                   % Wheelbase distance in m
EI=3200000000;              % bending module of car body
ib= 0.8;ic=7.6;             % radius of curvature of the carbody and the
bogies
Jb= 0.5* mb.*( ib)^2;       % moment of inertia of bogie 1 and 2
Jc = 0.5* mc.*(ic)^2;       % moment of inertia of car body
dcs = (bzc/4)./ (2*(Kzc/4 * mc).^0.5);   % damping ratio of secondary suspension
dcb = (Czb)/ (2*(Kzb/4 * mb)^0.5);       % damping ratio of primary suspension
dmmc = (bmc)/ (2*(kmc * mmc)^0.5);
clear bzc
dcs=0.6
bzc =4* dcs*(2*(Kzc/4 * mc).^0.5);       %damping ratio of the car body

Bi=sqrt((wi.^2.*mg./EI));
Xi=sin(Bi.*x_i)+ sinh(Bi.*x_i)-...
((sin(Bi.*L)- sinh(Bi.*L))./...
(cos(Bi.*L)-cosh(Bi.*L)))....
.*(cos(Bi.*x_i)-cosh(Bi.*x_i));   % Eigen function of the rigid car body bending
mode
```

%% Simulink results

```
sim('symmetrical.slx')      % calling Simulink blocks
```

```
Ac_1    =ans.Acb1;          %bounce accelerations data
t       =Ac_1.time;
acb_cb_1  =Ac_1.signals.values(:,1); %bounce accelerations of carbody
acb_bm  =Ac_1.signals.values(:,2);   %bounce accelerations of bm car body
acb_b  =Ac_1.signals.values(:,3);    %bounce accelerations of bogie
Ac_2    =ans.Acp;                    %calling pitch accelerations data
acp_cb_1  =Ac_2.signals.values(:,1);  %pitch accelerations of carbody
acp_bm  =Ac_2.signals.values(:,2);    %pitch accelerations of bm carbody
acp_b  =Ac_2.signals.values(:,3);     %pitch accelerations of bogie
plot(t,acb_cb_1,t,acb_bm,t,acb_b)
xlabel('time(seconds)')
ylabel('bounce acceleration in m/s^2')
legend ('carbody','bending mode vibration','bogie')
figure(2)
plot(t,acp_cb_1,t,acp_bm,t,acp_b)
xlabel('time(seconds)')
ylabel('pitch acceleration in rad/s^2')
legend ('carbody','bending mode vibration','bogie')
Fs=1000;                                %sampling frequency of the signal
signal= cat(2,acb_cb_1,acp_cb_1);    % pitch and bounce car body.....
                                        %accelerations signal
grid on;
[WZ, WR] = sperling(signal,Fs)        % ride quality and ride comfort ....
                                         % measuring functions
 function [wz, wr] = sperling(signal,fs)
%-------------------------------------------------------------------------
%This function calculates the sperling ride index value by the method
%
%SIGNAL is the acceleration data in m/s2, for which Wz ride index to be
%calculated.
%
%FS is sampling frequency.
%
```

```
%WZ is the ride index comfort value.
%WR is the ride quality factor.
%-------------------------------------------------------------------------
f=zeros(1,246);
Bw=zeros(1,246);
Bs=zeros(1,246);
for ij=4:246
   f(ij)=ij*1000/8192;

%*************************************************************************
   % Ride comfort weightening factor for
   %           horizontal direction
   %           of the acceleration

%*************************************************************************
   Bw(ij)=0.737*((1.911*f(ij)^2+(0.25*f(ij)^2)^2)/ ...
   ((1-0.277*f(ij)^2)^2 + (1.563*f(ij)-0.0368*f(ij)^3)^2))^0.5;

%*************************************************************************
   % Ride comfort weightening factor for
   %           vertical direction
   %           of the acceleration

%*************************************************************************
   Bs(ij)=Bw(ij)/1.25;

%*************************************************************************
   aa = f(ij);
   bb =(1 - 0.056*aa^2)^2;
   cc= ( (0.645*aa)^2 )* (3.55*aa^2);
   dd = (1- 0.252*aa^2)^2 ;
   ee = (1.547*aa - 0.00444*aa^3)^2 ;
   ff = 1 + 3.55*aa^2;
```

```
%************************************************************************
   % Vehicle ride quality

%************************************************************************
   B(ij) = 1.14*(( bb+ cc )/((dd +ee)*ff))^0.5;
end
hold on;
plot(f(4:end),Bw(4:end),'r');
plot(f(4:end),Bs(4:end),'g');
plot(f(4:end),B(4:end),'b');
set(gca,'fontsize',18)
xlabel('frequency([hz]');
ylabel('weghtininig frequency function');
hleg1 = legend('weghtining for horizontal','weightining for vertical',' ride quality');
set(gca,'fontsize',24)
title('weightining functions');
% Freq = w/2*pi;
%semilogx(f,20*log10(Bs),'m');
%semilogx(f,20*log10(Bs),'m');
% plot(f(4:end),Bw(4:end));
% xlabel('frequency(hz)');


for a=1:2
   sum=0;sum2=0;
   [Pxx,~] = pwelch(signal(:,a),[],[],8192,fs);
   for ij=4:246
      if (a~=3)&&(a~=4)&&(a~=9)&&(a~=12)&&(a~=15)
         Pxx2(ij)=2*Pxx(ij+1)*(Bs(ij)*Bs(ij));
      else
         Pxx2(ij)=2*Pxx(ij+1)*(Bw(ij)*Bw(ij));
      end
```

```
    end
    for ij=4:246
        Pxx3(ij)=2*Pxx(ij+1)*(B(ij)*B(ij));
    end
    for ij=4:246
        sum = Pxx2(ij)+sum;
        sum2 =Pxx3(ij)+sum2;
    end
    % A factor of 10000 is applied for conversion from m/s^2 to cm/s^2
    % 1000/8192 is df or the discrete frequency step used in integration
    integral1 = sum*1000/8192*10000;
    integral2 = sum2*1000/8192*10000;
    wz(a) = integral1^(1/6.67);
    wr(a) = integral2^(1/6.67);
end
```

C. Simulink Block

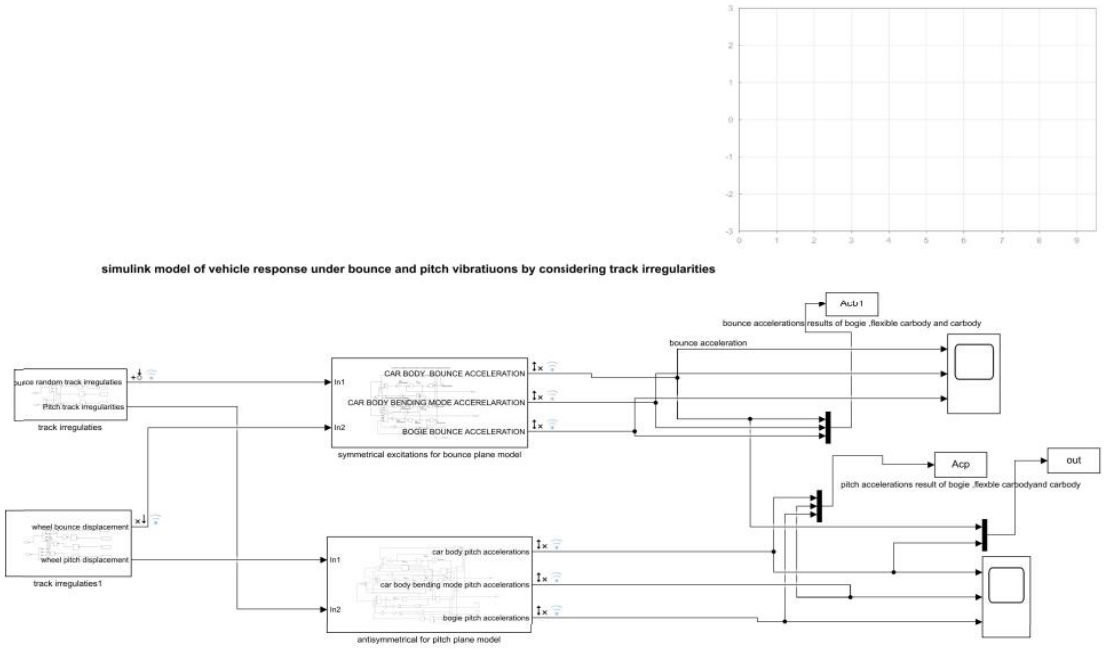

Figure c. 1 Simulink block of vertical vibrations of the carbody, bending mode carbody, and bogie pitch and bounce vibrations

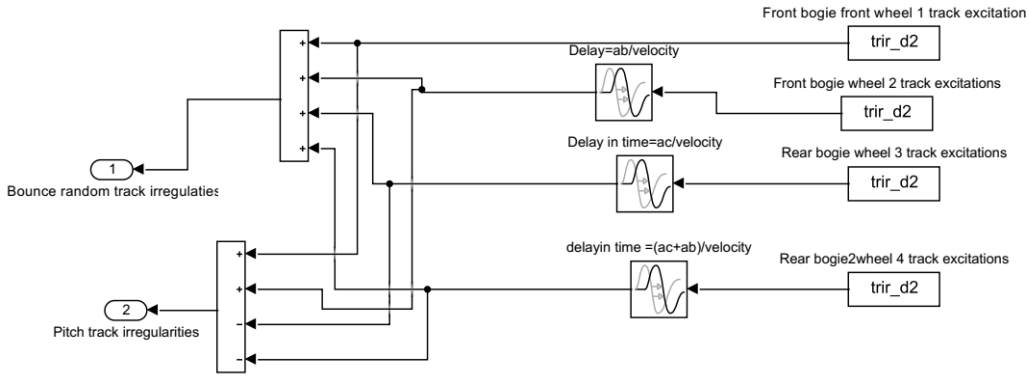

Figure c. 2 **vertical track excitation of AALRT**

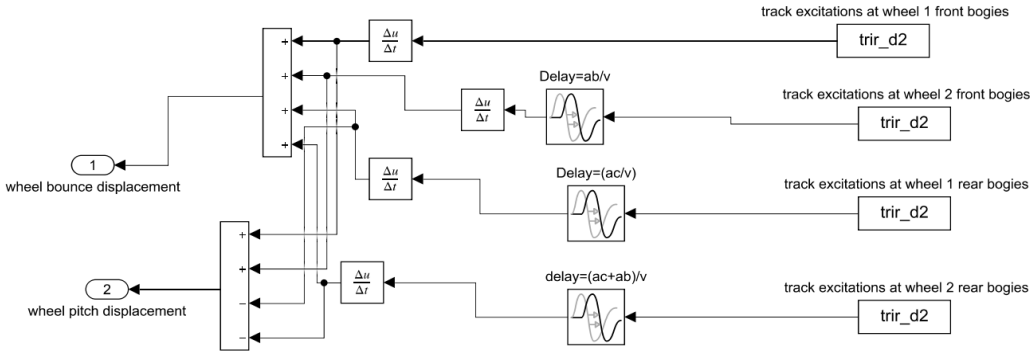

Figure c. 3 **velocity excitation of the track input**

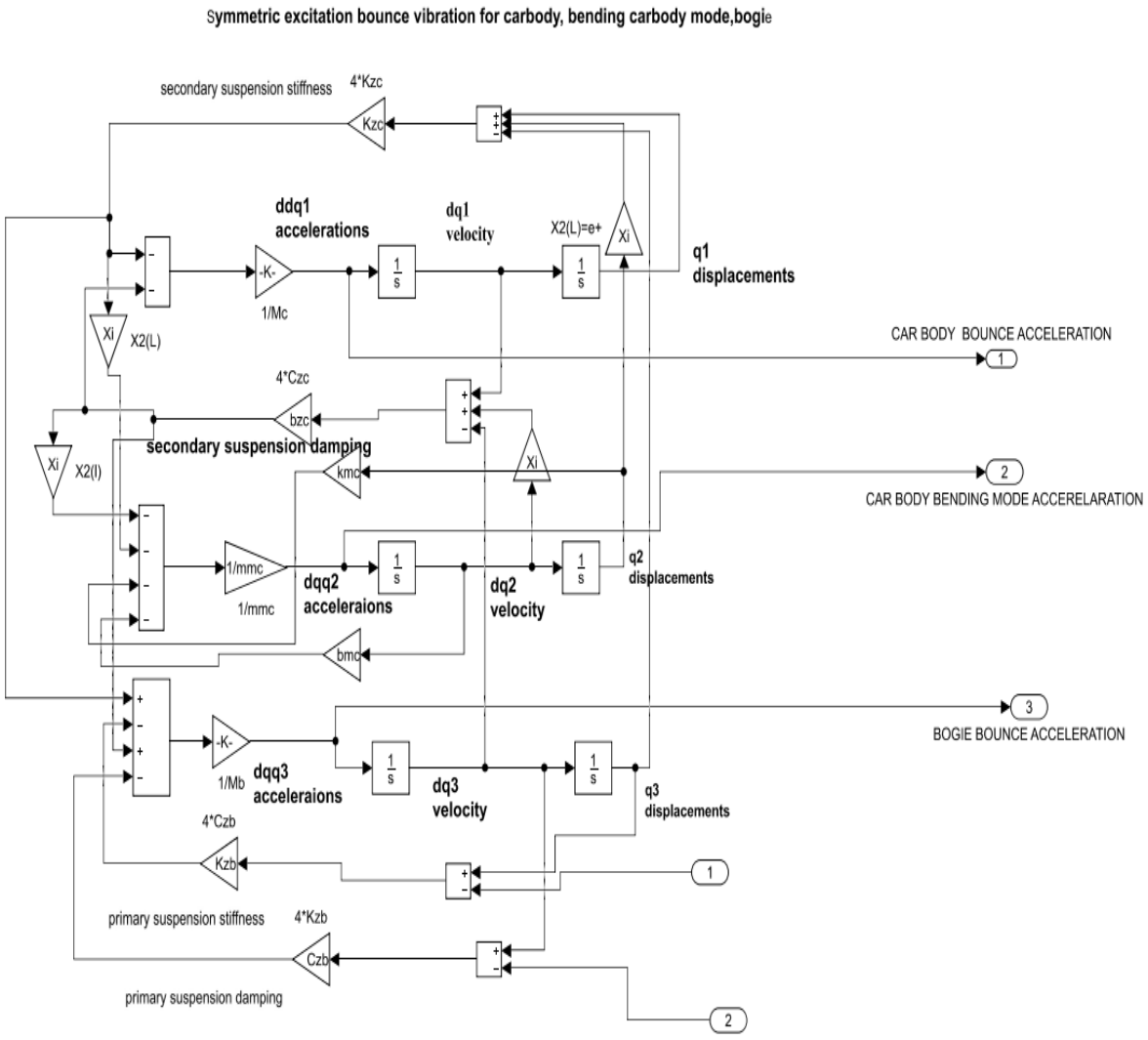

Figure c. 4 symmetrical excited bounce vibrations of the vehicle.

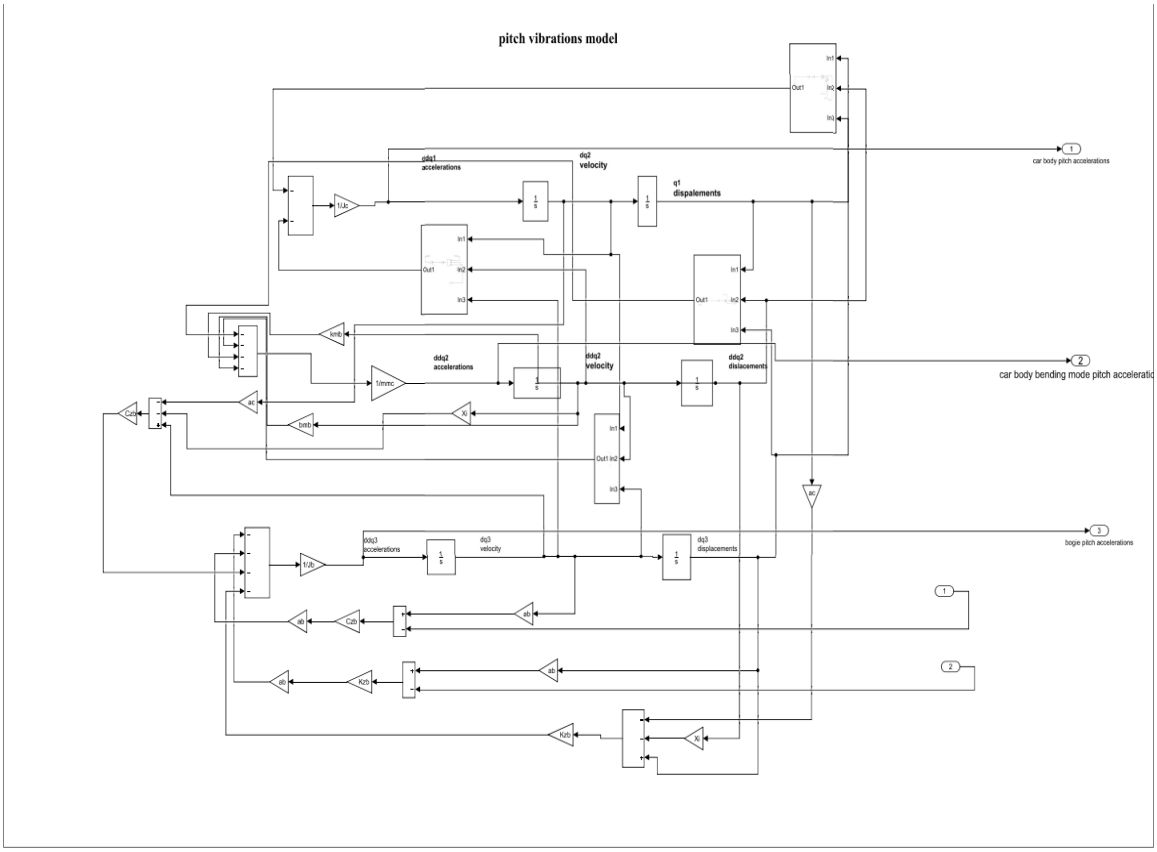

Figure c. 5 Simulink block for Anti symmetrical excitations of the vehicle pitch vibrations response.

D. Universal Mechanism software programs

- Identifiers
  - 1: v0
  - 2: my_car.v0
  - 3: my_car.BrakingForce
  - 4: my_car.bogie1_x
  - 5: my_car.bogie2_x
  - 6: my_car.xc
  - 7: my_car.zc
  - 8: my_car.beta1
  - 9: my_car.mcarbody
  - 10: my_car.Bogie1.v0
  - 11: my_car.Bogie1.rr
  - 12: my_car.Bogie1.wheelbase
  - 13: my_car.Bogie1.x1
  - 14: my_car.Bogie1.y1
  - 15: my_car.Bogie1.h1
  - 16: my_car.Bogie1.PrimaryStaticForce
  - 17: my_car.Bogie1.cx1
  - 18: my_car.Bogie1.cy1
  - 19: my_car.Bogie1.cz1
  - 20: my_car.Bogie1.x2
  - 21: my_car.Bogie1.y2
  - 22: my_car.Bogie1.z2
  - 23: my_car.Bogie1.h2
  - 24: my_car.Bogie1.beta1
  - 25: my_car.Bogie1.dxy1
  - 26: my_car.Bogie1.SecondaryStaticForce
  - 27: my_car.Bogie1.cx2
  - 28: my_car.Bogie1.cy2
  - 29: my_car.Bogie1.cz2
  - 30: my_car.Bogie1.x3

  - 30: my_car.Bogie1.x3
  - 31: my_car.Bogie1.y3
  - 32: my_car.Bogie1.length3
  - 33: my_car.Bogie1.z3
  - 34: my_car.Bogie1.y4
  - 35: my_car.Bogie1.z4
  - 36: my_car.Bogie1.length4
  - 37: my_car.Bogie1.z1
  - 38: my_car.Bogie1.beta2
  - 39: my_car.Bogie1.mcarbody
  - 40: my_car.Bogie1.dxy2
  - 41: my_car.Bogie1.WheelSet1.mwset
  - 42: my_car.Bogie1.WheelSet1.ixwset
  - 43: my_car.Bogie1.WheelSet1.iywset
  - 44: my_car.Bogie1.WheelSet1.axlelength
  - 45: my_car.Bogie1.WheelSet1.y_axlebox
  - 46: my_car.Bogie1.WheelSet2.mwset
  - 47: my_car.Bogie1.WheelSet2.ixwset
  - 48: my_car.Bogie1.WheelSet2.iywset
  - 49: my_car.Bogie1.WheelSet2.axlelength
  - 50: my_car.Bogie1.WheelSet2.y_axlebox
  - 51: my_car.Bogie2.v0
  - 52: my_car.Bogie2.rr
  - 53: my_car.Bogie2.wheelbase
  - 54: my_car.Bogie2.x1
  - 55: my_car.Bogie2.y1
  - 56: my_car.Bogie2.h1
  - 57: my_car.Bogie2.PrimaryStaticForce
  - 58: my_car.Bogie2.cx1
  - 59: my_car.Bogie2.cy1
  - 60: my_car.Bogie2.cz1

61: my_car.Bogie2.x2
62: my_car.Bogie2.y2
63: my_car.Bogie2.z2
64: my_car.Bogie2.h2
65: my_car.Bogie2.beta1
66: my_car.Bogie2.dxy1
67: my_car.Bogie2.SecondaryStaticForce
68: my_car.Bogie2.cx2
69: my_car.Bogie2.cy2
70: my_car.Bogie2.cz2
71: my_car.Bogie2.x3
72: my_car.Bogie2.y3
73: my_car.Bogie2.length3
74: my_car.Bogie2.z3
75: my_car.Bogie2.y4
76: my_car.Bogie2.z4
77: my_car.Bogie2.beta2
78: my_car.Bogie2.mcarbody
79: my_car.Bogie2.dxy2
80: my_car.Bogie2.length4
81: my_car.Bogie2.WheelSet1.mwset
82: my_car.Bogie2.WheelSet1.ixwset
83: my_car.Bogie2.WheelSet1.iywset_l
84: my_car.Bogie2.WheelSet1.iywset_r
85: my_car.Bogie2.WheelSet1.axlelength
86: my_car.Bogie2.WheelSet1.y_axlebox
87: my_car.Bogie2.WheelSet2.mwset
88: my_car.Bogie2.WheelSet2.ixwset
89: my_car.Bogie2.WheelSet2.iywset_l
90: my_car.Bogie2.WheelSet2.iywset_r
91: my_car.Bogie2.WheelSet2.axlelength
92: my_car.Bogie2.WheelSet2.y_axlebox

Subsystems
1: my_car
2: my_car.Bogie1
3: my_car.Bogie2
4: my_car.Bogie1.WheelSet1
5: my_car.Bogie1.WheelSet2
6: my_car.Bogie2.WheelSet1
7: my_car.Bogie2.WheelSet2


Images
1: my_car.bottom
2: my_car.part1
3: my_car.part2
4: my_car.middle
5: my_car.middle_gray
6: my_car.middle_darkblue
7: my_car.right_eye
8: my_car.left_eye
9: my_car.side_wind
10: my_car.front_wind
11: my_car.frond_wind1
12: my_car.eye
13: my_car.rubber1
14: my_car.Carbody
15: my_car.Bogie1.SpringGO
16: my_car.Bogie1.Damper
17: my_car.Bogie1.AirSpringGO
18: my_car.Bogie1.FrameGO
19: my_car.Bogie1.SecondarySpringGO
20: my_car.Bogie1.WheelSet1.goWSet
21: my_car.Bogie1.WheelSet2.goWSet
22: my_car.Bogie2.SpringGO
23: my_car.Bogie2.Damper
24: my_car.Bogie2.AirSpringGO
25: my_car.Bogie2.FrameGO
26: my_car.Bogie2.SecondarySpringGO
27: my_car.Bogie2.WheelSet1.goWSet
28: my_car.Bogie2.WheelSet1.goWheelRight
29: my_car.Bogie2.WheelSet2.goWSet
30: my_car.Bogie2.WheelSet2.goWheelRight
Bodies
1: my_car.Car body
2: my_car.Bogie1.BogieFrame
3: my_car.Bogie1.WheelSet1.WSet
4: my_car.Bogie1.WheelSet1.WSetRotat
5: my_car.Bogie1.WheelSet2.WSet
6: my_car.Bogie1.WheelSet2.WSetRotat
7: my_car.Bogie2.BogieFrame
8: my_car.Bogie2.WheelSet1.WSet
9: my_car.Bogie2.WheelSet1.WSetRotat
10: my_car.Bogie2.WheelSet1.WSetRightWheel
11: my_car.Bogie2.WheelSet2.WSet
12: my_car.Bogie2.WheelSet2.WSetRotat
13: my_car.Bogie2.WheelSet2.WSetRightWheel


Coordinates
1: my_car.jCar body(1)
2: my_car.jCar body(2)
3: my_car.jCar body(3)
4: my_car.jCar body(4)
5: my_car.jCar body(5)
6: my_car.jCar body(6)
7: my_car.Bogie1.jBogieFrame(1)
8: my_car.Bogie1.jBogieFrame(2)
9: my_car.Bogie1.jBogieFrame(3)
10: my_car.Bogie1.jBogieFrame(4)
11: my_car.Bogie1.jBogieFrame(5)
12: my_car.Bogie1.jBogieFrame(6)
13: my_car.Bogie1.WheelSet1.jWSet(1)
14: my_car.Bogie1.WheelSet1.jWSet(2)
15: my_car.Bogie1.WheelSet1.jWSet(3)
16: my_car.Bogie1.WheelSet1.jWSet(4)
17: my_car.Bogie1.WheelSet1.jWSet(5)
18: my_car.Bogie1.WheelSet1.jWSetRotat(1)
19: my_car.Bogie1.WheelSet2.jWSet(1)
20: my_car.Bogie1.WheelSet2.jWSet(2)
21: my_car.Bogie1.WheelSet2.jWSet(3)
22: my_car.Bogie1.WheelSet2.jWSet(4)
23: my_car.Bogie1.WheelSet2.jWSet(5)
24: my_car.Bogie1.WheelSet2.jWSetRotat(1)
25: my_car.Bogie2.jBogieFrame(1)
26: my_car.Bogie2.jBogieFrame(2)
27: my_car.Bogie2.jBogieFrame(3)
28: my_car.Bogie2.jBogieFrame(4)
29: my_car.Bogie2.jBogieFrame(5)
30: my_car.Bogie2.jBogieFrame(6)
31: my_car.Bogie2.WheelSet1.jWSet(1)
32: my_car.Bogie2.WheelSet1.jWSet(2)
33: my_car.Bogie2.WheelSet1.jWSet(3)
34: my_car.Bogie2.WheelSet1.jWSet(4)
35: my_car.Bogie2.WheelSet1.jWSet(5)
36: my_car.Bogie2.WheelSet1.jWSetRotat(1)
37: my_car.Bogie2.WheelSet1.jWSetRightWheel(1)
38: my_car.Bogie2.WheelSet2.jWSet(1)
39: my_car.Bogie2.WheelSet2.jWSet(2)
40: my_car.Bogie2.WheelSet2.jWSet(3)
41: my_car.Bogie2.WheelSet2.jWSet(4)
42: my_car.Bogie2.WheelSet2.jWSet(5)
43: my_car.Bogie2.WheelSet2.jWSetRotat(1)
44: my_car.Bogie2.WheelSet2.jWSetRightWheel(1)

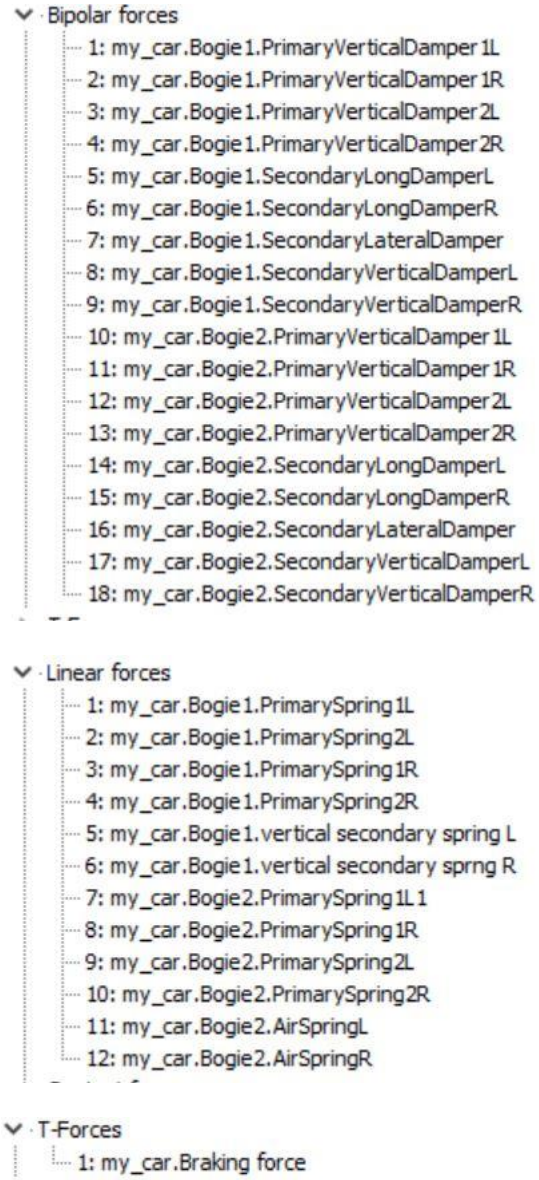
Bipolar forces
1: my_car.Bogie1.PrimaryVerticalDamper1L
2: my_car.Bogie1.PrimaryVerticalDamper1R
3: my_car.Bogie1.PrimaryVerticalDamper2L
4: my_car.Bogie1.PrimaryVerticalDamper2R
5: my_car.Bogie1.SecondaryLongDamperL
6: my_car.Bogie1.SecondaryLongDamperR
7: my_car.Bogie1.SecondaryLateralDamper
8: my_car.Bogie1.SecondaryVerticalDamperL
9: my_car.Bogie1.SecondaryVerticalDamperR
10: my_car.Bogie2.PrimaryVerticalDamper1L
11: my_car.Bogie2.PrimaryVerticalDamper1R
12: my_car.Bogie2.PrimaryVerticalDamper2L
13: my_car.Bogie2.PrimaryVerticalDamper2R
14: my_car.Bogie2.SecondaryLongDamperL
15: my_car.Bogie2.SecondaryLongDamperR
16: my_car.Bogie2.SecondaryLateralDamper
17: my_car.Bogie2.SecondaryVerticalDamperL
18: my_car.Bogie2.SecondaryVerticalDamperR
Linear forces
1: my_car.Bogie1.PrimarySpring1L
2: my_car.Bogie1.PrimarySpring2L
3: my_car.Bogie1.PrimarySpring1R
4: my_car.Bogie1.PrimarySpring2R
5: my_car.Bogie1.vertical secondary spring L
6: my_car.Bogie1.vertical secondary sprng R
7: my_car.Bogie2.PrimarySpring1L1
8: my_car.Bogie2.PrimarySpring1R
9: my_car.Bogie2.PrimarySpring2L
10: my_car.Bogie2.PrimarySpring2R
11: my_car.Bogie2.AirSpringL
12: my_car.Bogie2.AirSpringR
T-Forces
1: my_car.Braking force